

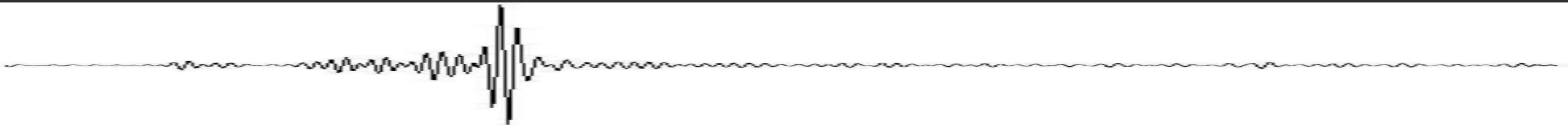
From 1D Layers to 3D Heterogeneous Structures: Insights into Earth's Interior



Xuzhang Shen(沈旭章)

The school of Earth Science and engineering of Sun Yat sen University

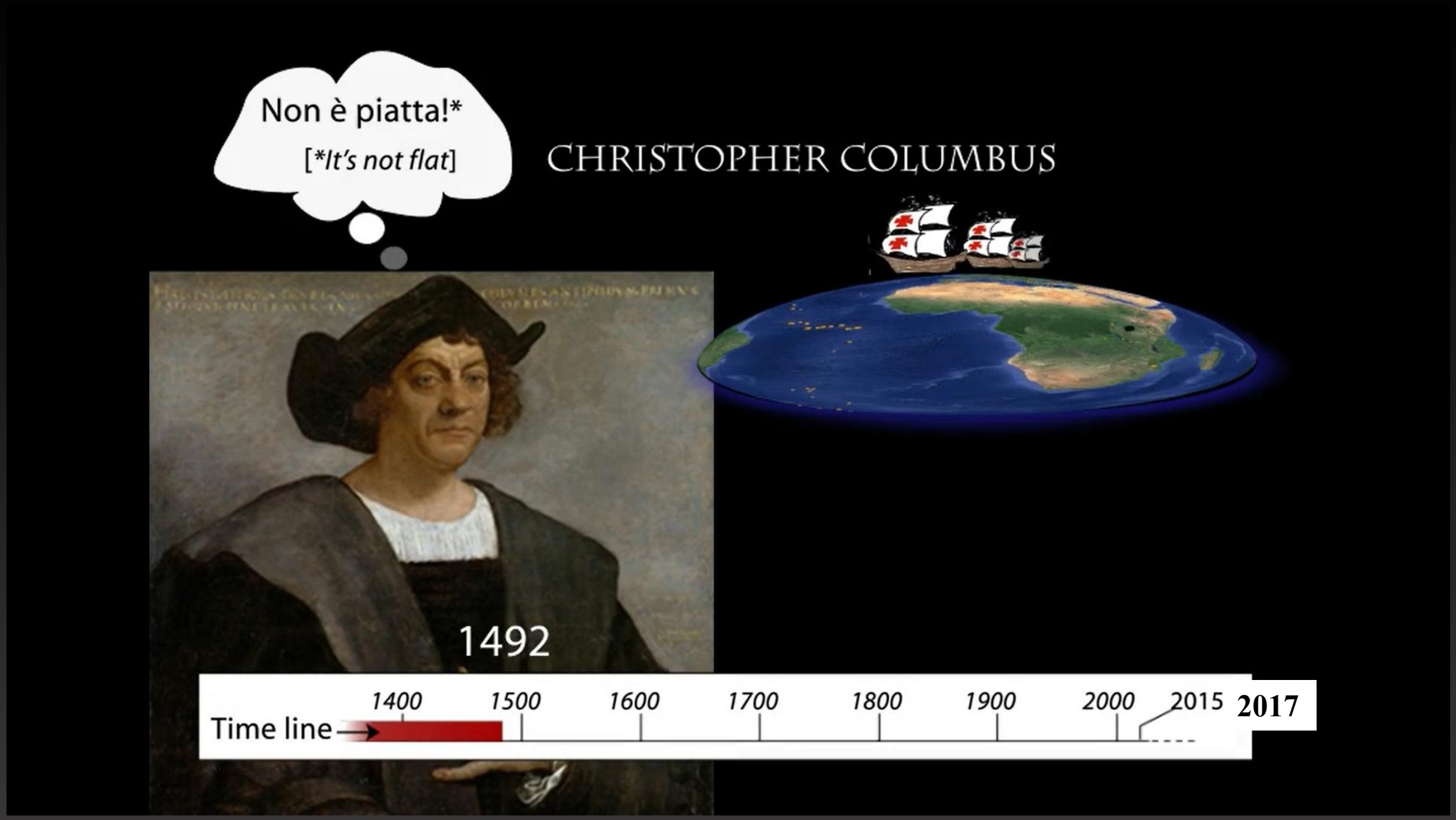
中山大学地球科学与工程学院



Outlines

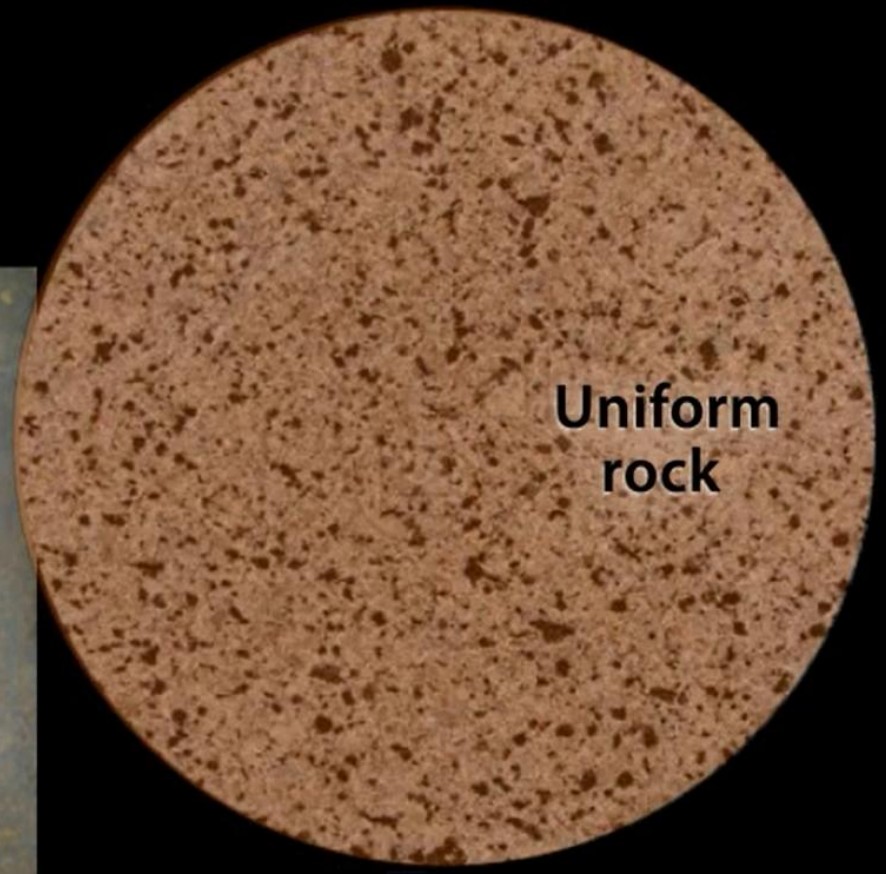
- Research history of the layered Earth
- Secondary discontinuities within the Earth's interior
- 3D Earth

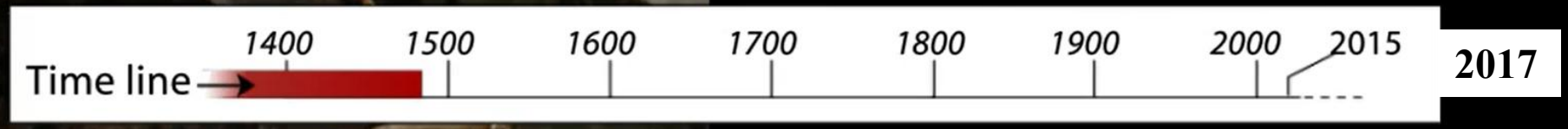
Understanding the Earth: From the Surface to the Center



Understanding the Earth: From the Surface to the Center

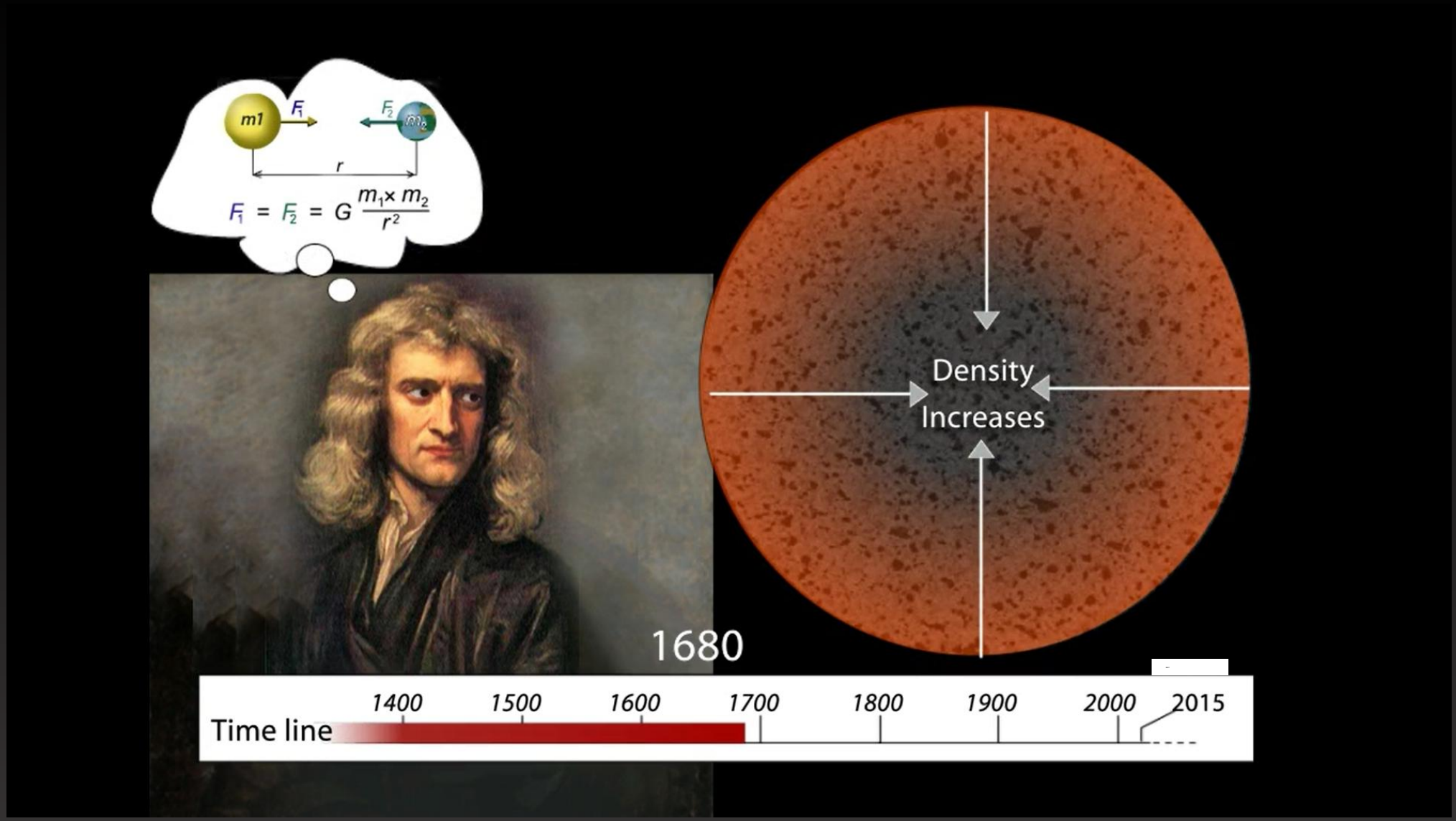






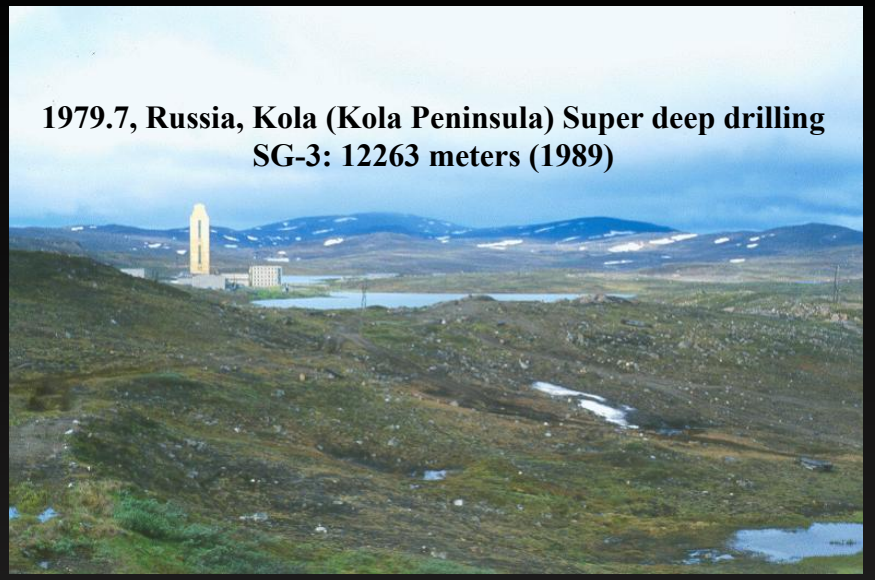
2017

Physicists' Early Understanding of Earth



How to study the internal structure of the Earth?





Drilling is the most direct way to understand the Earth!

The interior of the solid Earth is invisible and intangible, how do we know it's right?

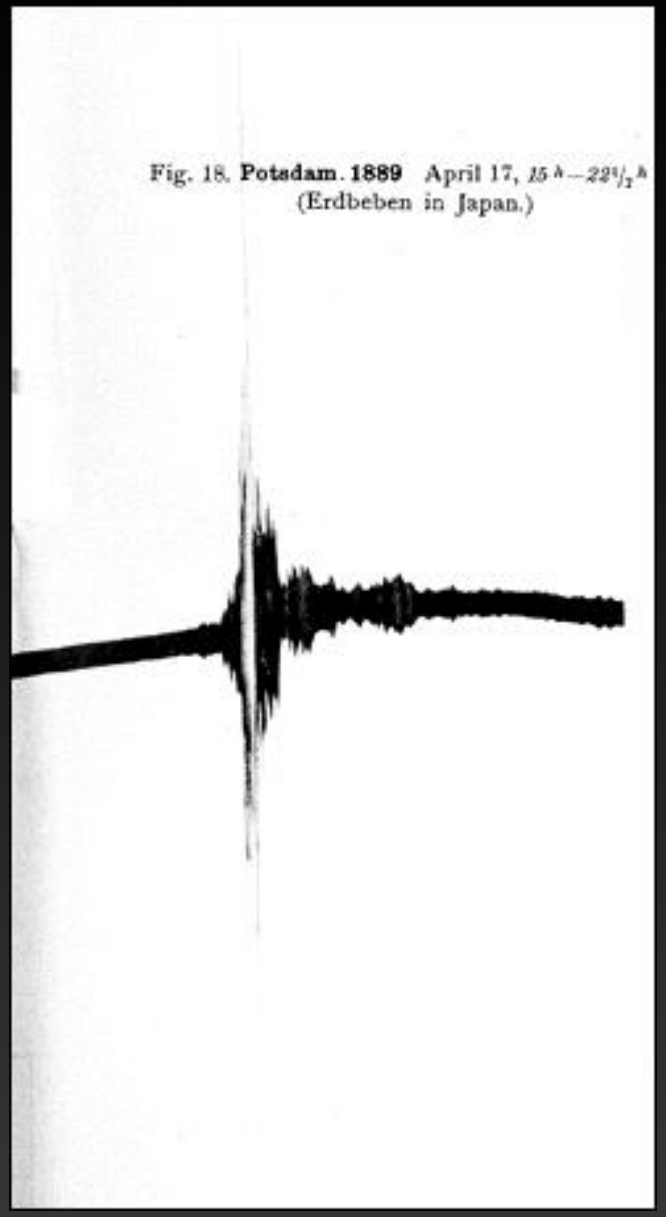


The world's first teleseismic record



（Ernst von Rebeur）

Astronomer

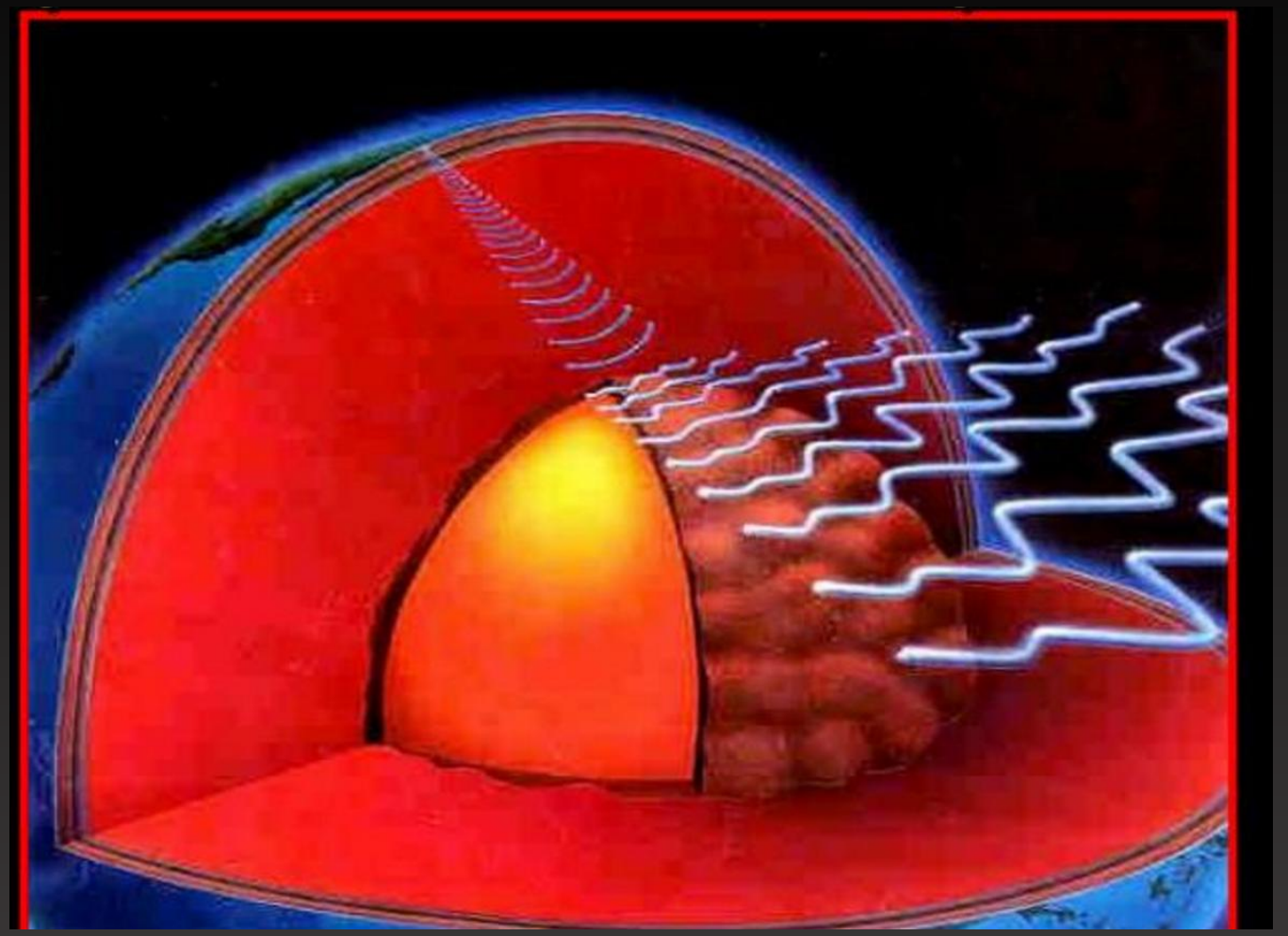

Fig. 18. **Potsdam. 1889** April 17, $15^h - 22\frac{1}{2}^h$
(Erdbeben in Japan.)

Gray-Milne seismograph
1885

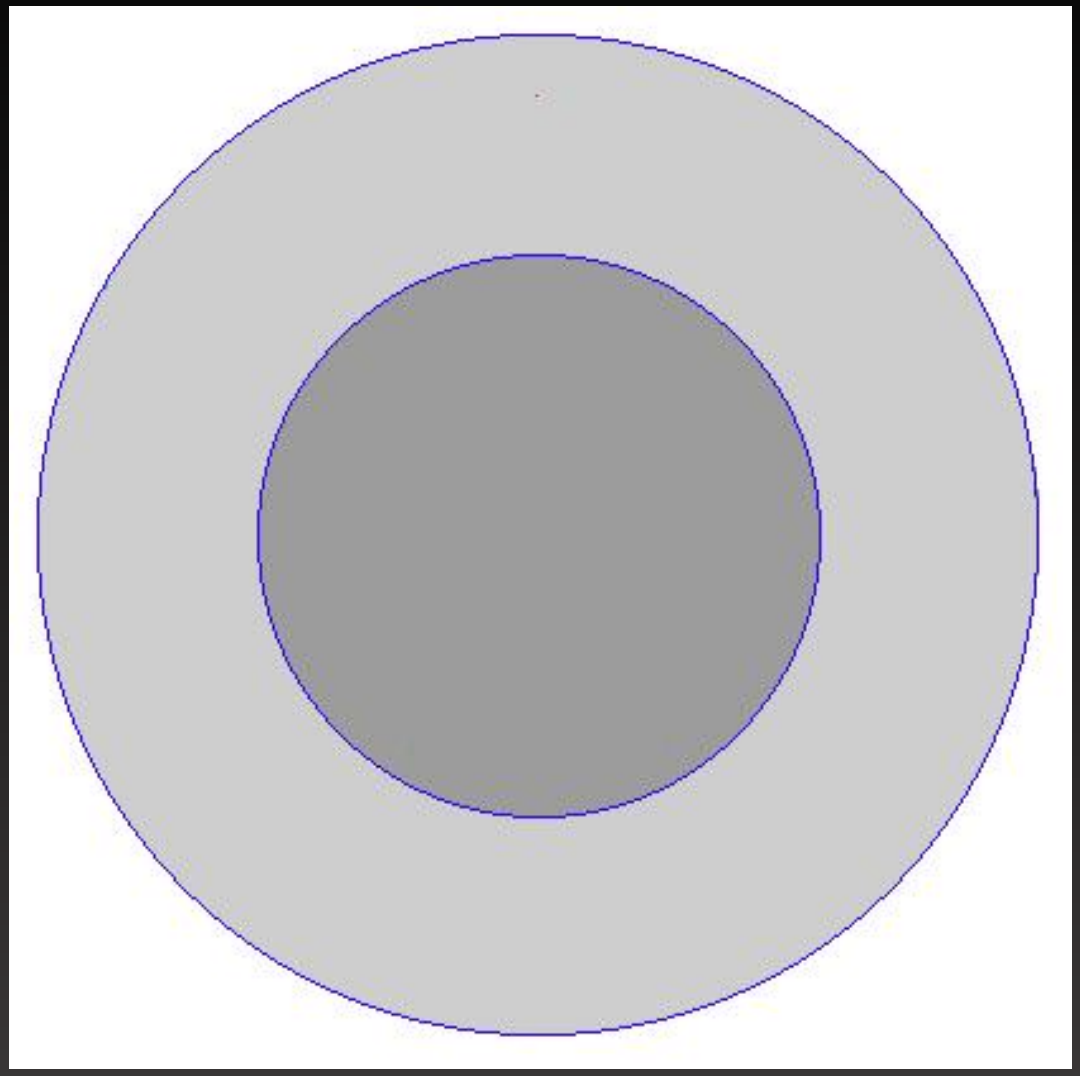


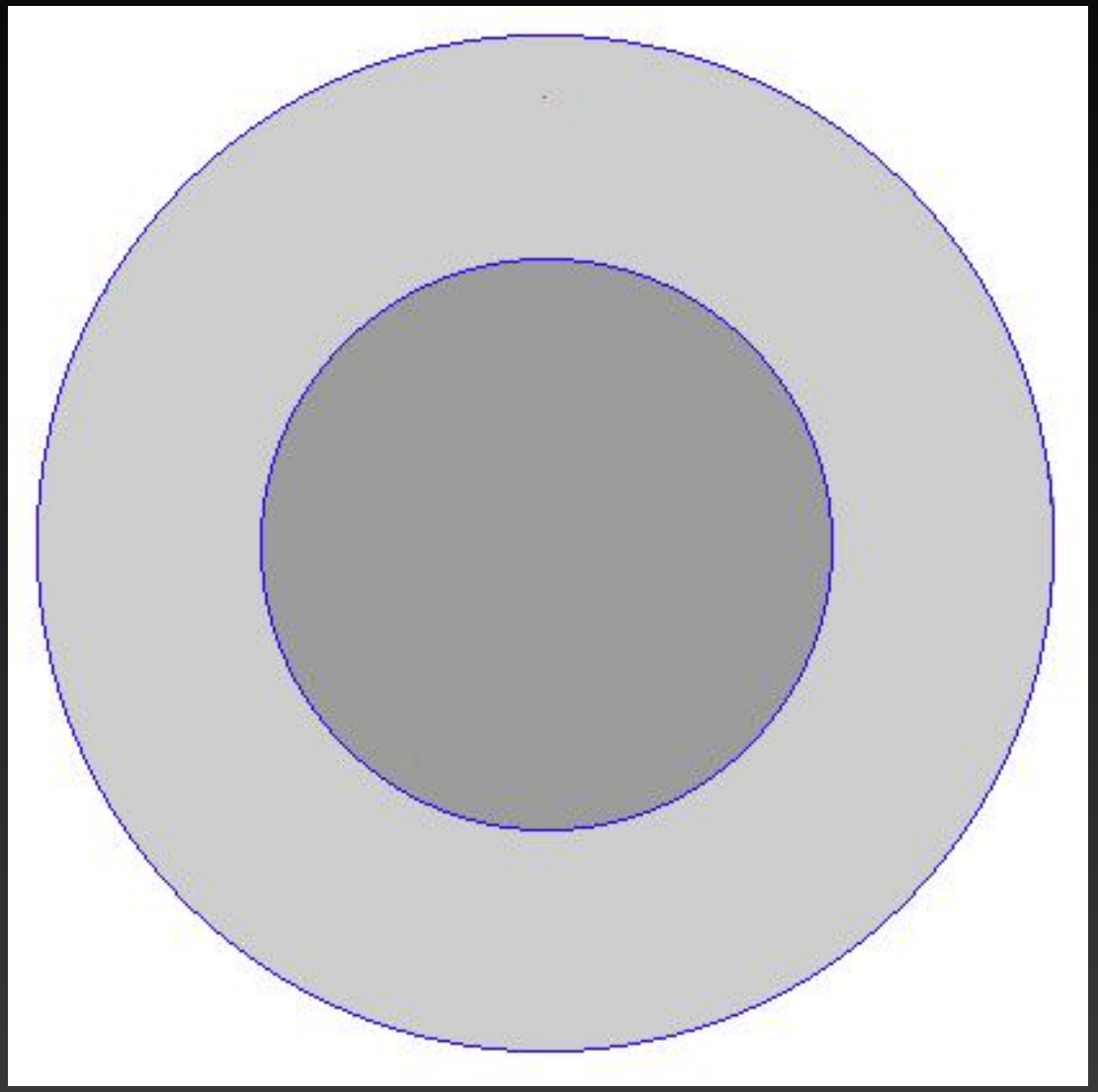
Seismic waves can travel across the entire Earth!

The seismic waves generated after a major earthquake can easily penetrate the Earth, so seismic waves contain information on their propagation paths and can be used for detecting the deep structures of the Earth.



Numerical simulation of P-wave propagation in Earth

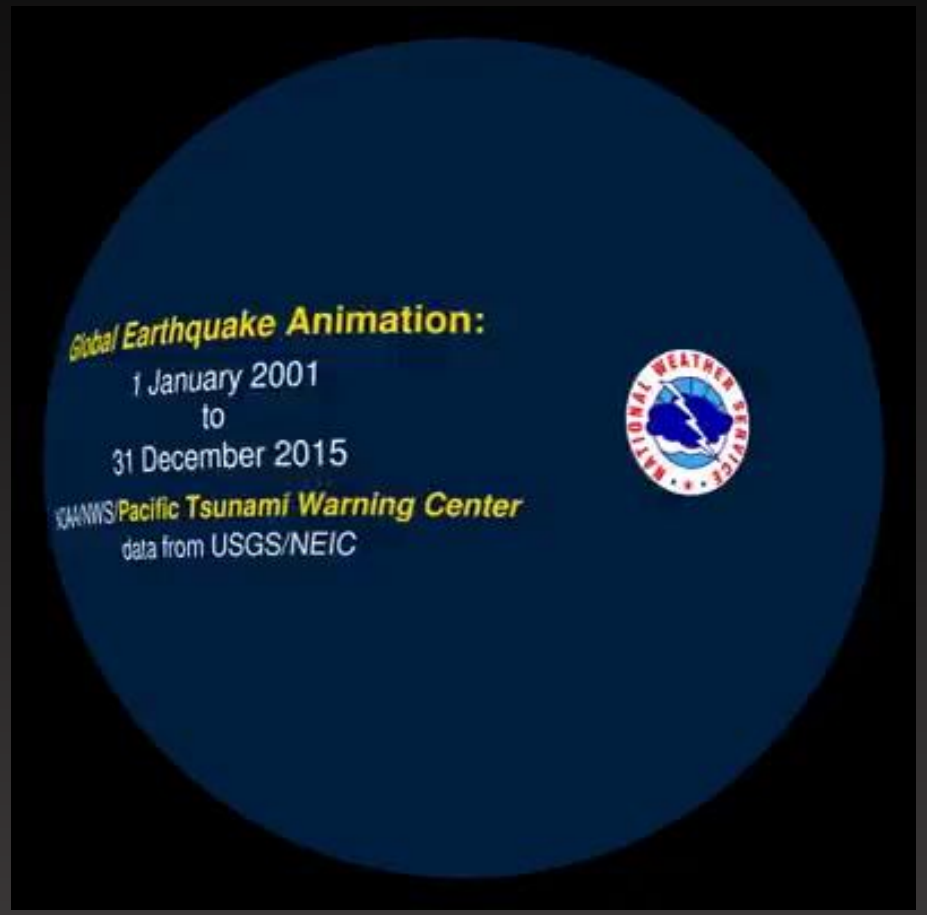


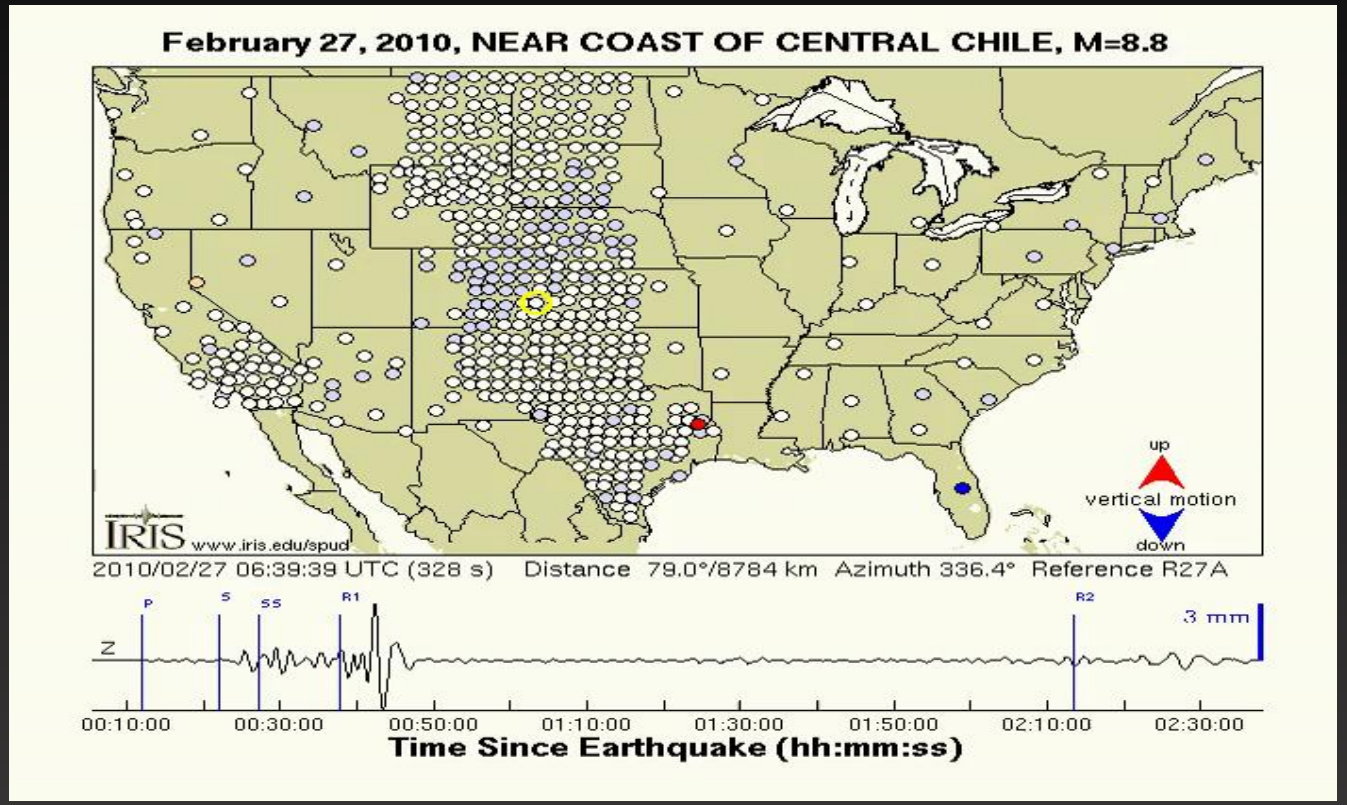


"Можно уподобить всякое землетрясение фонарю, который зажигается на короткое время и освещает нам внутренность Земли, позволяя тем самым рассмотреть то, что там происходит. Свет этого фонаря пока еще очень тусклый, но не подлежит сомнению, что со временем он станет гораздо ярче и позволит нам разобраться в этих сложных явлениях природы.

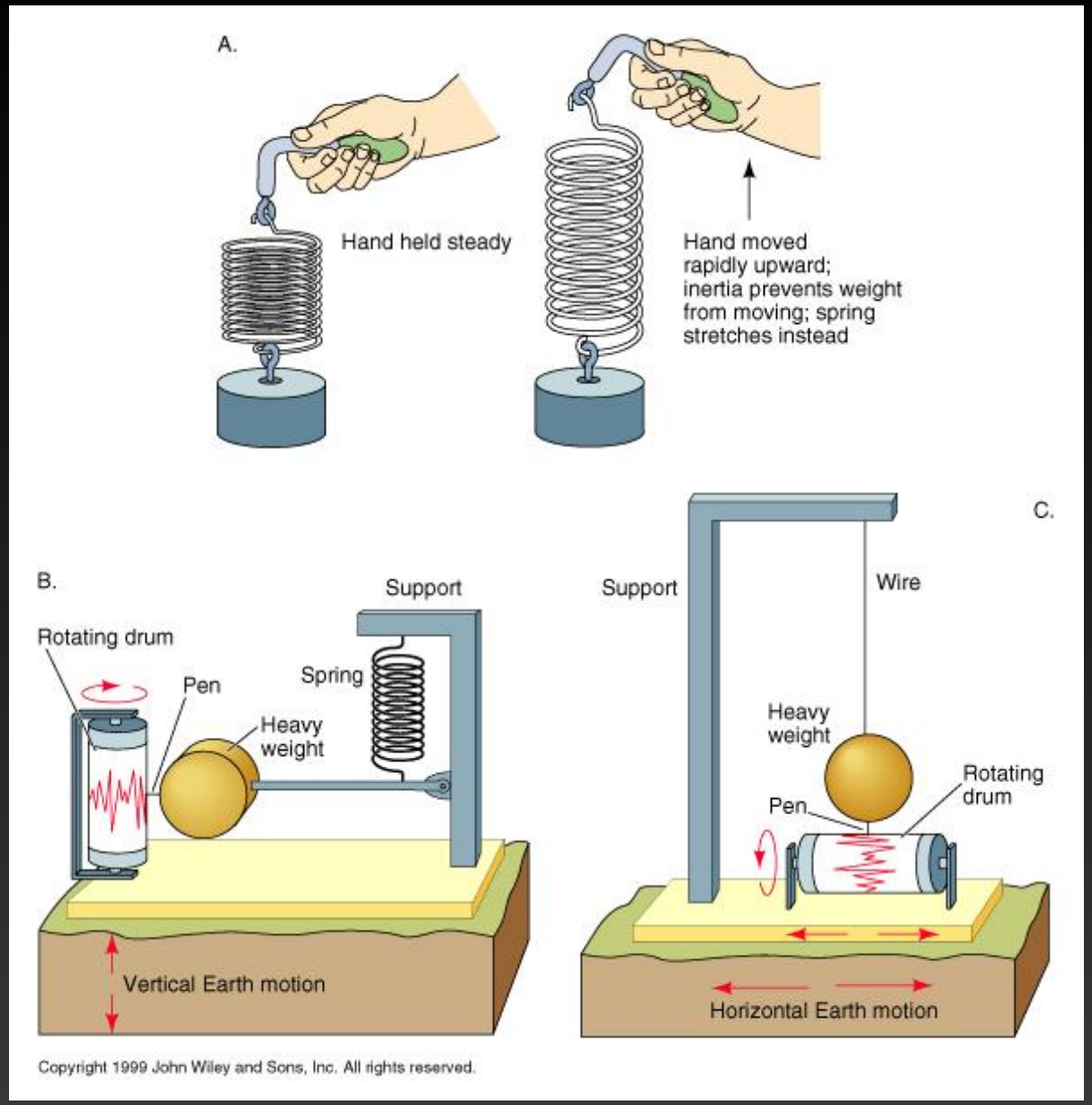
Russian seismologist Galitsyn

"Every earthquake can be likened to a lantern that **is lit for a short time and illuminates the interior of the Earth**, thereby helping us to examine what is happening there.The light of this lantern is still very dim, but there is no doubt that in time it will become much brighter and allow us to understand these complex natural phenomena." **Russian seismologist Galitsyn**



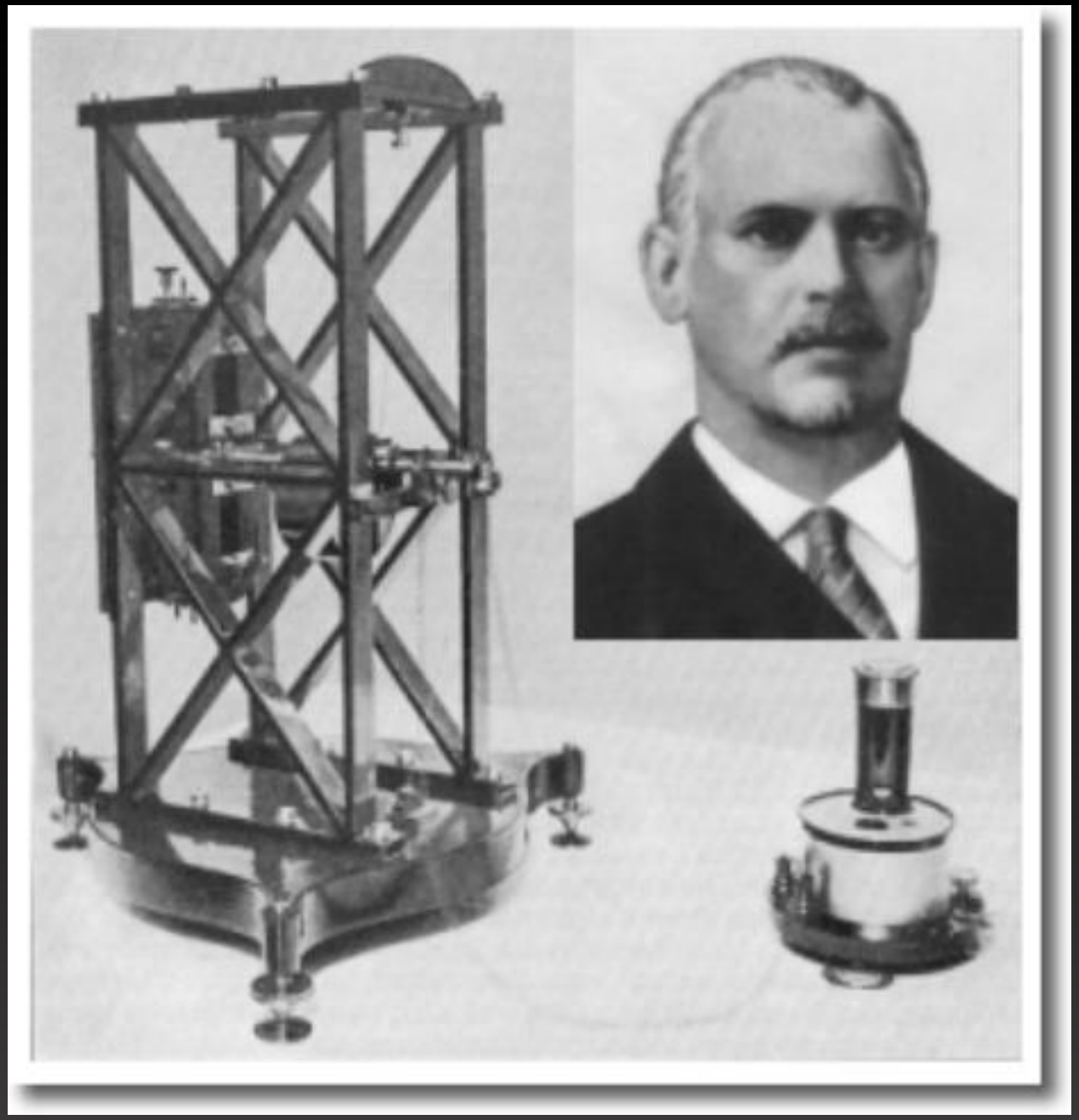


Modern seismograph





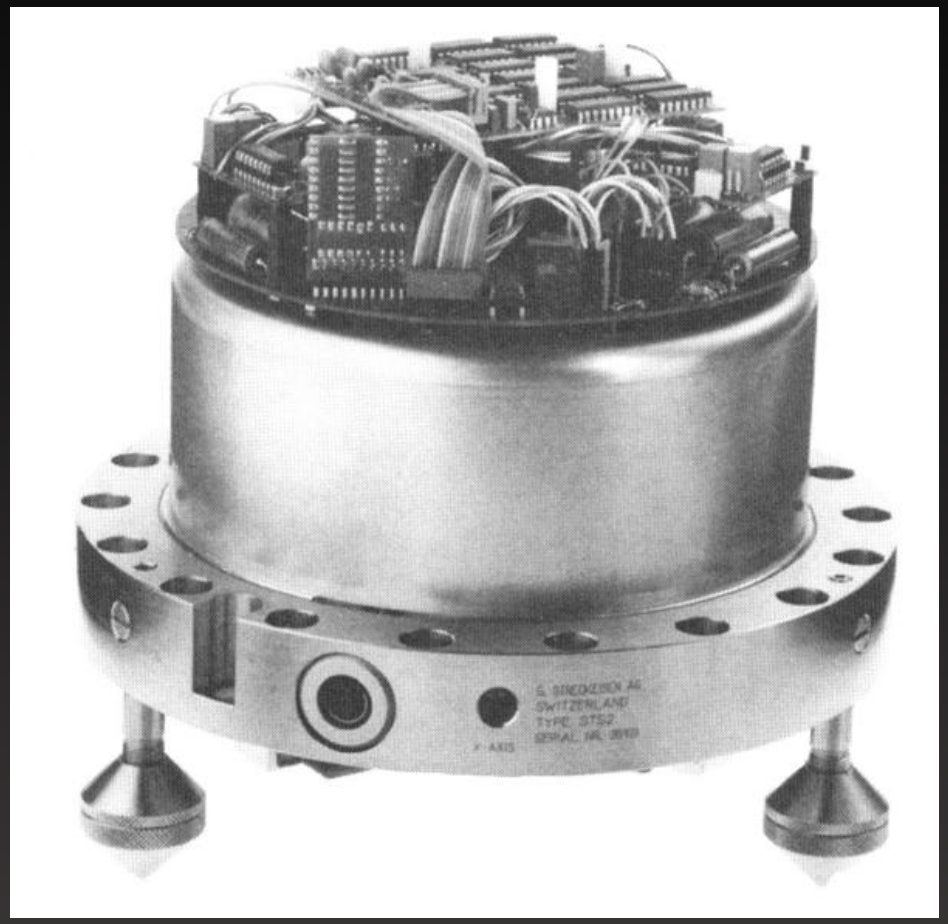
Horizontal 1000 kg Wiechert seismograph in Zagreb (built in 1909)



Electromagnetic seismometer

- The first seismometer that use a electromagnetic transducer to sense ground motion was invented by Galitzin of Russia in 1914.

STS-2 Seismometer

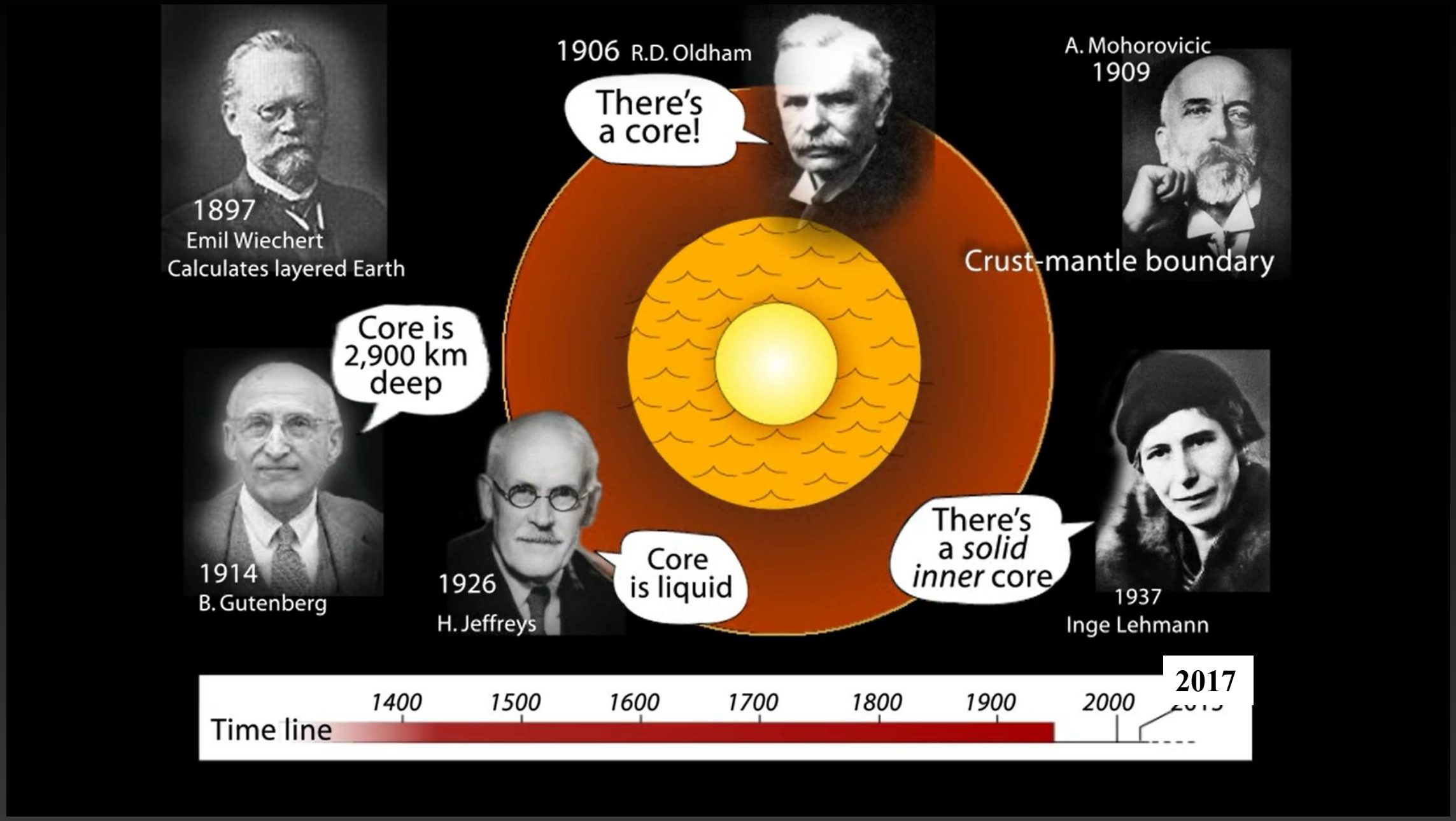




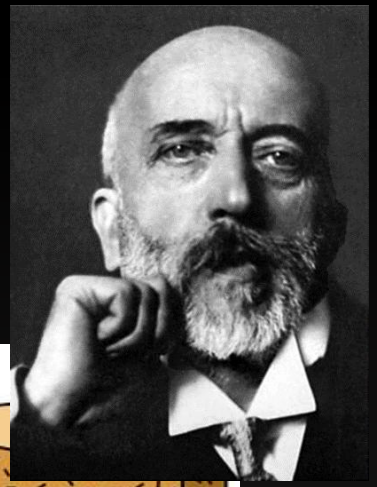


Meridian Compact PH

Outstanding contributor to the structure of the Earth's internal layers

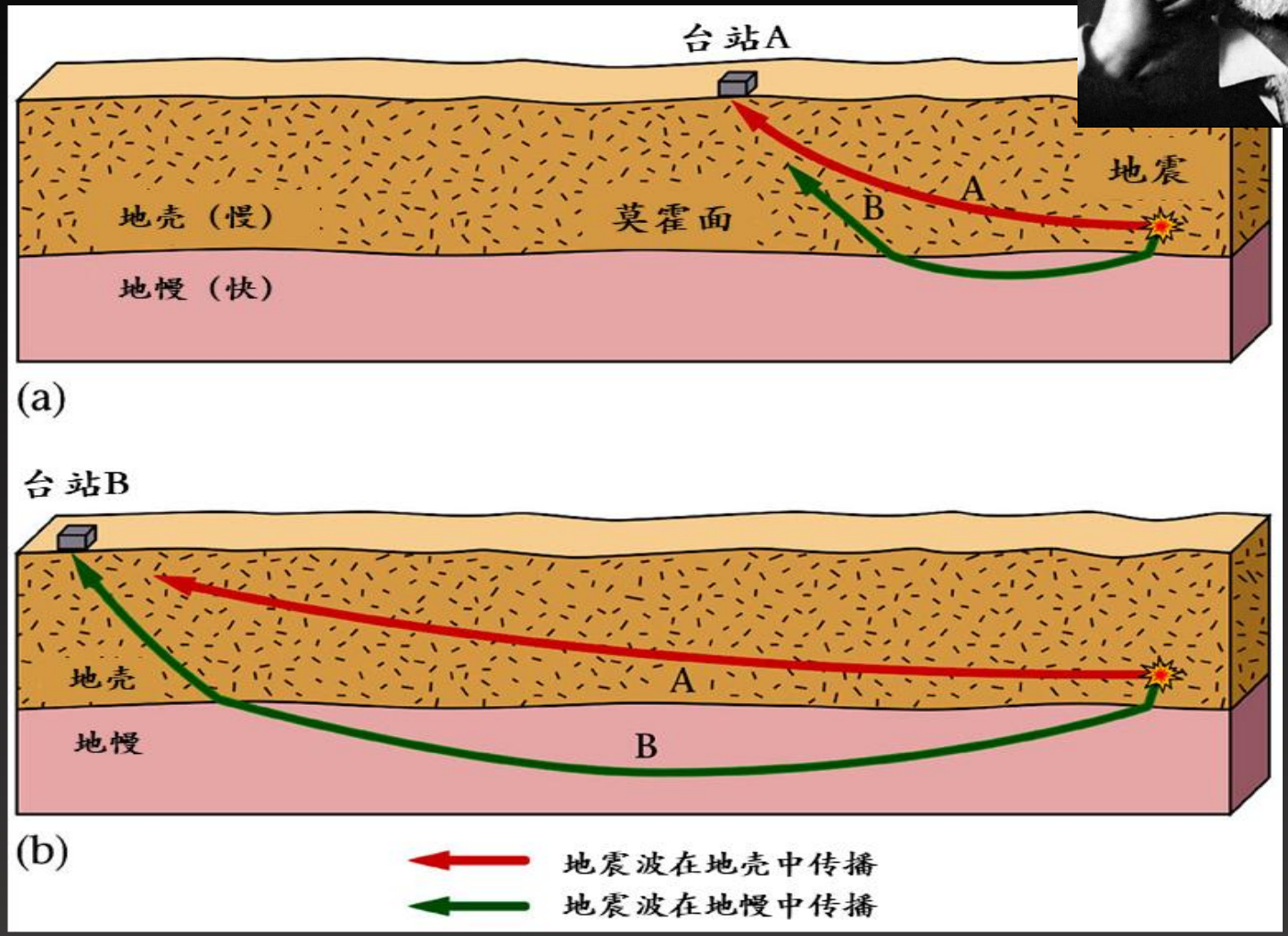


Discovery of the boundary between the crust and mantle

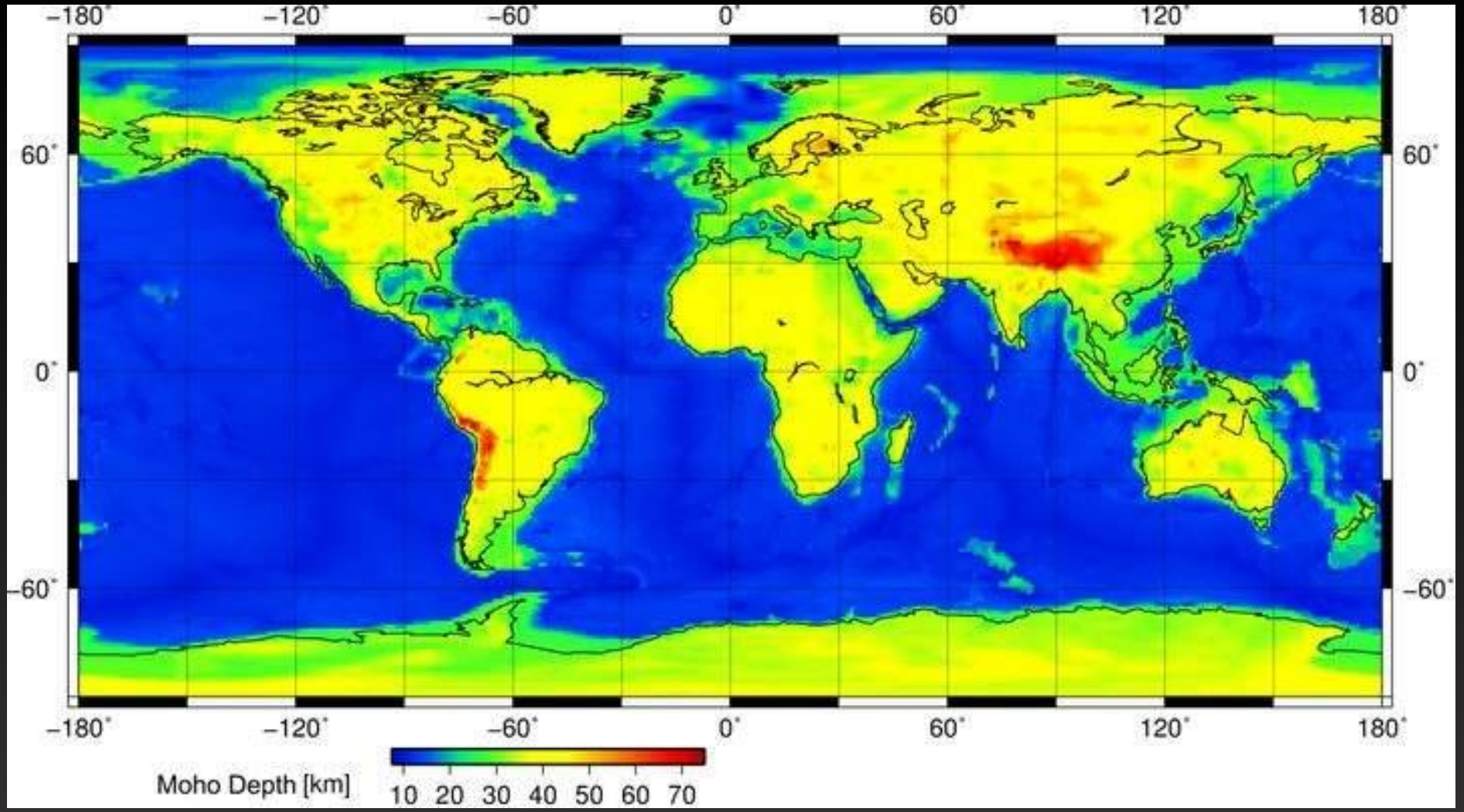


- In 1909, Andrija Mohorovi č i ć discovered that the average velocity of waves that first reached seismic stations within 200 kilometers of the epicenter was 6 kilometers per second. Station>200 kilometers away: average wave speed of 8 kilometers per second.
- To commemorate this discovery, the boundary between the Earth's crust and mantle is now known as the Moho discontinuity.

- **Vp:~7.0 km/s to ~8.1 km/s，Vs: ~4.2 km/s to ~ 4.4km/s.**

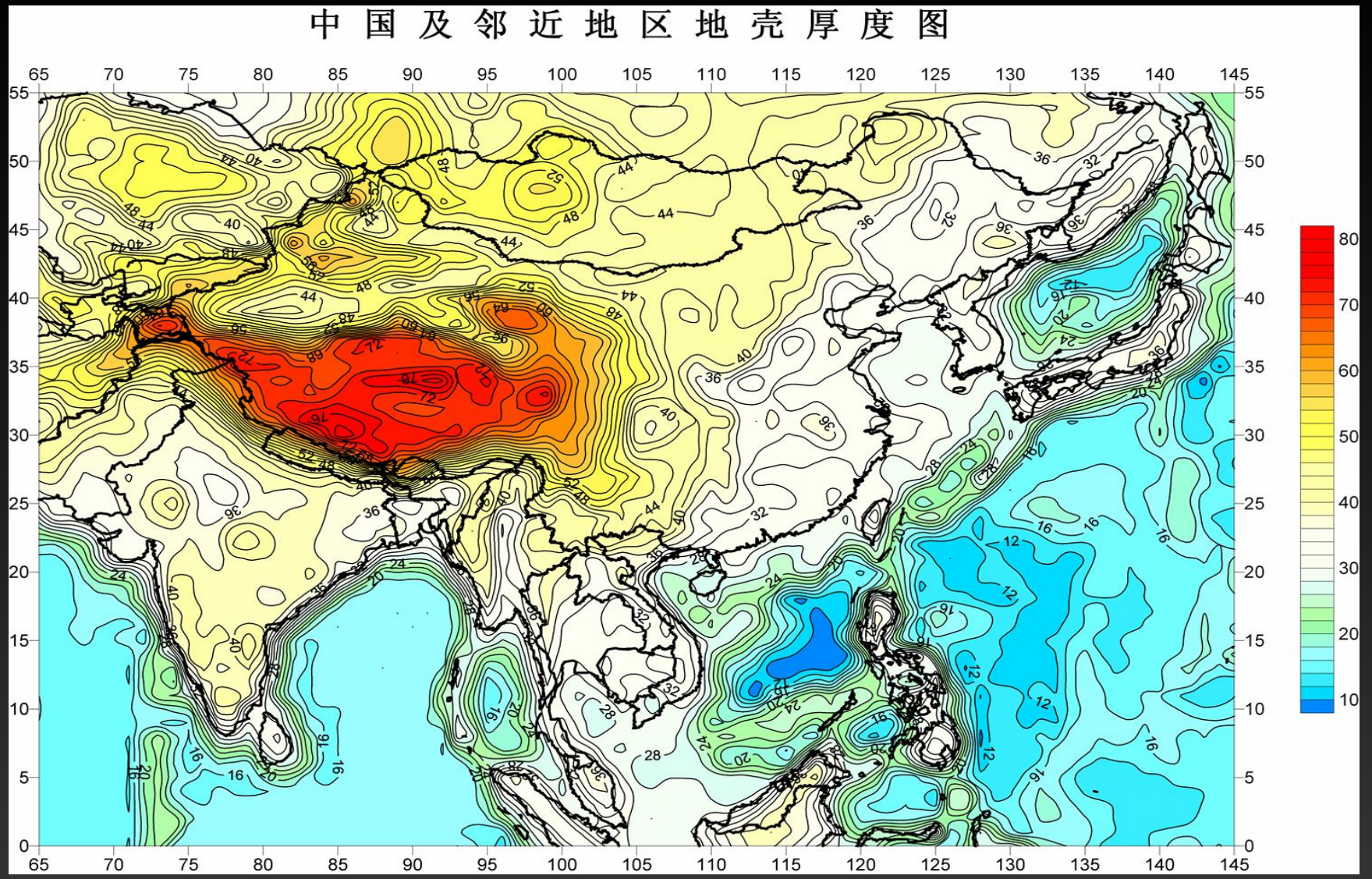


Global crustal thickness



The depth at which the Moho discontinuity appears is an average of 33 km globally and only 7 km beneath the ocean

Crustal thickness in China and neighboring regions



Where is the thickest crust in the world?

How were the boundaries between the mantle and the Earth's core, as well as the outer core, discovered?

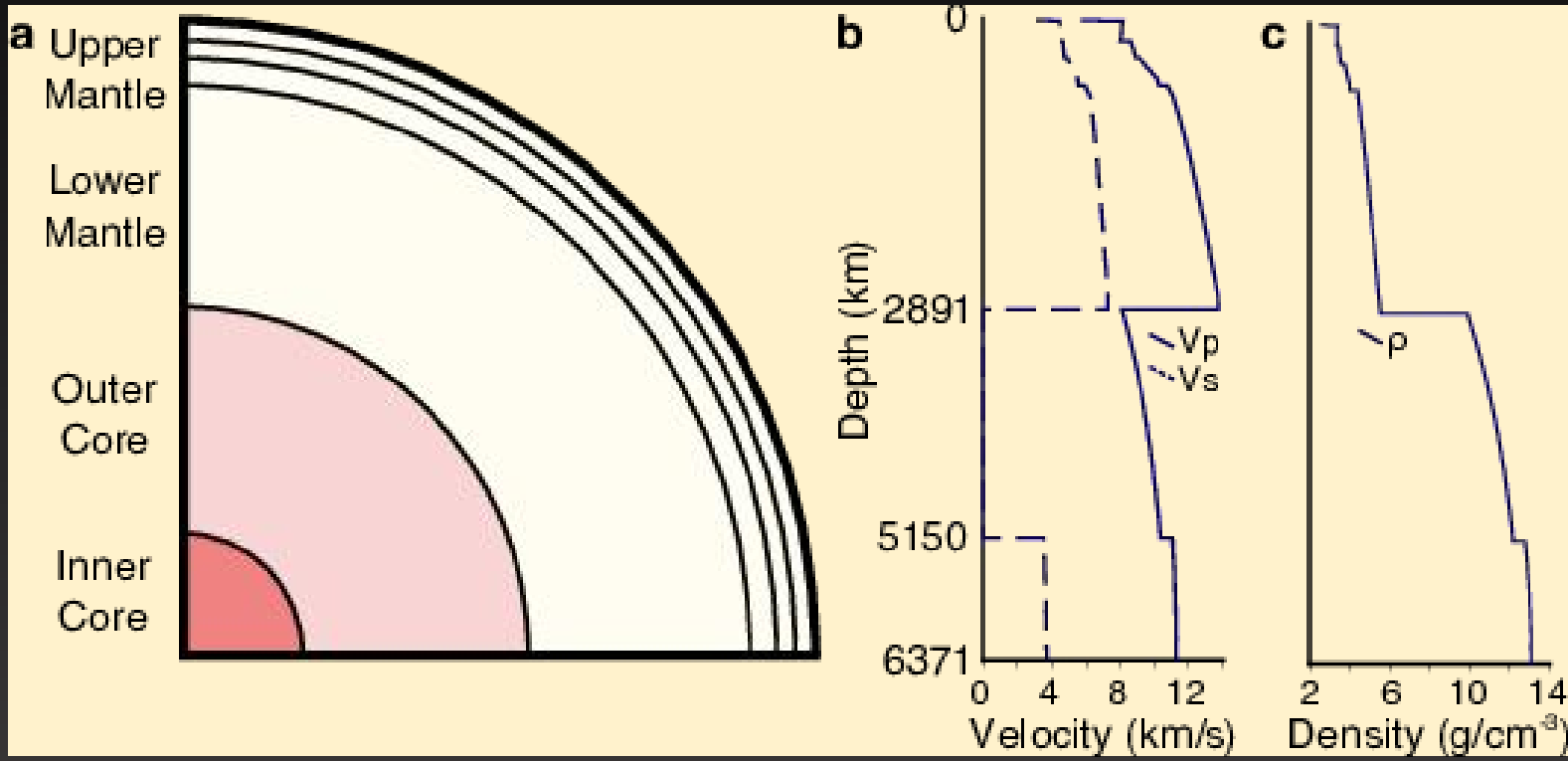


- **Gutenberg discontinuity**

➢ Discovered by German American scholar B. Gutenberg (1889-1960) in 1914;

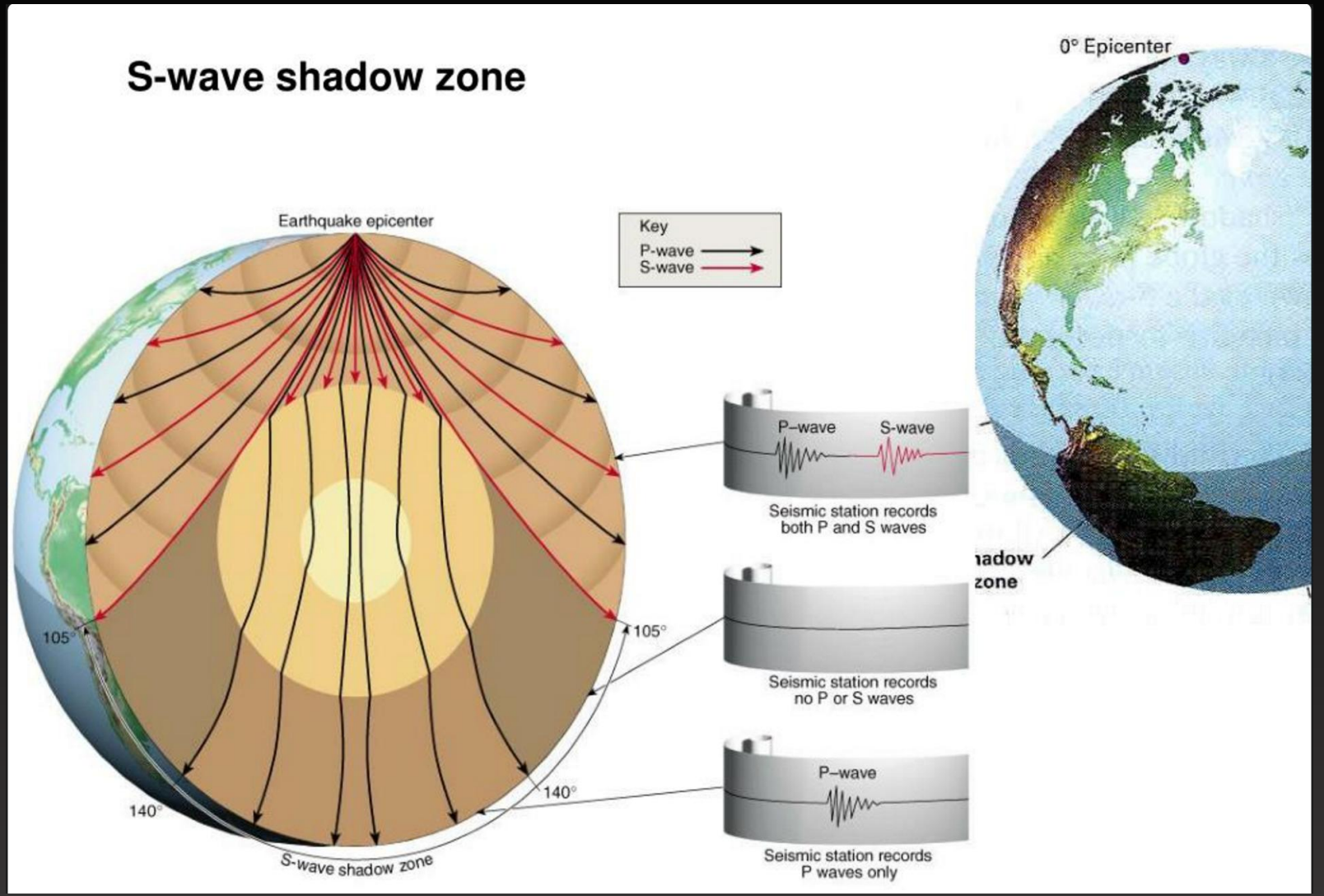
➢ Across this discontinuity, P- wave velocity drops abruptly from 13.6 km/s to 7.98 km/s; S- wave velocity (7.23 km/s above) vanishes abruptly.

➢ This interface is located at 2885 km depth. The zone below it extending to the Earth's center is the core.

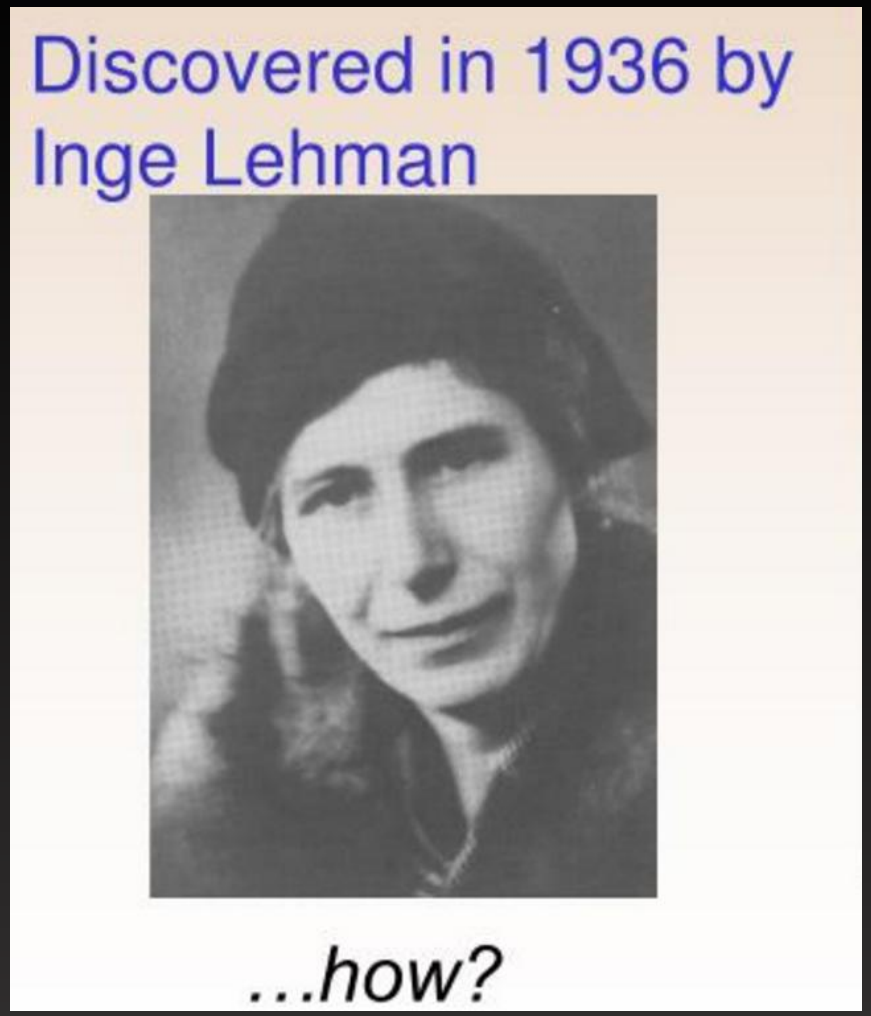


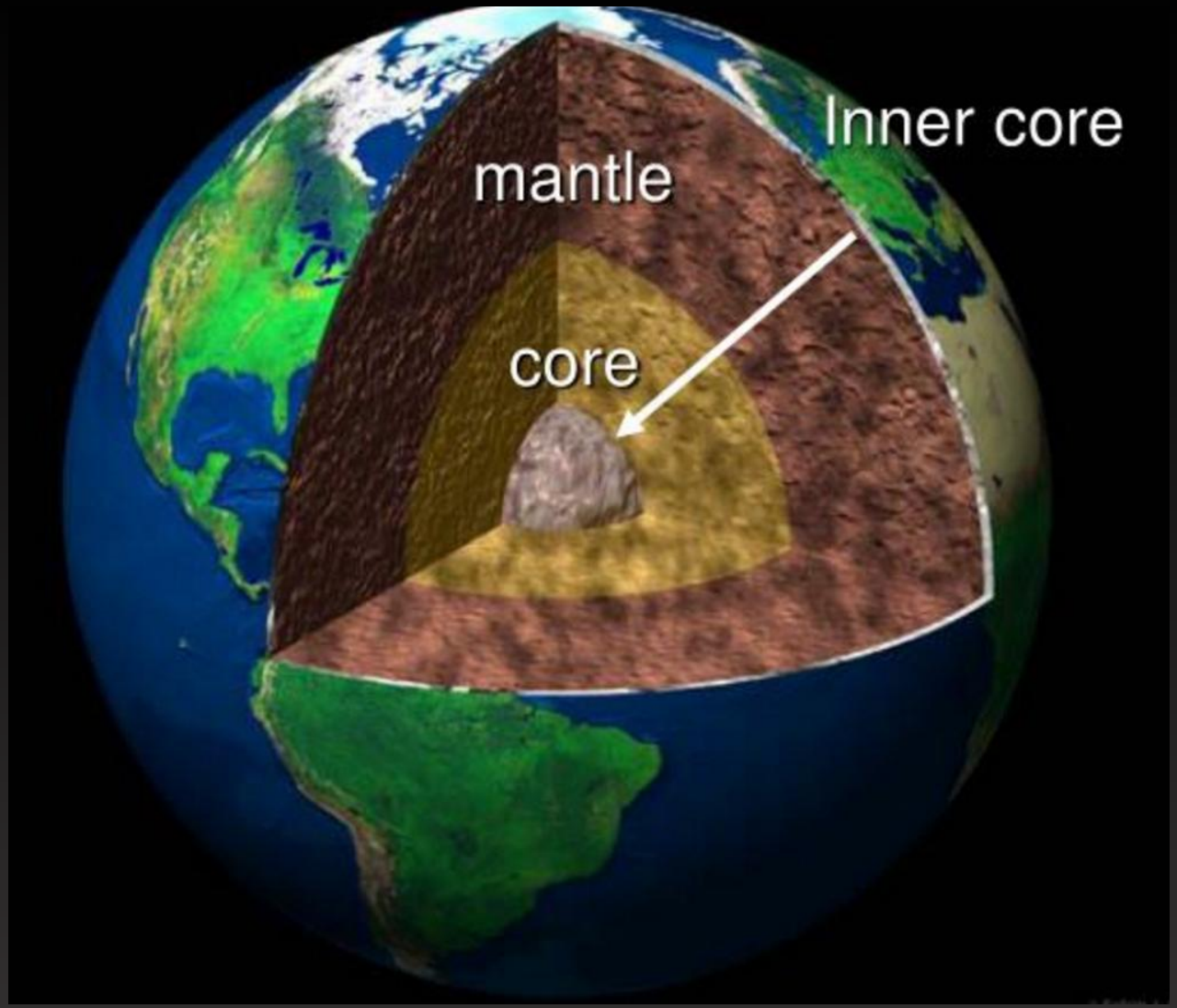
Seismic shadow caused by the low-velocity zone in the outer core

- In reality, direct P-waves do not arrive at all seismic stations worldwide. The P-wave **shadow zone spans the angular range of 103° to 143°**.
- This can be easily explained by deep seismic velocity discontinuities. This is due to the existence of the liquid outer core.



solid inner core

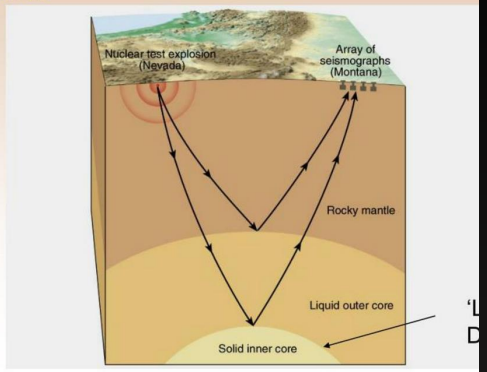


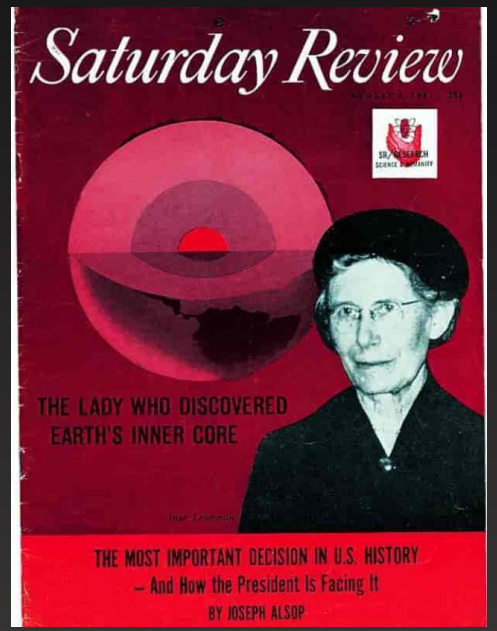


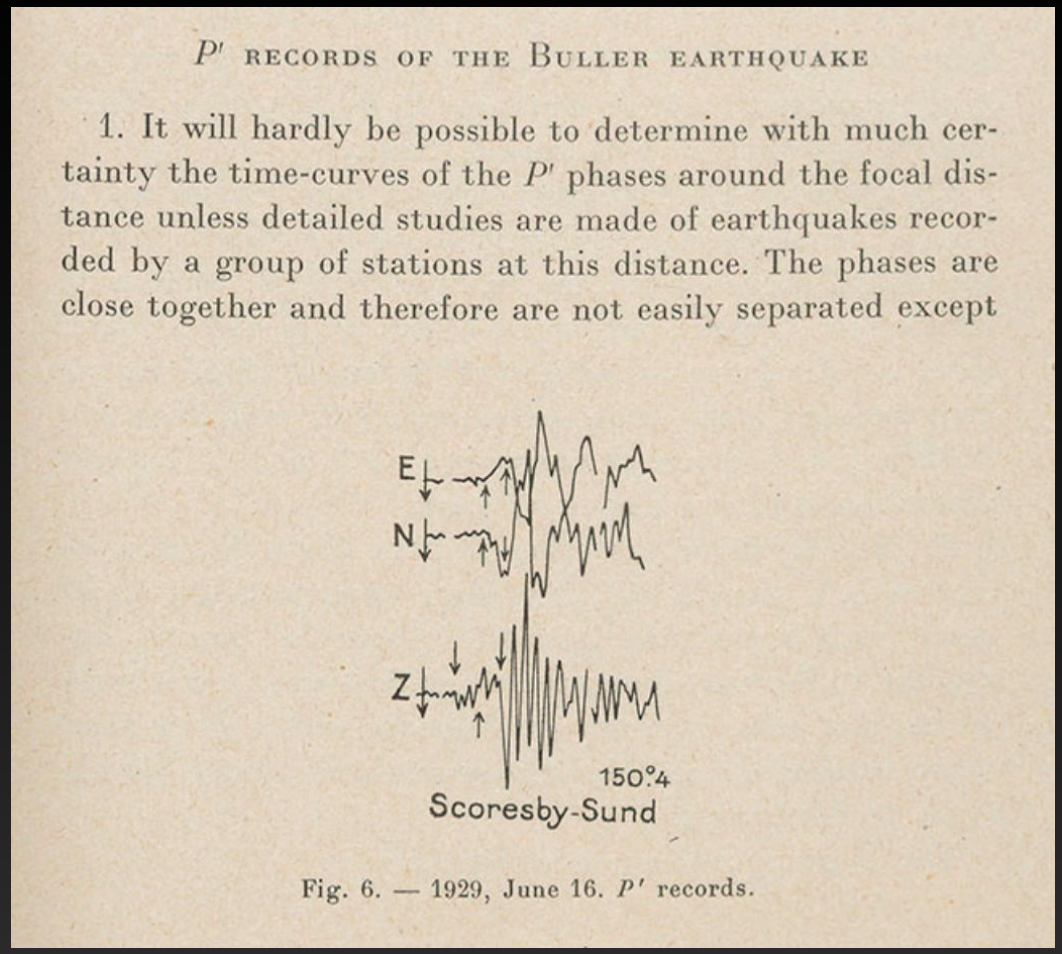
- Inge Lehmann, the distinguished Danish seismologist, discovered the inner core. She lived to be 105 years old, the longest-lived seismologist.

solid inner core

She discovered reflections ('echoes') of seismic waves



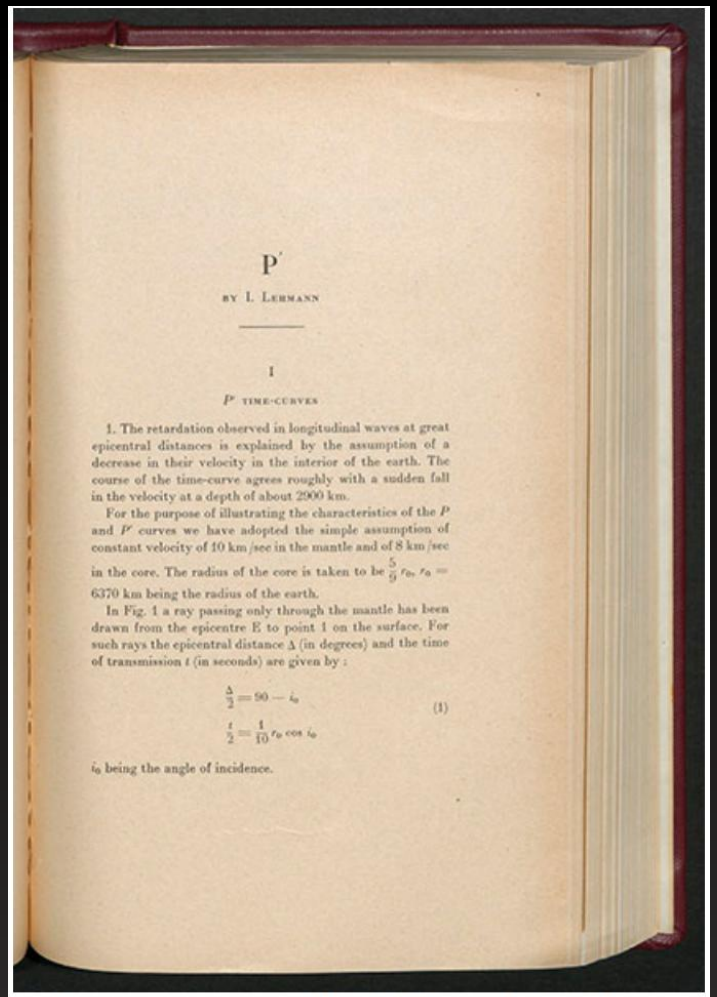




P′ RECORDS OF THE BULLER EARTHQUAKE

1. It will hardly be possible to determine with much certainty the time-curves of the P' phases around the focal distance unless detailed studies are made of earthquakes recorded by a group of stations at this distance. The phases are close together and therefore are not easily separated except

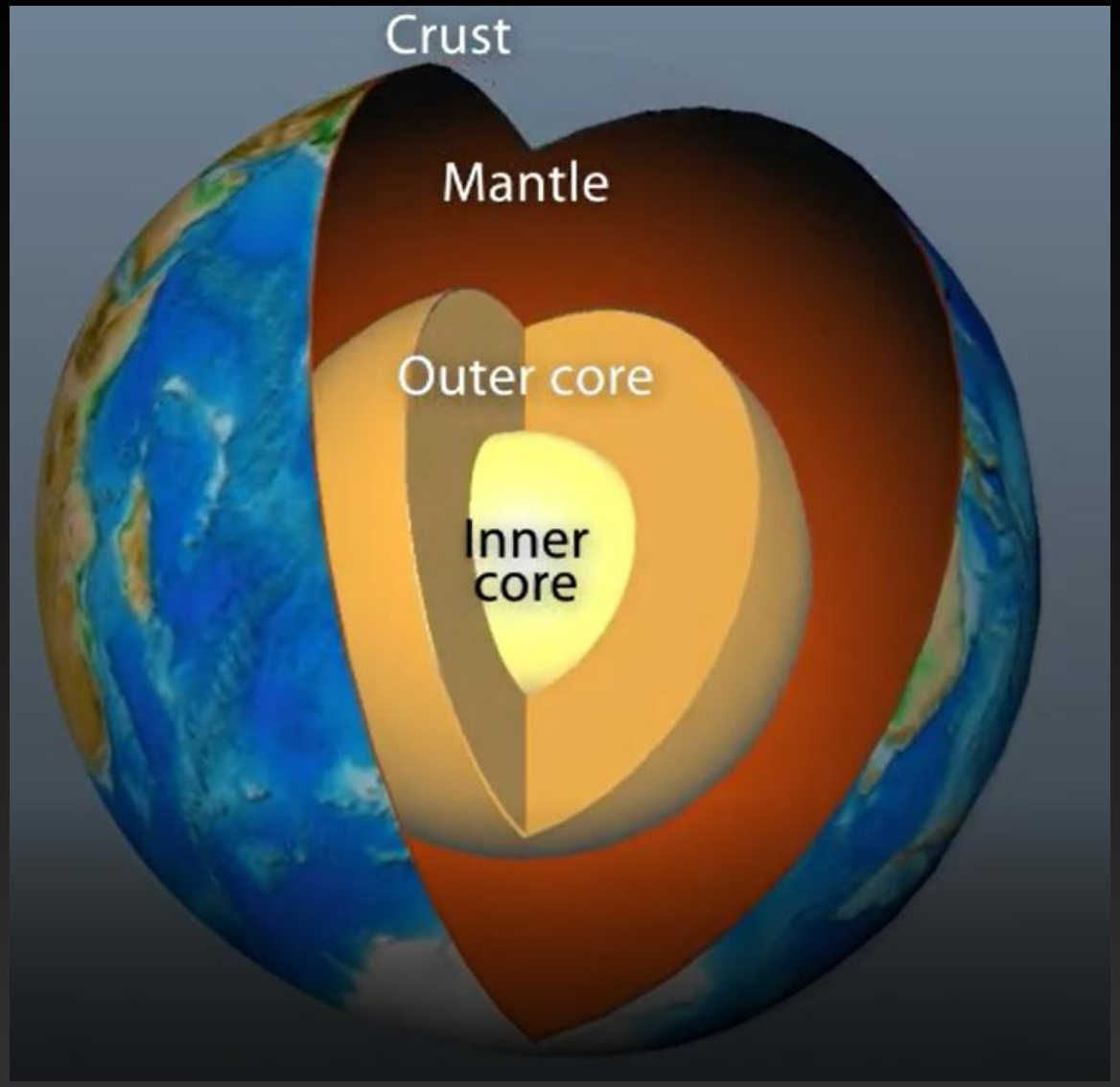
Fig. 6. — 1929, June 16. P' records.

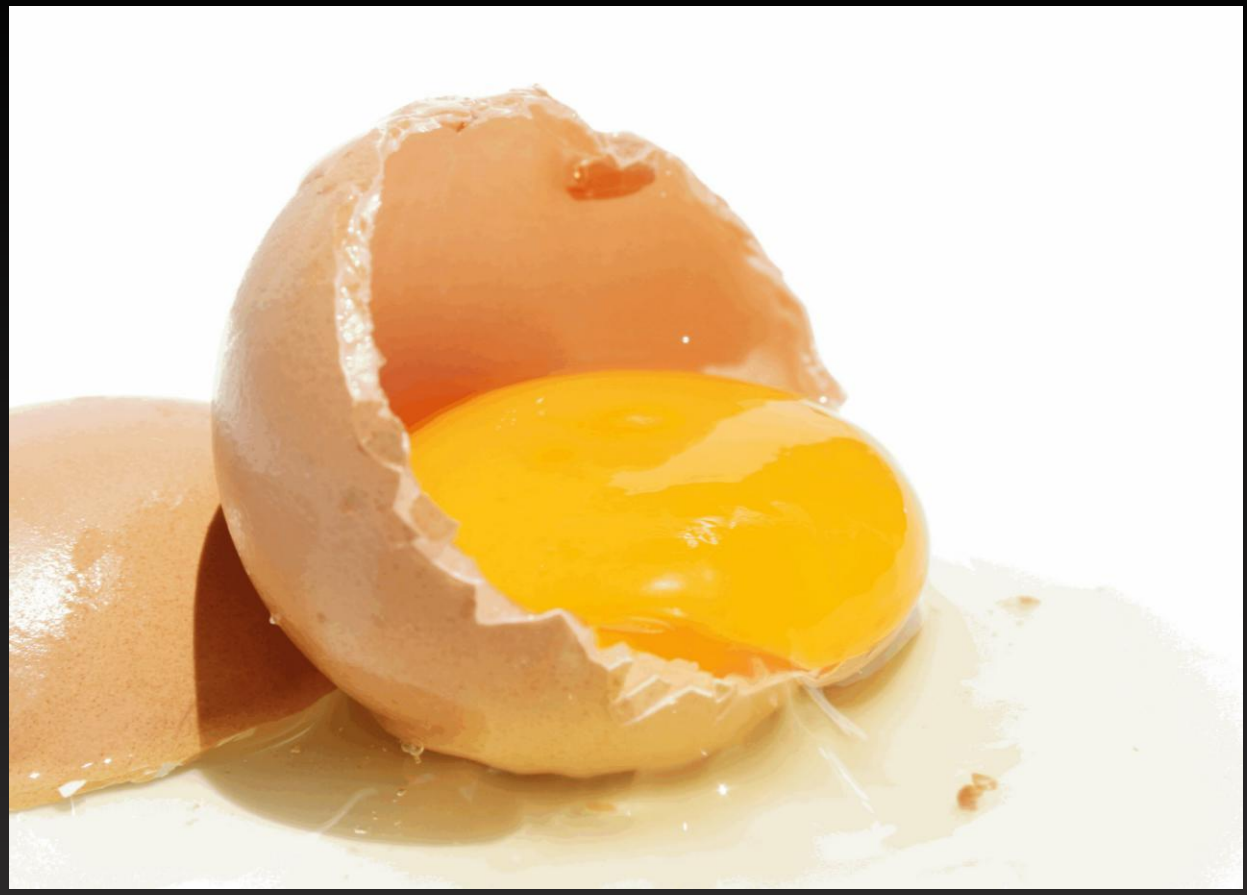


First page of Lehmann's article, " P′ ", *Publications du Bureau Central Séismologique*, 1936 (Linda Hall Library)

Analyzing waveforms from the great 1929 New Zealand earthquake, Inge Lehmann recognized the inner-core reflected phase and argued for a solid inner core. Her paper bears one of the shortest titles ever: **P′**.

Earth's Basic Layered Structure





◆Research history of the layered Earth

◆Secondary discontinuities within the Earth's interior

◆3D Earth

- Lithosphere–asthenosphere boundary（LAB）
- Upper mantle discontinuities（‘410’ and ‘660’）
- D”
- …

What is the lithosphere?

岩石圈
Lithosphere

软流圈
Asthenosphere



The lithosphere is the mobile plate in plate tectonics. The basic plate-tectonic model describes buoyant lithosphere floating over the asthenosphere.

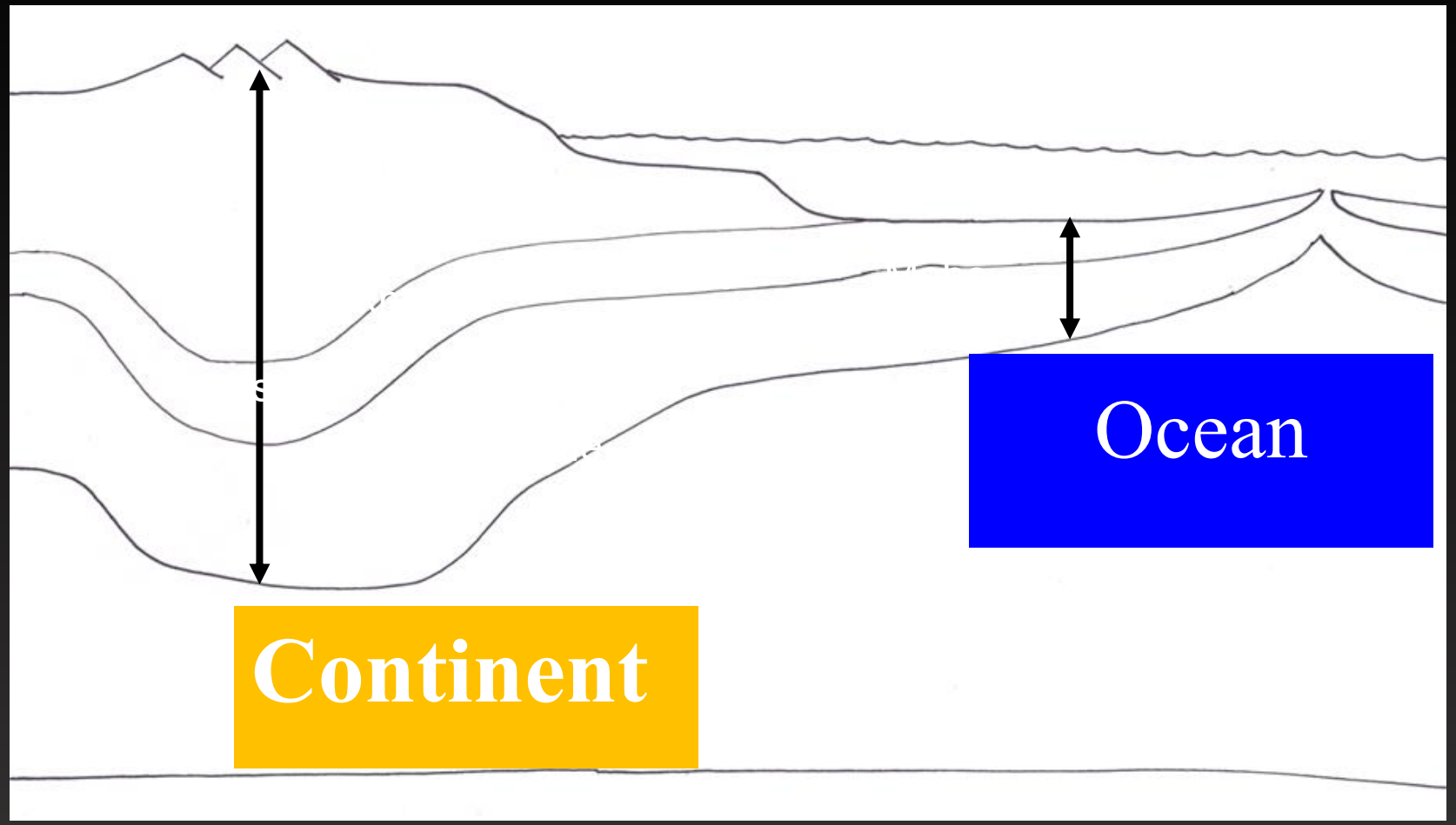
岩石圈/Lithosphere

- the Earth's outermost layer
- the crust and a portion of the upper mantle
- High mechanical strength.
- Brittle
- Cold (< 1300°C)
- High velocity

软流圈/Asthenosphere

- Beneath the lithosphere
- It is part of the mantle
- Low mechanical strength
- Visco- plastic
- Hot (>1300°C)
- Low velocity
- Partial melt (<0.5%)

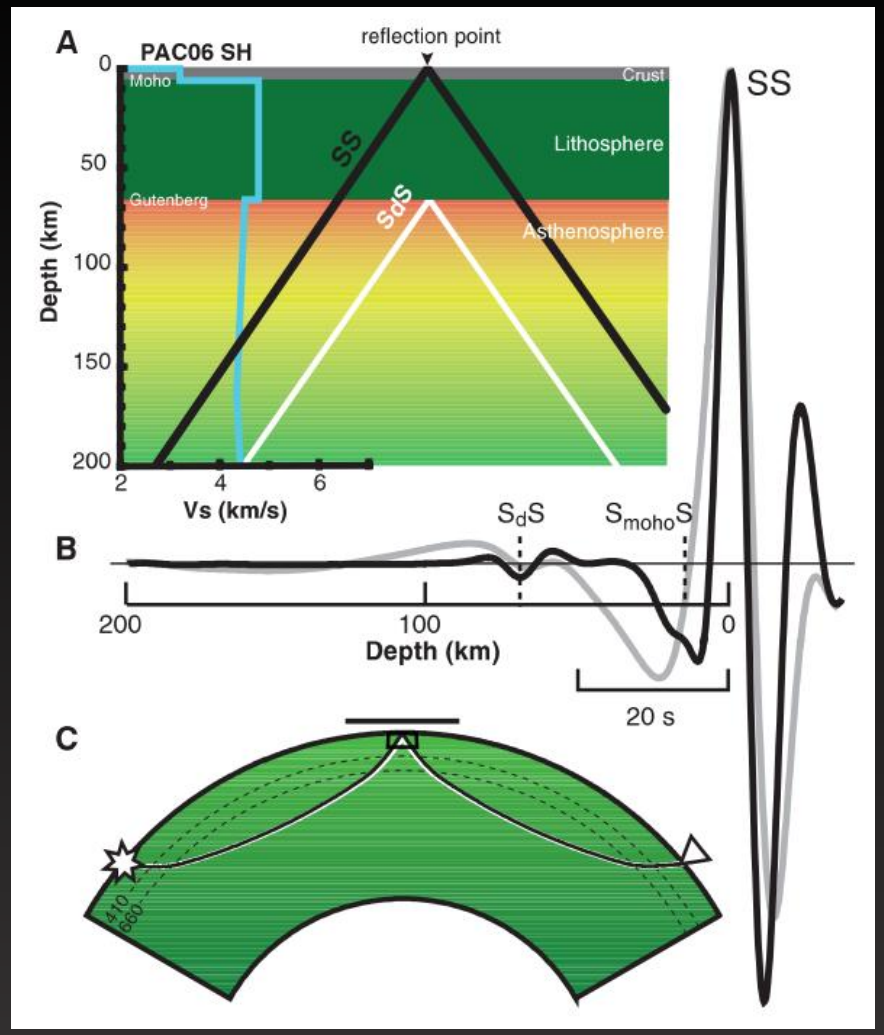
Stratification of Oceanic and Continental Lithosphere

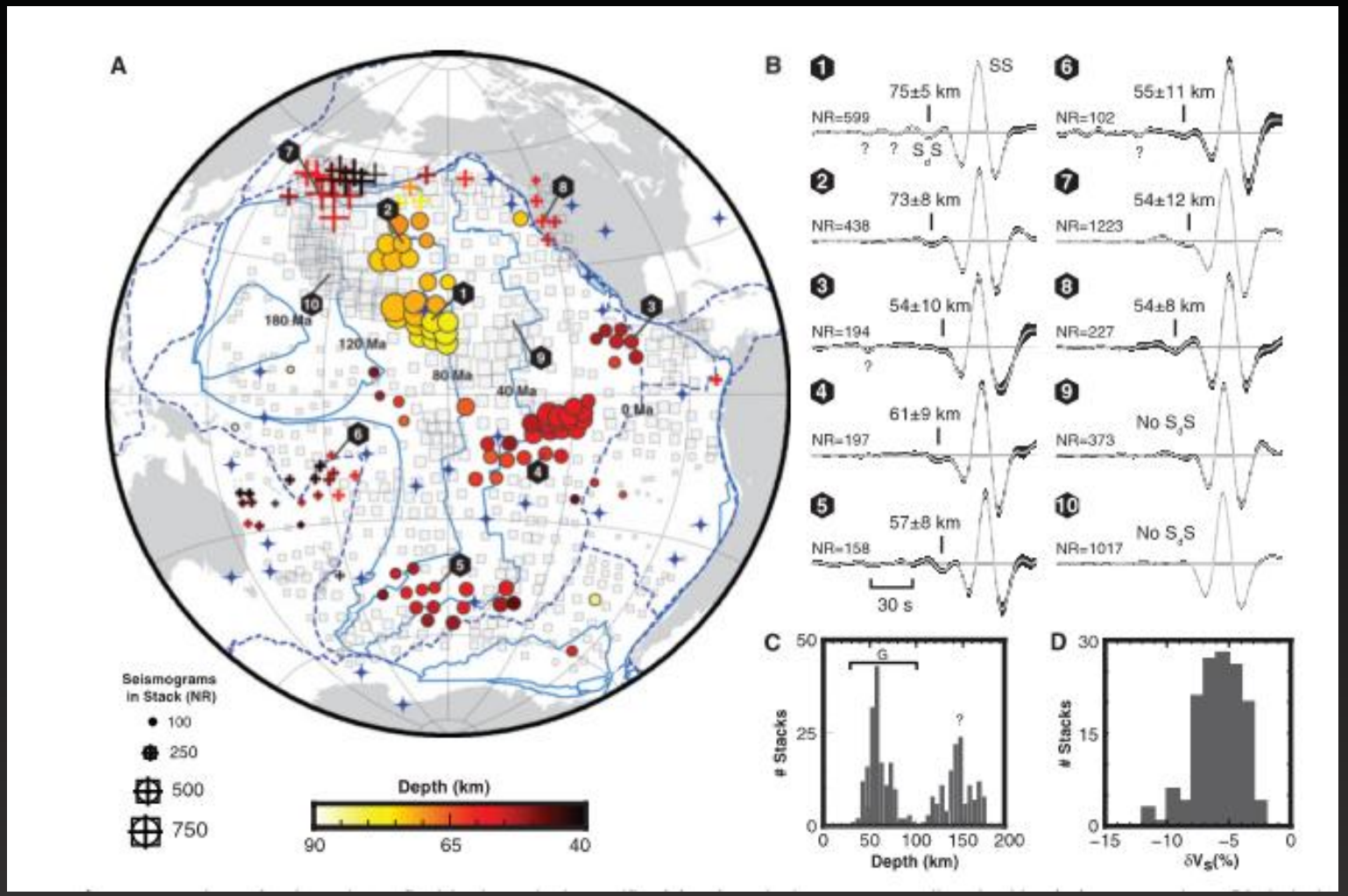


Mantle

Seismic lithosphere

Schmerr, 2012@Science





- Defined by seismic wave velocities, it refers to the high-velocity lid overlying the low-velocity asthenosphere.

Scientific implications of lithospheric thickness for lithospheric age and dynamic evolution

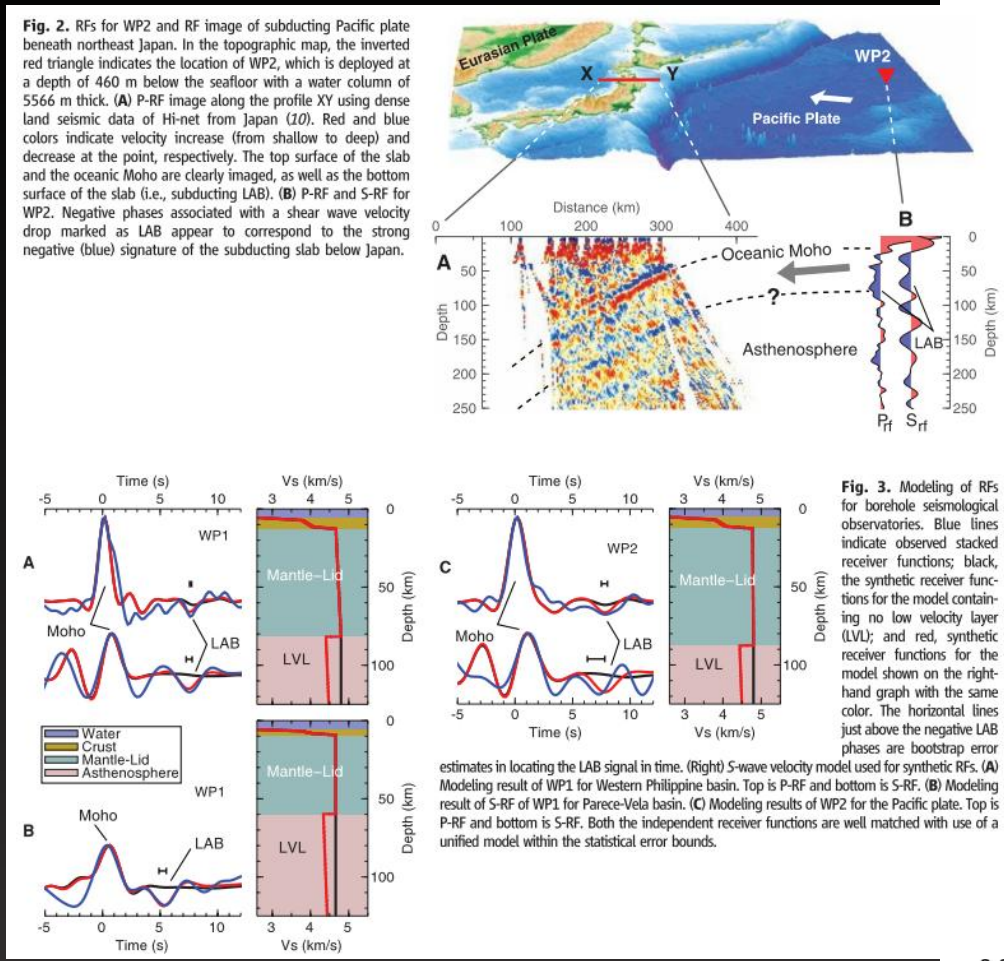
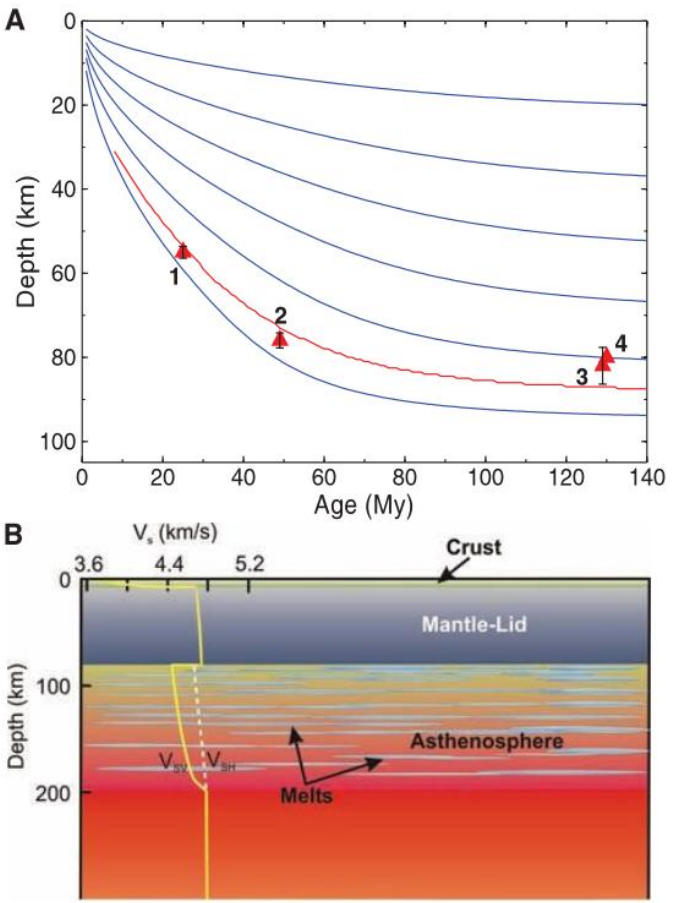


Fig. 2. RFs for WP2 and RF image of subducting Pacific plate beneath northeast Japan. In the topographic map, the inverted red triangle indicates the location of WP2, which is deployed at a depth of 460 m below the seafloor with a water column of 5566 m thick. (**A**) P-RF image along the profile XY using dense land seismic data of Hi-net from Japan (*10*). Red and blue colors indicate velocity increase (from shallow to deep) and decrease at the point, respectively. The top surface of the slab and the oceanic Moho are clearly imaged, as well as the bottom surface of the slab (i.e., subducting LAB). (**B**) P-RF and S-RF for WP2. Negative phases associated with a shear wave velocity drop marked as LAB appear to correspond to the strong negative (blue) signature of the subducting slab below Japan.

Fig. 3. Modeling of RFs for borehole seismological observatories. Blue lines indicate observed stacked receiver functions; black, the synthetic receiver functions for the model containing no low velocity layer (LVL); and red, synthetic receiver functions for the model shown on the right-hand graph with the same color. The horizontal lines just above the negative LAB phases are bootstrap error estimates in locating the LAB signal in time. (Right) *S*-wave velocity model used for synthetic RFs. (**A**) Modeling result of WP1 for Western Philippine basin. Top is P-RF and bottom is S-RF. (**B**) Modeling result of S-RF of WP1 for Parece-Vela basin. (**C**) Modeling results of WP2 for the Pacific plate. Top is P-RF and bottom is S-RF. Both the independent receiver functions are well matched with use of a unified model within the statistical error bounds.



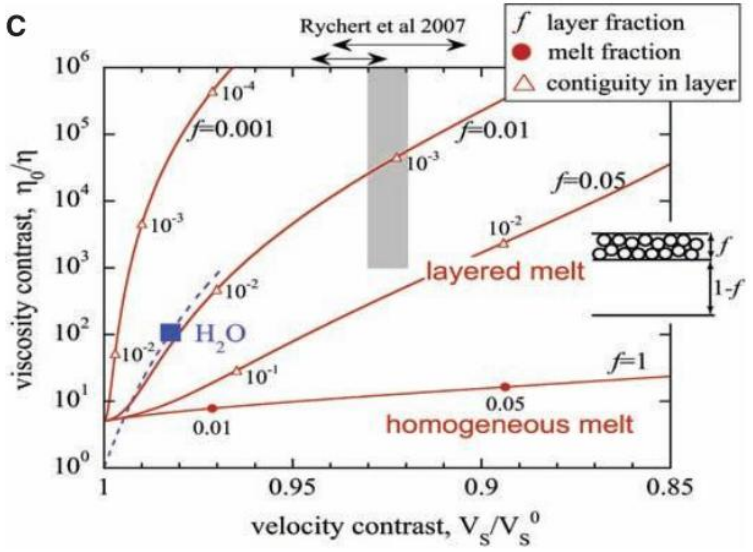


Fig. 4. Age dependence of observed LAB depths and a model for LAB and asthenosphere. (**A**) Observed LAB depths are plotted as a function of the plate age (red triangles; 1 indicates PVB; 2, WPB; 3, WP2; and 4, northeast Japan) over the isotherms given in a 200° intervals (blue lines) (*18*). Red line indicates the top of partial melting region calculated on the basis of the model of Mierdel *et al*. defined by the water solubility of 1000 parts per million H_2O (*16*). (**B**) A schematic illustration for the LAB and the asthenosphere. A schematic model for a *S*-wave seismic velocity structure of a radial anisotropy is superposed. (**C**) Viscosity (η) versus *S*-wave velocity (V_S) contrasts at LAB predicted from models of wet asthenosphere (bule) and partially molten asthenosphere (red), with seismological and geodynamical requirements (shaded) (*30*). Subscript 0 denotes lithospheric values. In the partially molten asthenosphere model, horizontal melt-rich layers are embedded in meltless mantle with various layer fractions from $f = 1$ (homogeneous) to $f = 0.001$. For $f = 1$ (homogeneous), melt has equilibrium geometry with variable melt fraction ϕ. For $f < 1$ (layered), ϕ in layers is close to the disaggregation melt fraction ϕ_c, and contiguity φ of grain-to-grain contact is small and variable [$\varphi = 1$ means melt-free and $\varphi = 0$ means disaggregation (*19*, *25*)]. Average ϕ in asthenosphere is given by $f\phi_c$.

Determination of lithospheric age from lithospheric thickness variations in the Western Pacific subduction zone

Kawakatsu et al., 2009@Science

Lithosphere–Asthenosphere System (LAS)

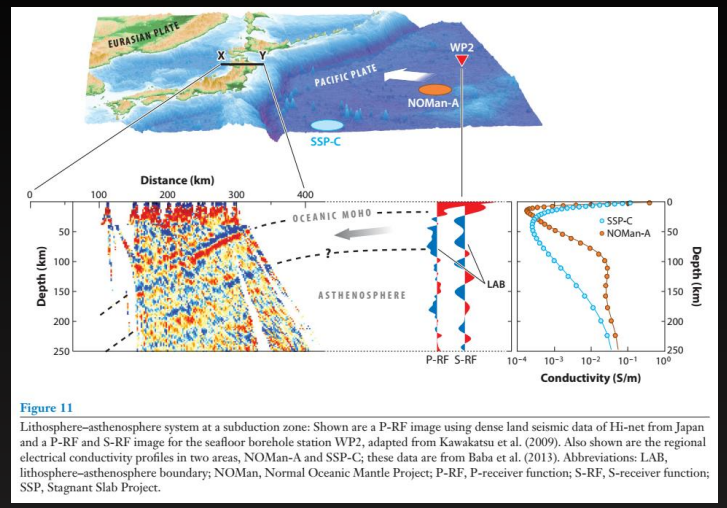


Figure 11

Lithosphere–asthenosphere system at a subduction zone: Shown are a P-RF image using dense land seismic data of Hi-net from Japan and a P-RF and S-RF image for the seafloor borehole station WP2, adapted from Kawakatsu et al. (2009). Also shown are the regional electrical conductivity profiles in two areas, NOMan-A and SSP-C; these data are from Baba et al. (2013). Abbreviations: LAB, lithosphere–asthenosphere boundary; NOMan, Normal Oceanic Mantle Project; P-RF, P-receiver function; S-RF, S-receiver function; SSP, Stagnant Slab Project.

RF

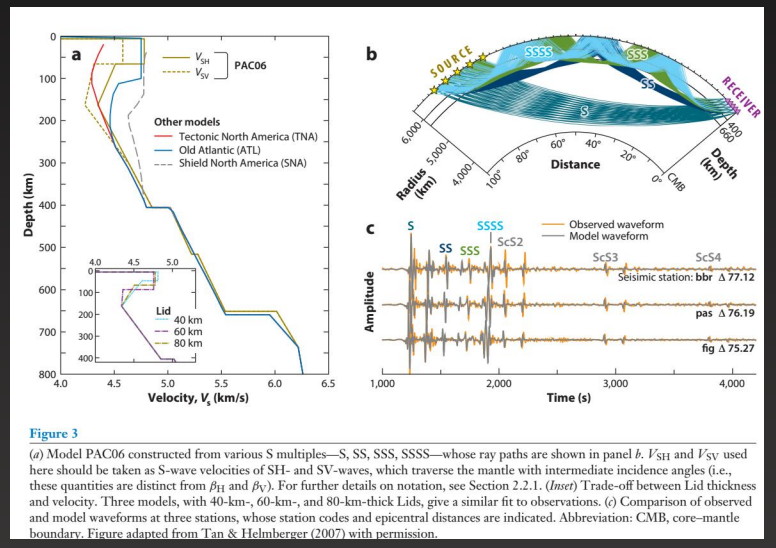


Figure 3

(*a*) Model PAC06 constructed from various S multiples—S, SS, SSS, SSSS—whose ray paths are shown in panel *b*. V_{SH} and V_{SV} used here should be taken as S-wave velocities of SH- and SV-waves, which traverse the mantle with intermediate incidence angles (i.e., these quantities are distinct from β_H and β_V). For further details on notation, see Section 2.2.1. (*Inset*) Trade-off between Lid thickness and velocity. Three models, with 40-km-, 60-km-, and 80-km-thick Lids, give a similar fit to observations. (*c*) Comparison of observed and model waveforms at three stations, whose station codes and epicentral distances are indicated. Abbreviation: CMB, core–mantle boundary. Figure adapted from Tan & Helmberger (2007) with permission.

SS precursor

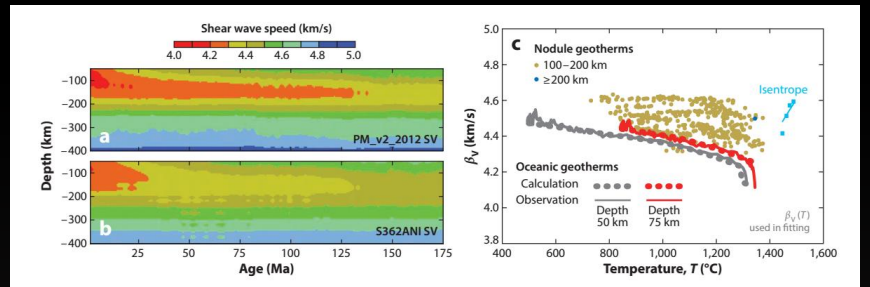


Figure 2

Shear wave (S-wave) velocity (β_V) profiles from tomographic models of the Pacific Ocean, stacked as functions of age. [Models are from (*a*) Priestley & McKenzie (2013), (*b*) Kustowski et al. (2008).] (*c*) β_V as a function of temperature estimated from panel *a*. The solid gray line shows the velocities at a depth of 50 km and the solid red line those at 75 km. All panels adapted from Priestley & McKenzie (2013) with permission.

Surface wave tomography

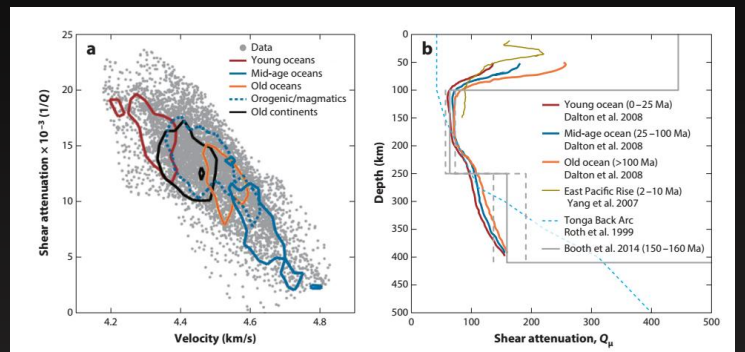


Figure 7

Seismic attenuation: (*a*) Scatter plot showing the shear velocity and shear attenuation values at a depth of 100 km. Panel *a* adapted from Dalton et al. (2009) with permission. (*b*) Shear attenuation model beneath old western Pacific seafloor (*solid gray line*; uncertainty ranges are denoted by *broken gray lines*) compared with other oceanic shear attenuation models. Panel *b* adapted from Booth et al. (2014) with permission.

Seismic attenuation

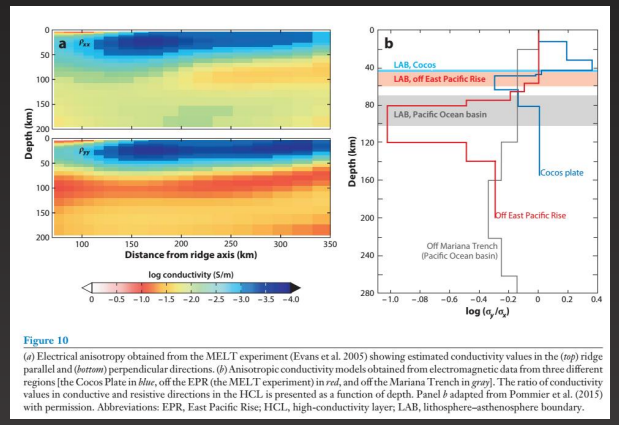


Figure 10

(*a*) Electrical anisotropy obtained from the MELT experiment (Evans et al. 2005) showing estimated conductivity values in the (*top*) ridge parallel and (*bottom*) perpendicular directions. (*b*) Anisotropic conductivity models obtained from electromagnetic data from three different regions [the Cocos Plate in *blue*, off the EPR (the MELT experiment) in *red*, and off the Mariana Trench in *gray*]. The ratio of conductivity values in conductive and resistive directions in the HCL is presented as a function of depth. Panel *b* adapted from Pommier et al. (2015) with permission. Abbreviations: EPR, East Pacific Rise; HCL, high-conductivity layer; LAB, lithosphere–asthenosphere boundary.

MT

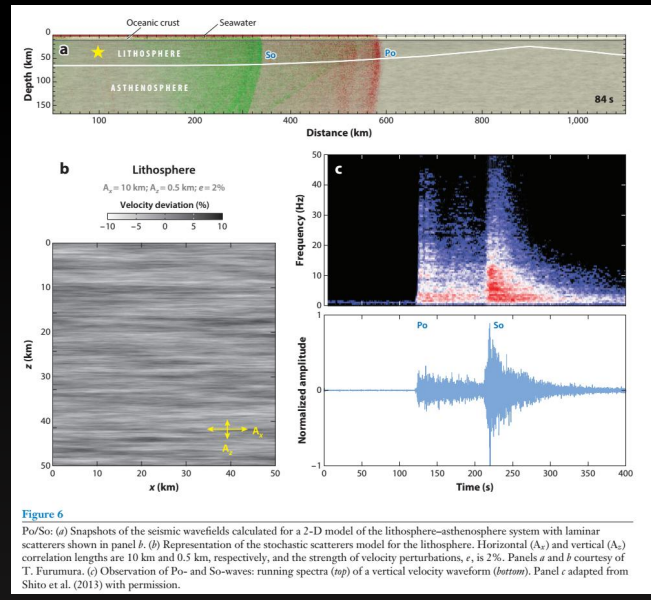


Figure 6

Po/So: (*a*) Snapshots of the seismic wavefields calculated for a 2-D model of the lithosphere–asthenosphere system with laminar scatterers shown in panel *b*. (*b*) Representation of the stochastic scatterers model for the lithosphere. Horizontal (A_x) and vertical (A_z) correlation lengths are 10 km and 0.5 km, respectively, and the strength of velocity perturbations, ϵ, is 2%. Panels *a* and *b* courtesy of T. Furumura. (*c*) Observation of Po- and So-waves: running spectra (*top*) of a vertical velocity waveform (*bottom*). Panel *c* adapted from Shito et al. (2013) with permission.

scattered wave

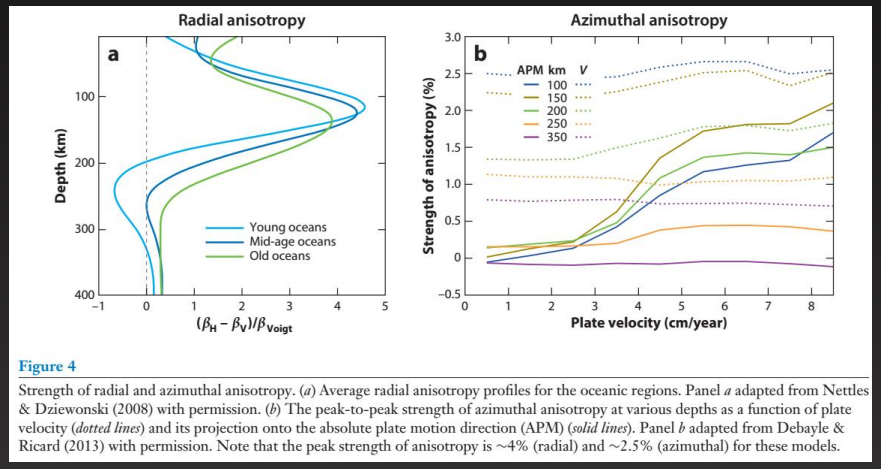
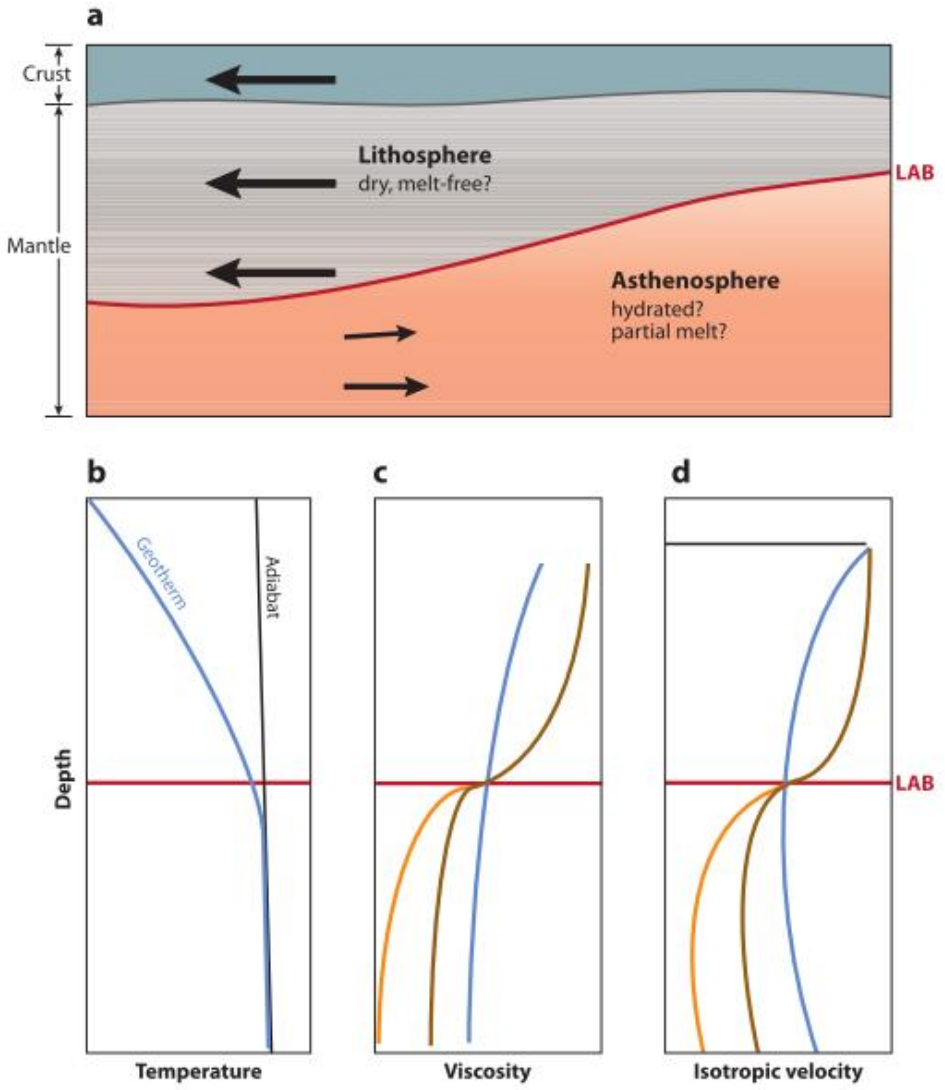


Figure 4

Strength of radial and azimuthal anisotropy. (*a*) Average radial anisotropy profiles for the oceanic regions. Panel *a* adapted from Nettles & Dziewonski (2008) with permission. (*b*) The peak-to-peak strength of azimuthal anisotropy at various depths as a function of plate velocity (*dotted lines*) and its projection onto the absolute plate motion direction (APM) (*solid lines*). Panel *b* adapted from Debayle & Ricard (2013) with permission. Note that the peak strength of anisotropy is ~4% (radial) and ~2.5% (azimuthal) for these models.

Seismic anisotropy

Kawakatsu and Utada,2017@Annu. Rev. Earth Planet. Sci.



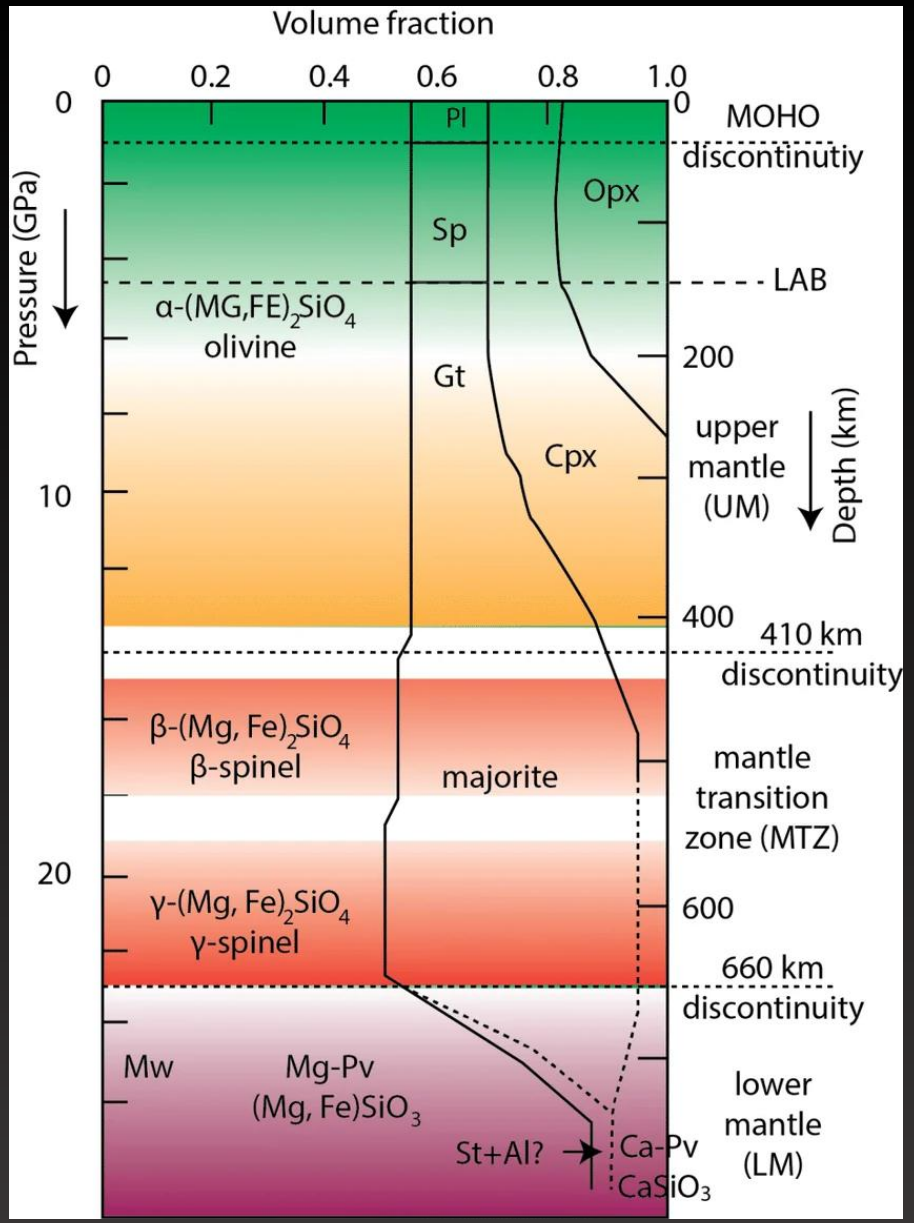
WHAT MAKES THE LITHOSPHERE PLATE-LIKE?

The concept of a strong lithosphere that translates as a relatively coherent layer over a weak asthenosphere is fundamental to a modern understanding of plate motions, tectonics, and mantle convection. **However, much remains to be learned about the physical and chemi-cal properties that create the rheological differences between the lithosphere and asthenosphere.**

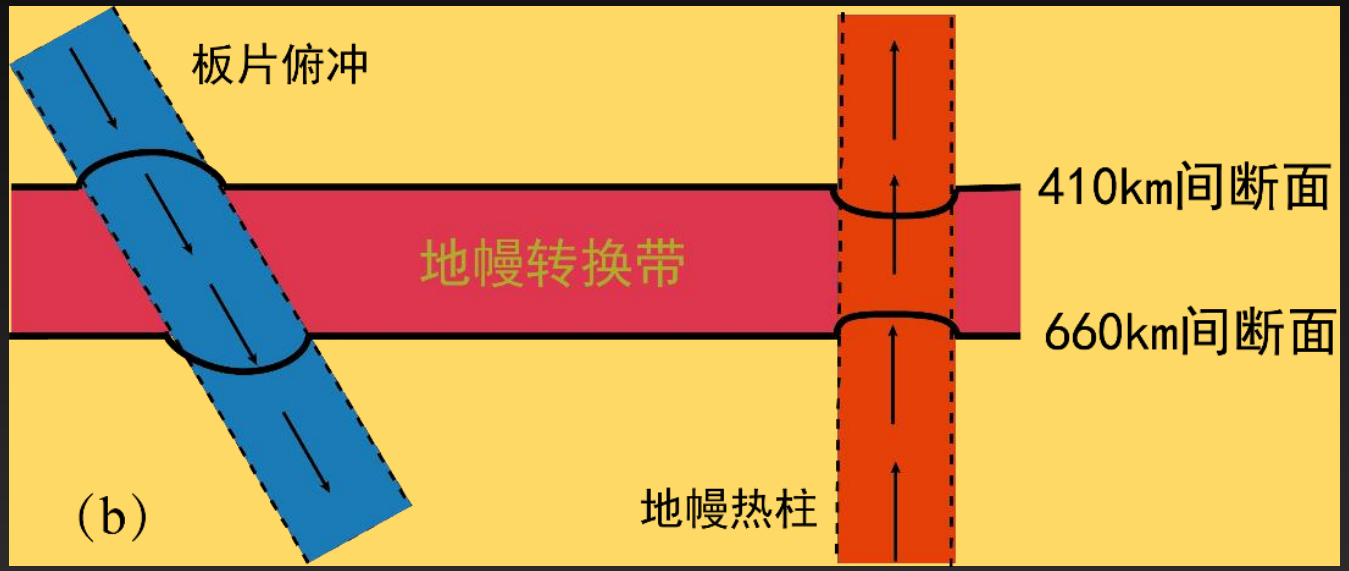
Fischer, et al., 2010@Annu. Rev. Earth Planet. Sci.

Our knowledge of the lithosphere is still very limited!

Upper mantle discontinuities: 410 and 660

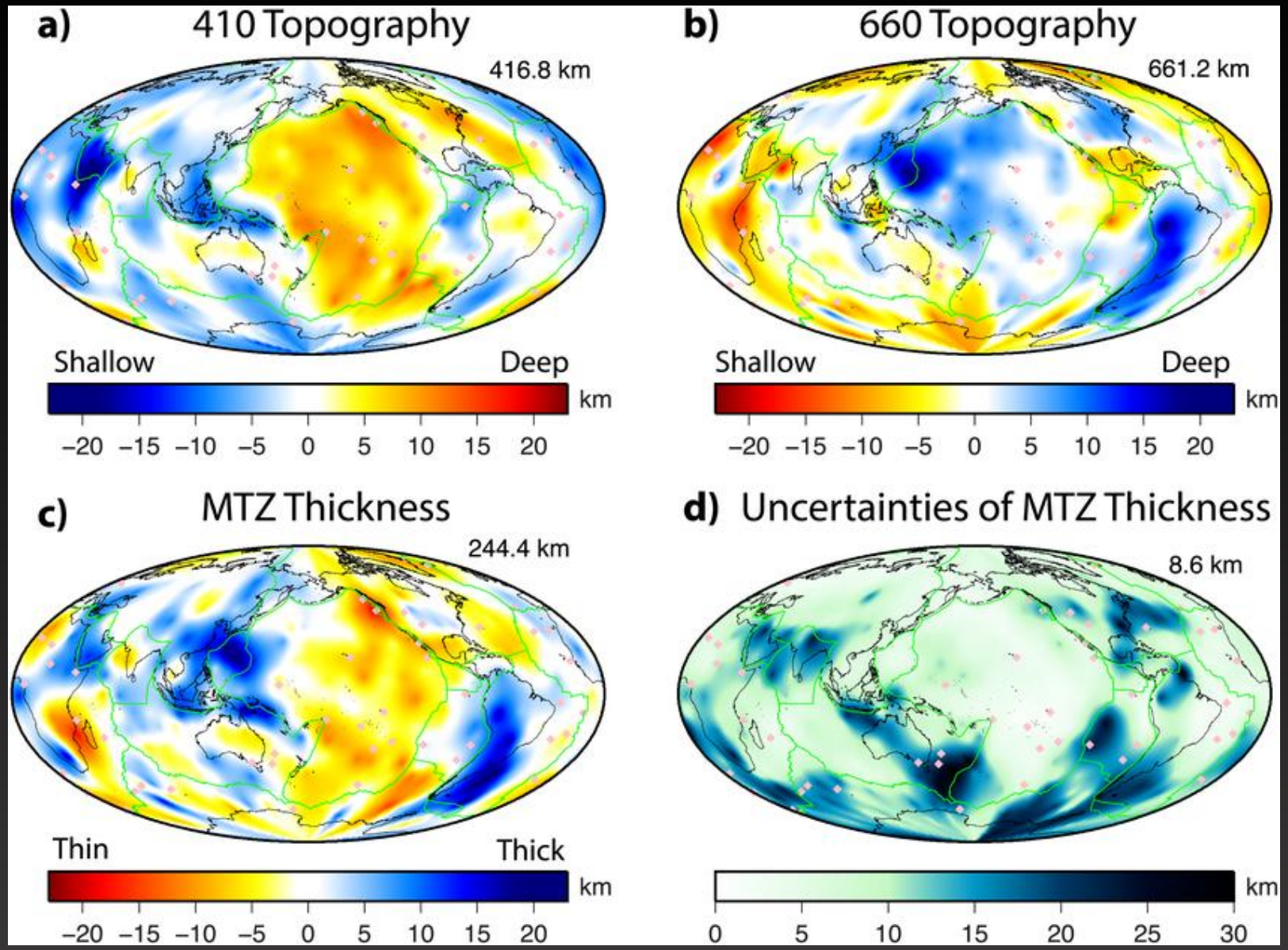


- The 410 and 660 are phase-transition discontinuities.
- Differences in Clapeyron slopes lead to distinct responses to hot and cold migrating materials.
- Subduction zone: 410 uplifted, 660 depressed
- Hot plume: 410 depressed, 660 uplifted



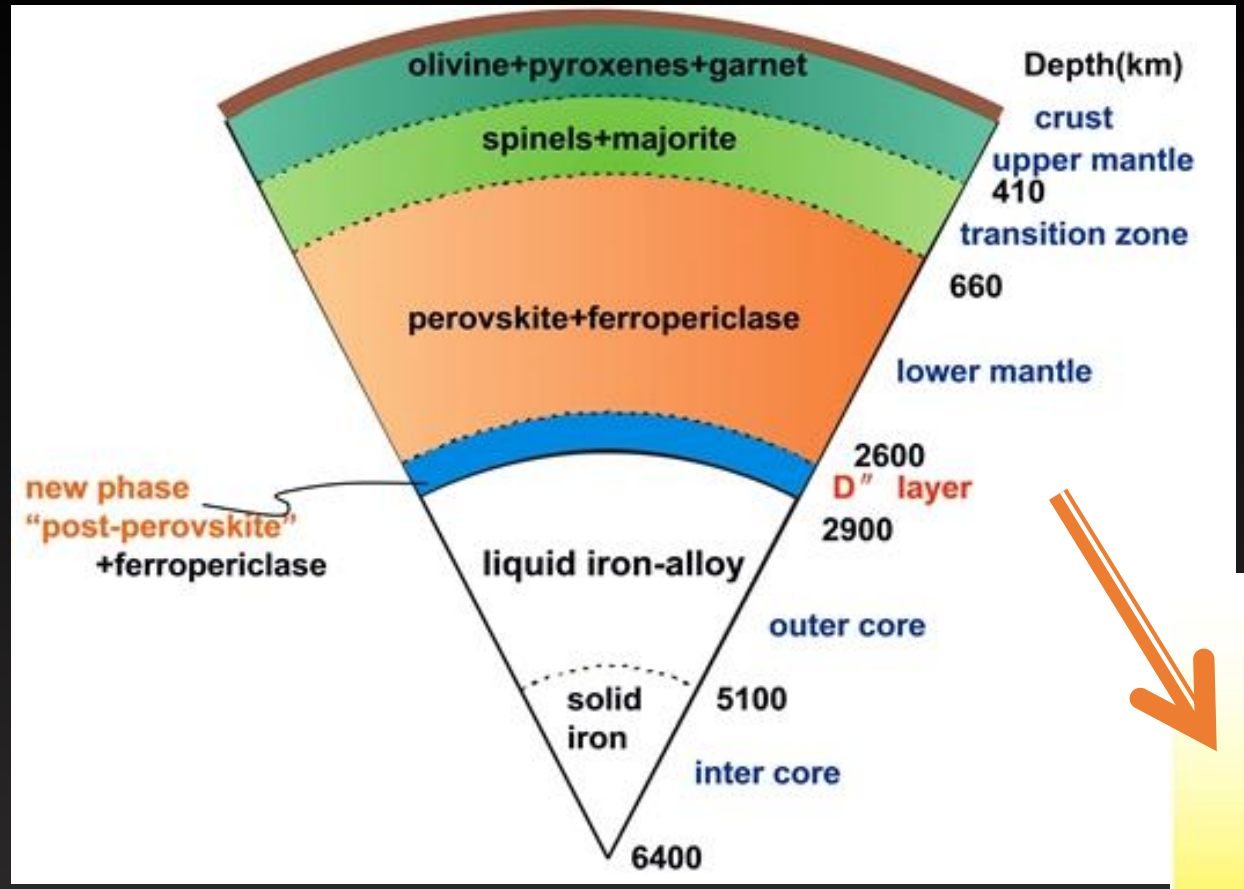
Material exchange between shallow and deep Earth leaves signatures on the 410 and 660 discontinuities. Hence, studies of their properties are critical for understanding large-scale geodynamic processes.

The global map of 410 and 660 topography

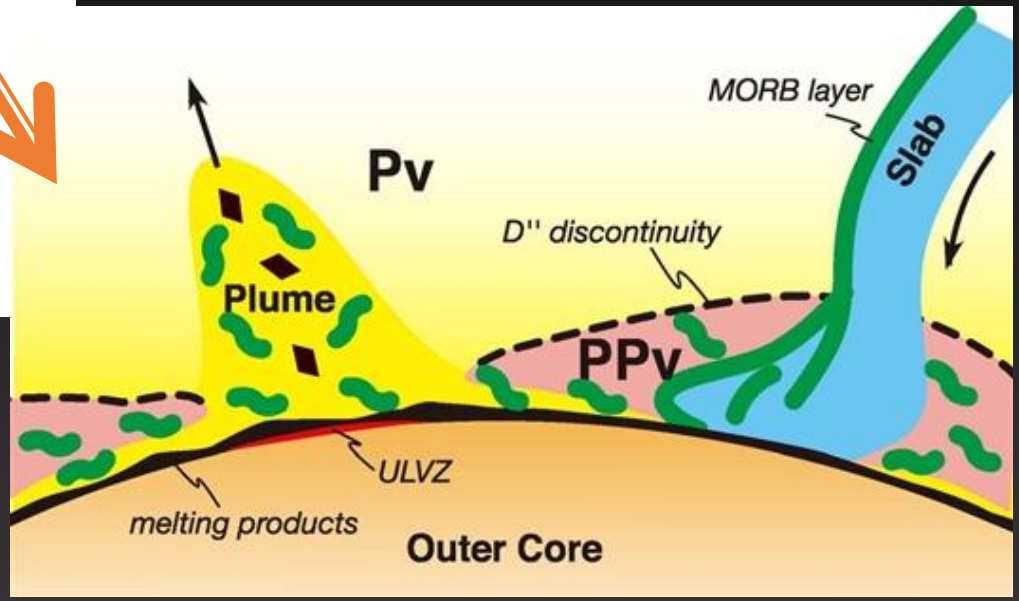


(Huang et al.,2019@JGR)

D”



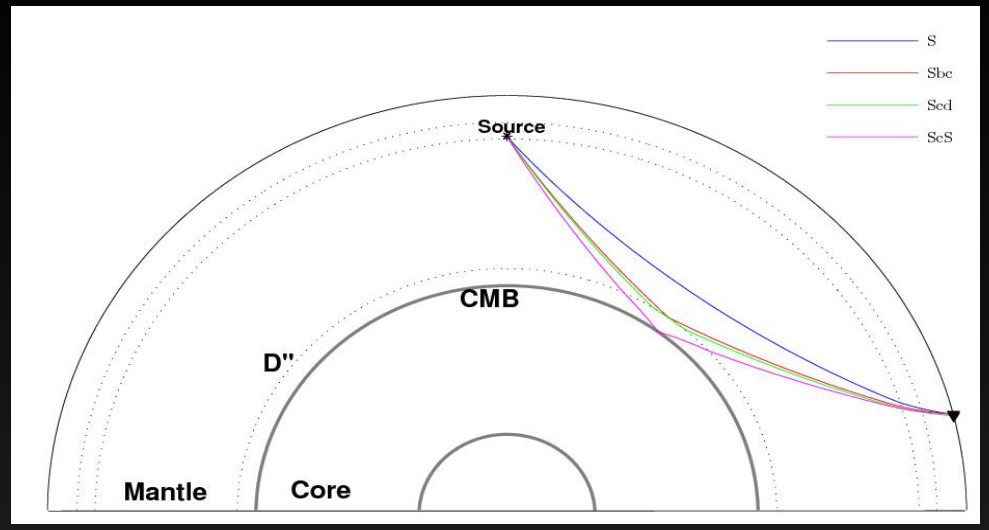
- Graveyard of subducting slabs
- Birthplace of mantle plumes



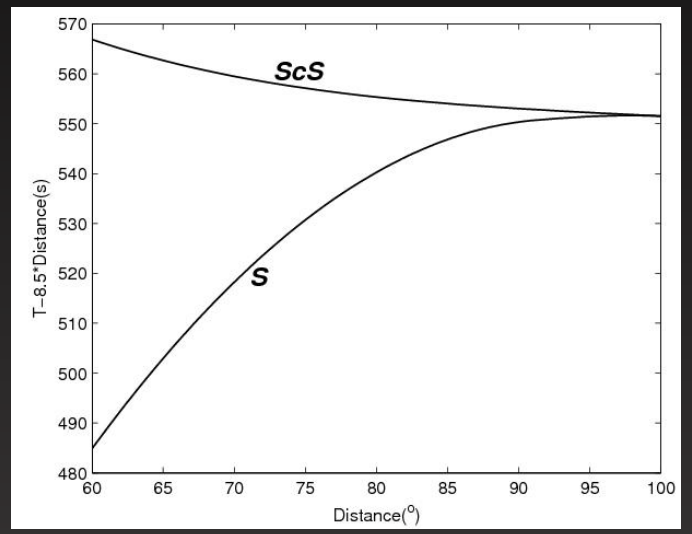
The D″ layer above the core- mantle boundary is a highly special region in the Earth’s interior.

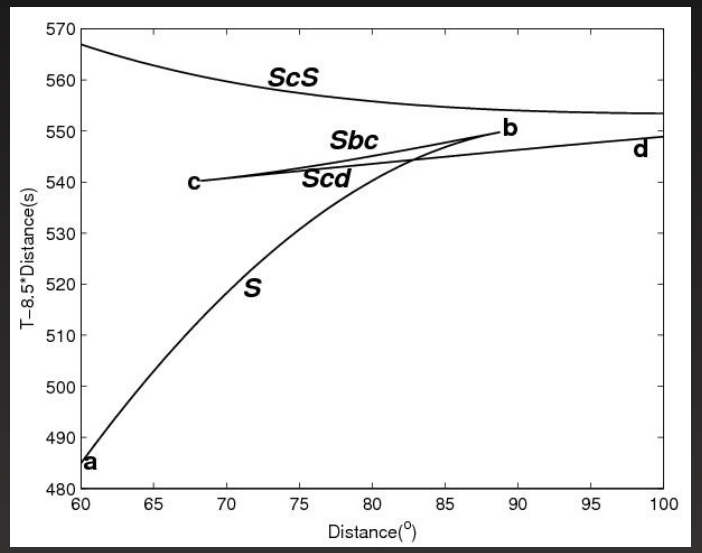
(Hirose and Lay,2008)

Seismological methods for constraining the D″ layer



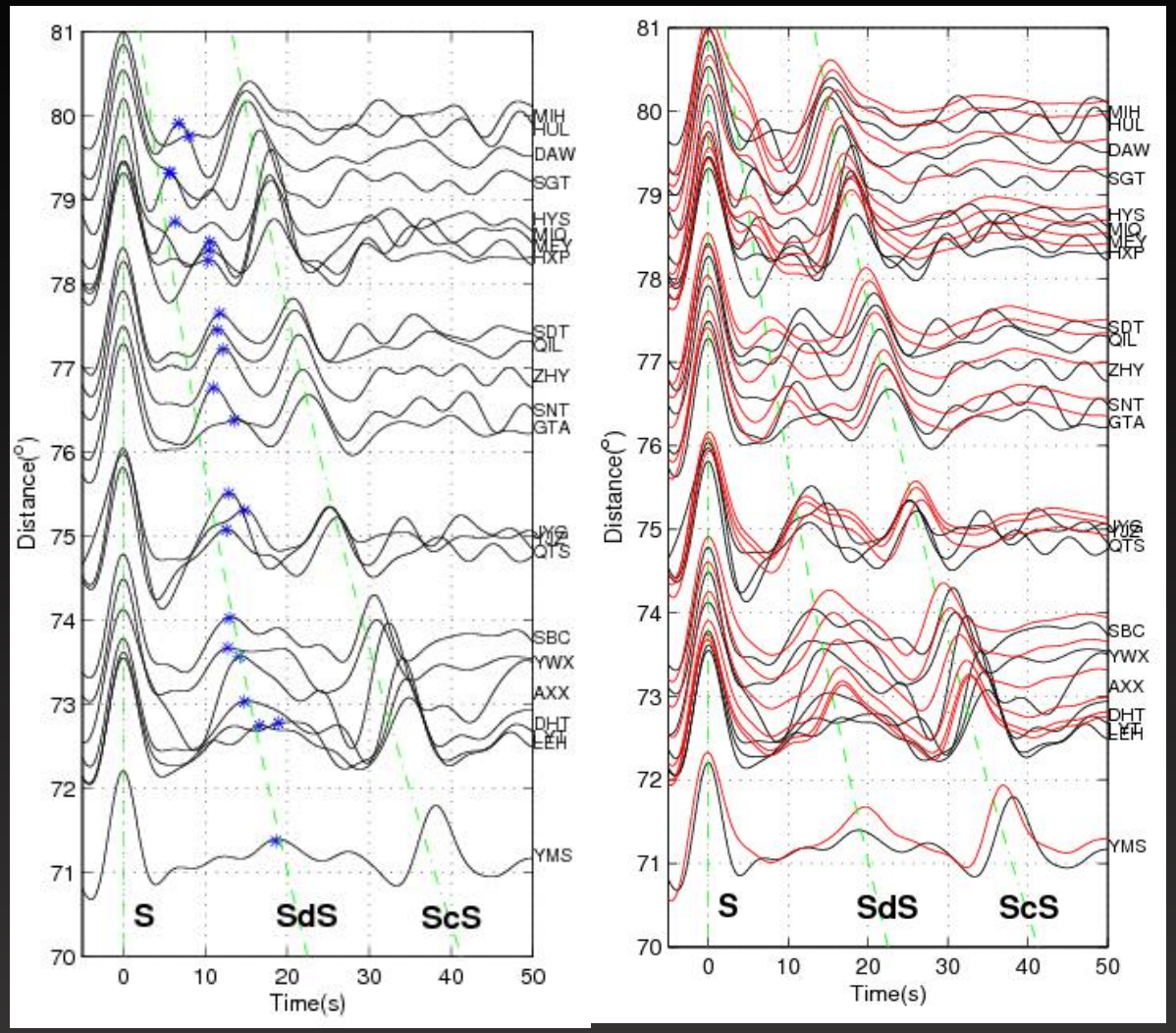
- Without D″ , no phases occur between ScS and S.
- D″ modifies seismic wave travel paths and produces D″ -related SdS phases (Sbc and Scd shown).
- Their arrival times can be analyzed to constrain the properties of the D″ layer.

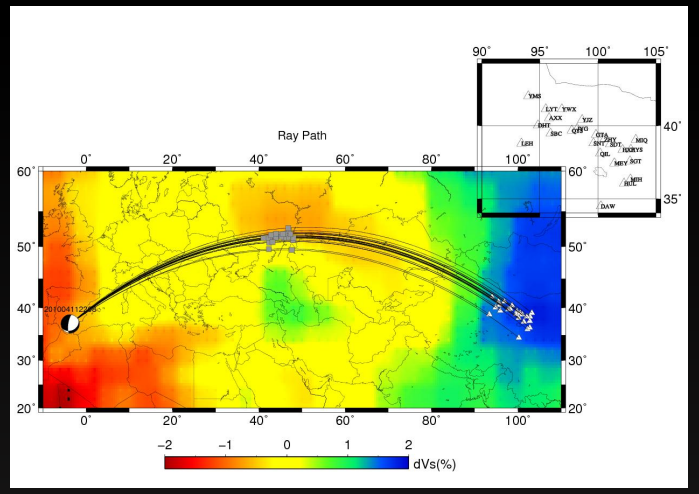




New seismic phases emerge where D″ exists.

Case studies of the D″ layer

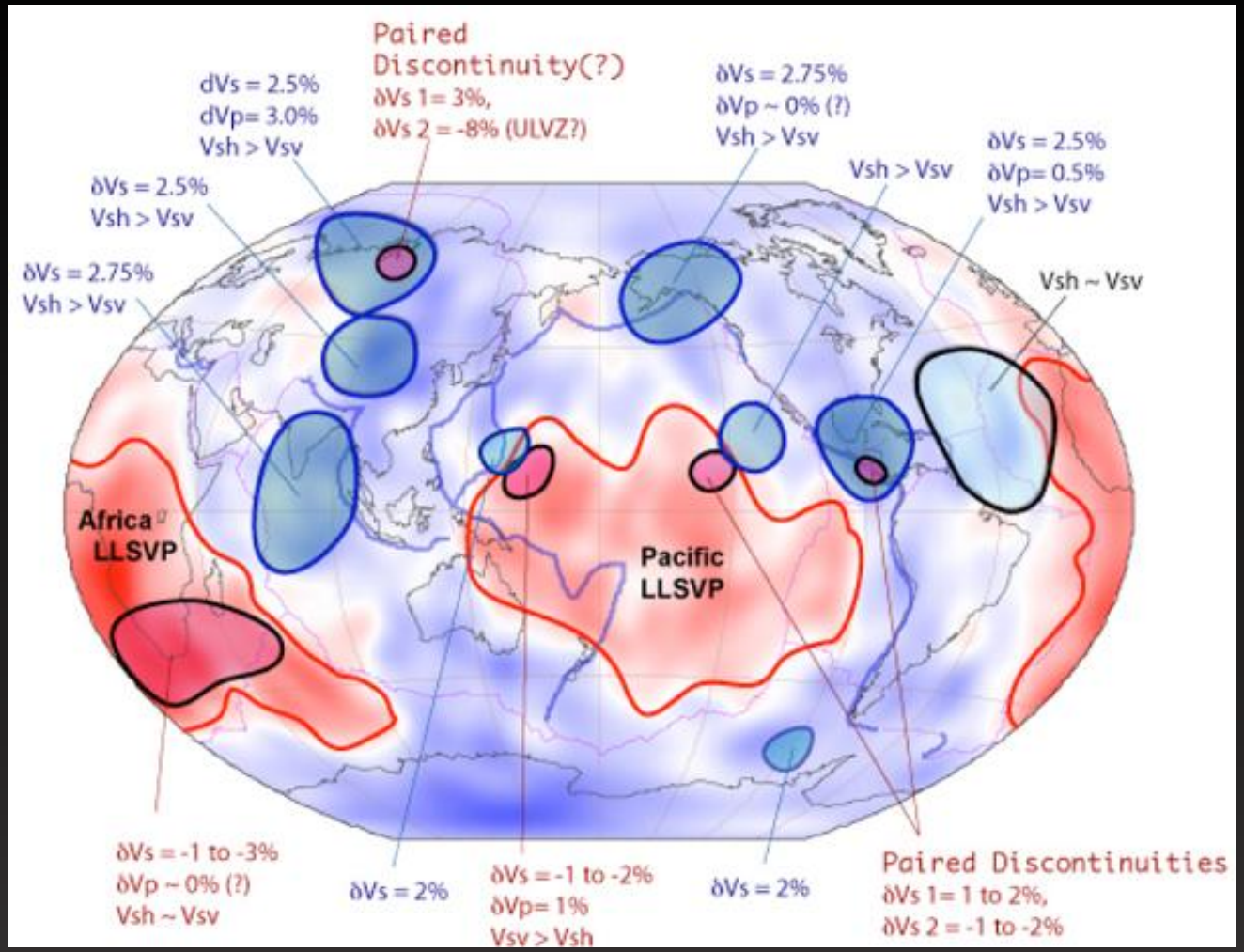


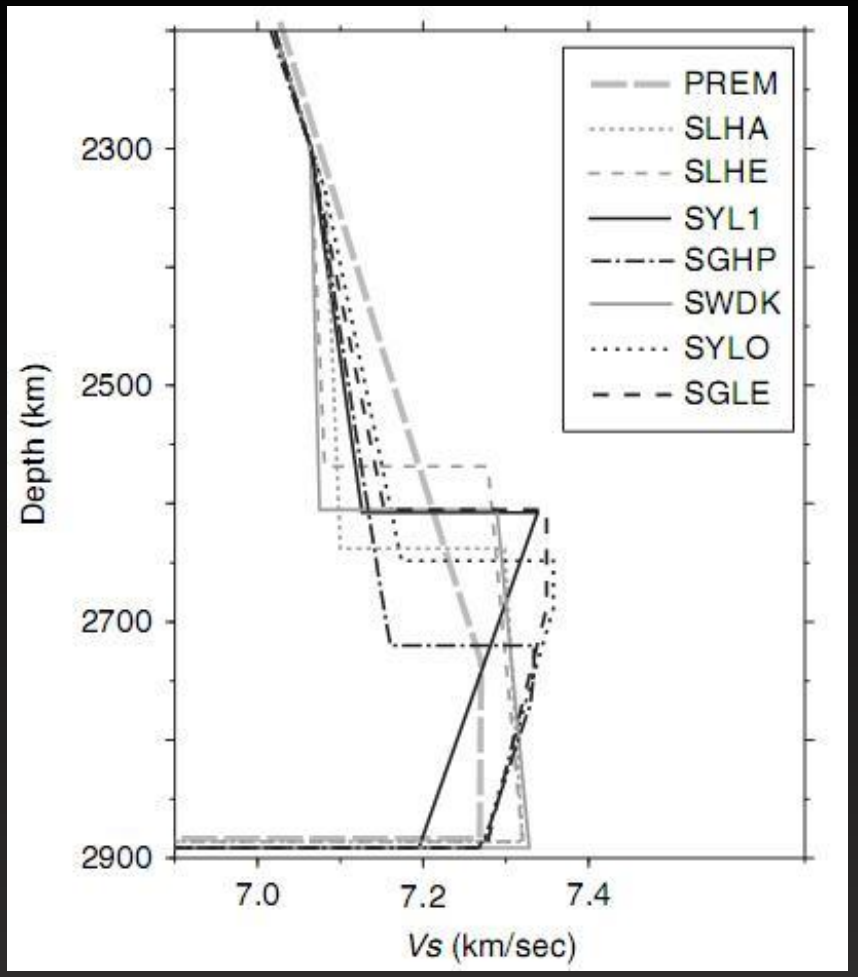


Observed phases between S and ScS indicate the presence of D″ .

(Shen et al., 2010)

Global map of D″ distribution



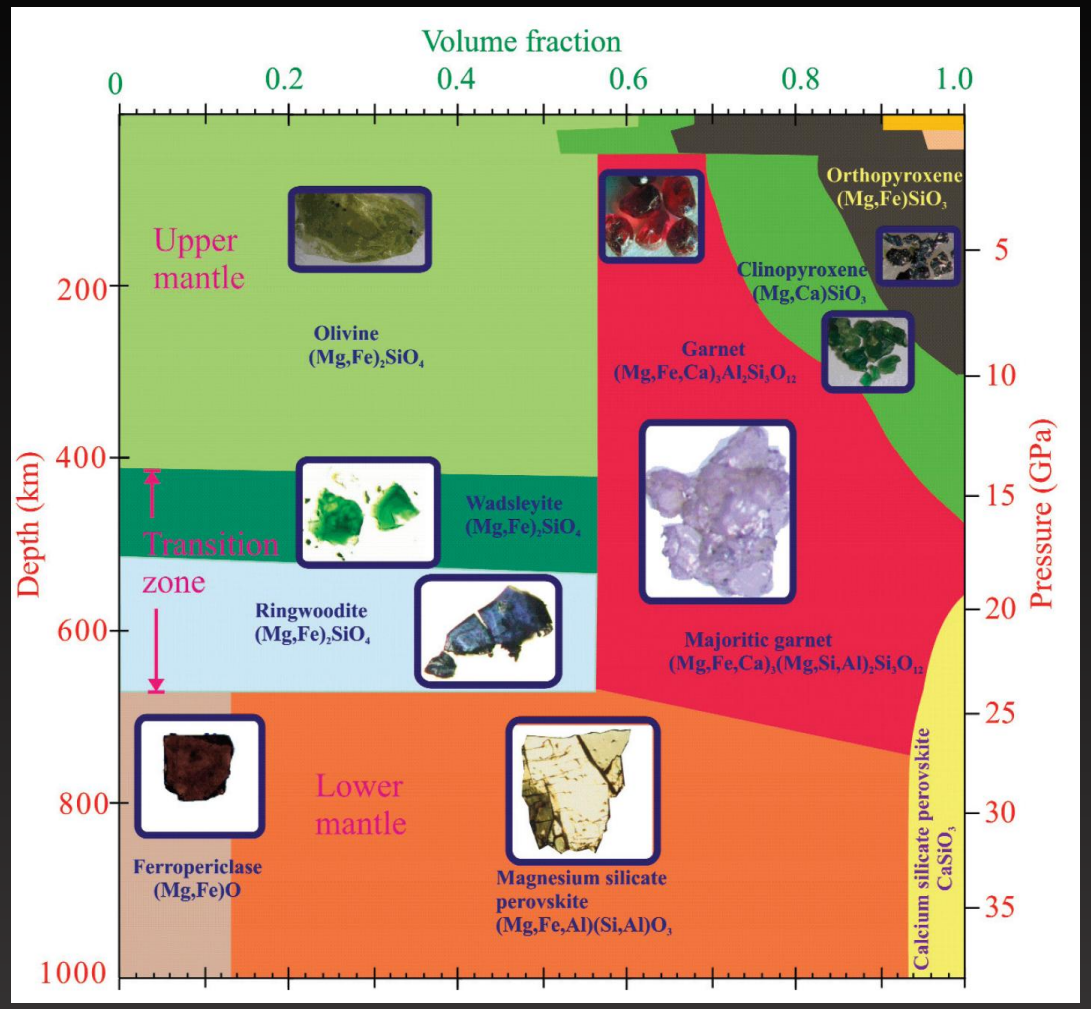


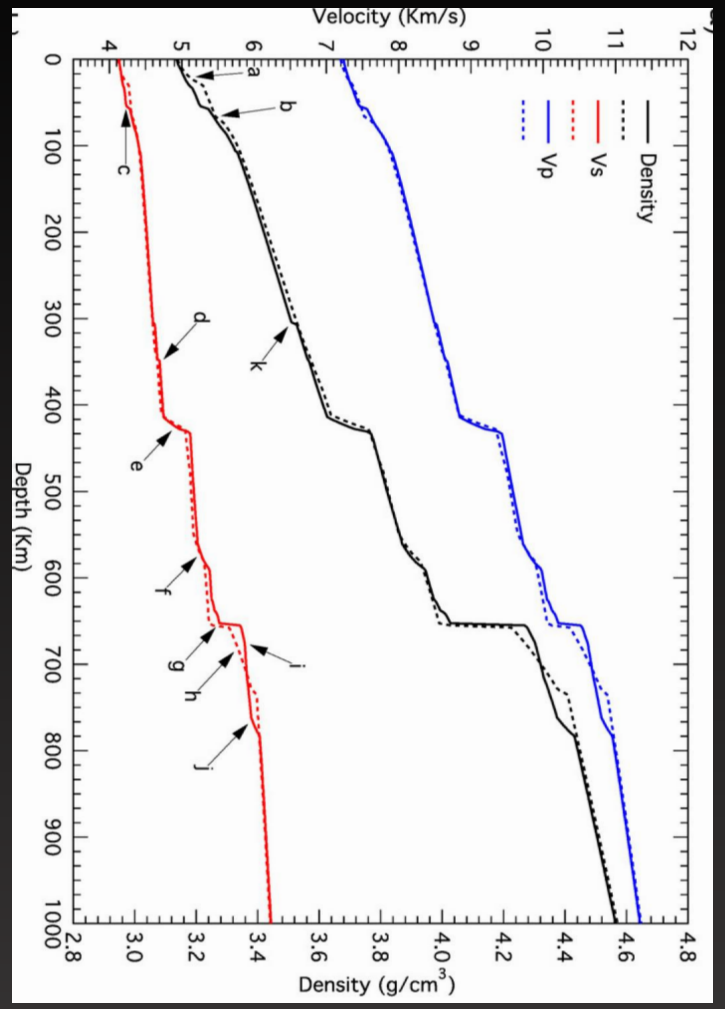
Regions with D″ have been reported in prior studies. Notably, low-velocity D″ occurs beneath Africa and the Pacific, the sites of mantle plumes.

(Lay and Garnero,2007)

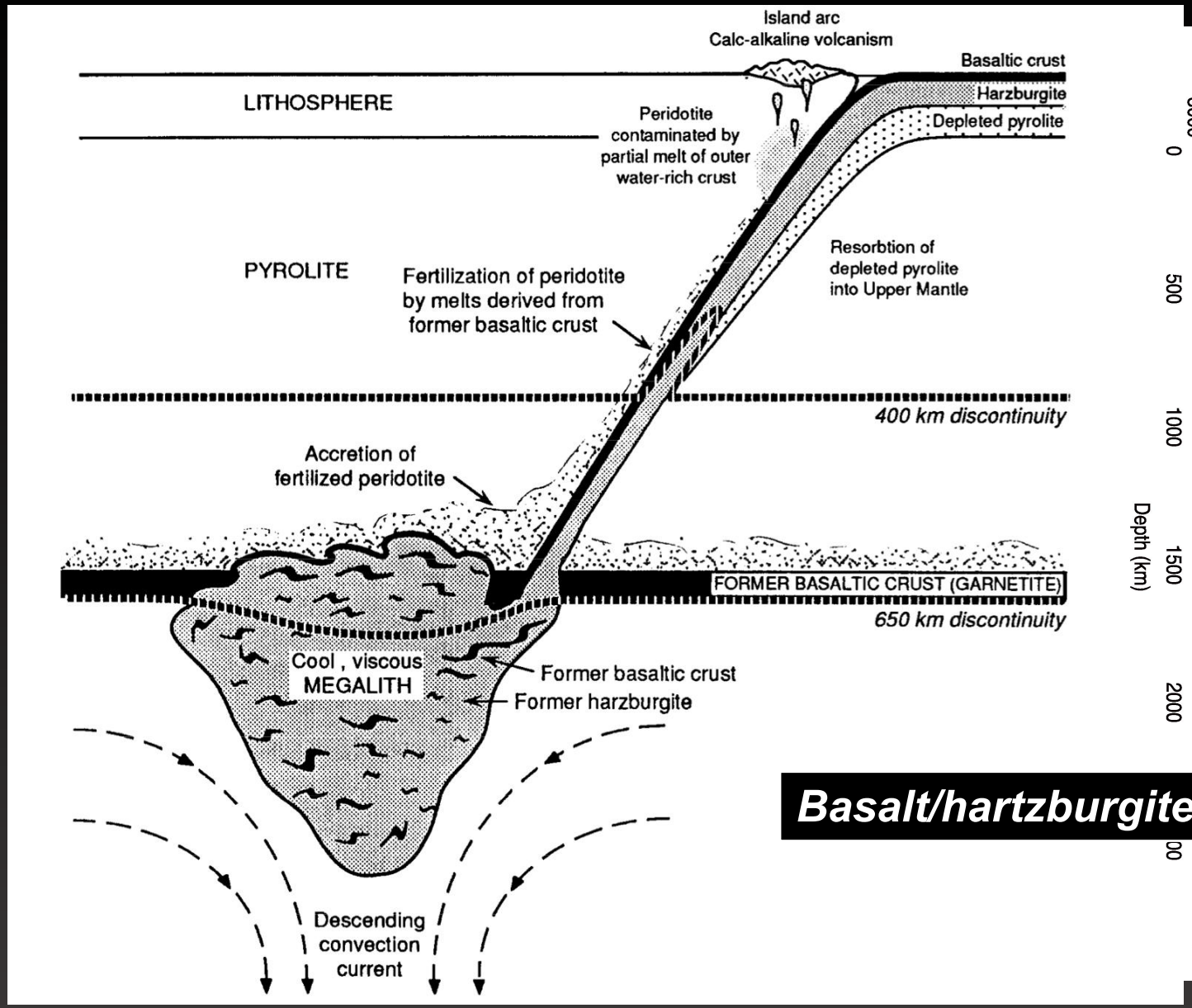
Other possible Secondary discontinuities within the Earth's interior

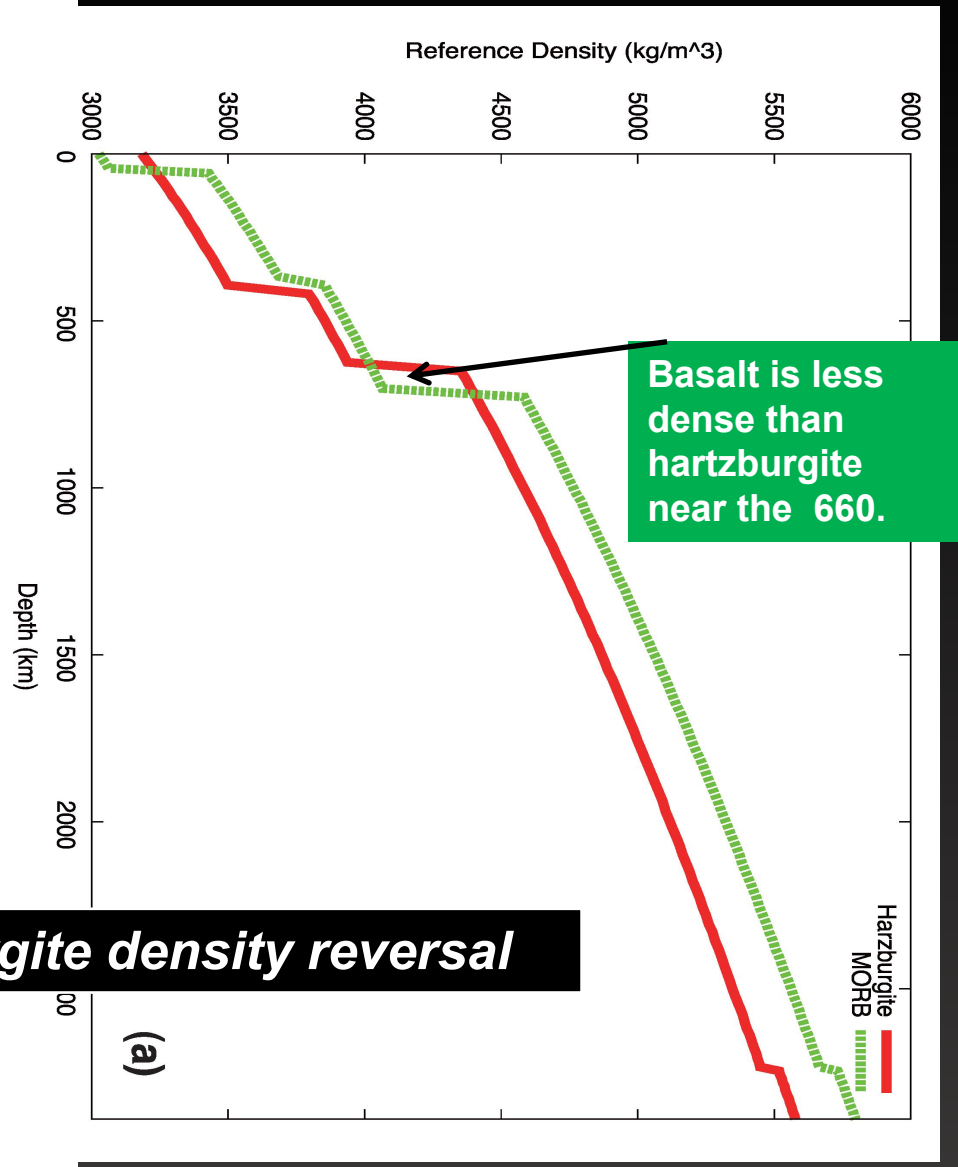
- 300
- 520
- 600
- 1000





Former crust/lithosphere near the 660

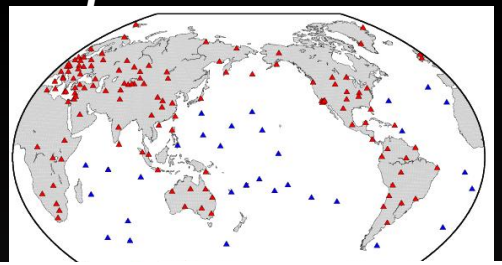


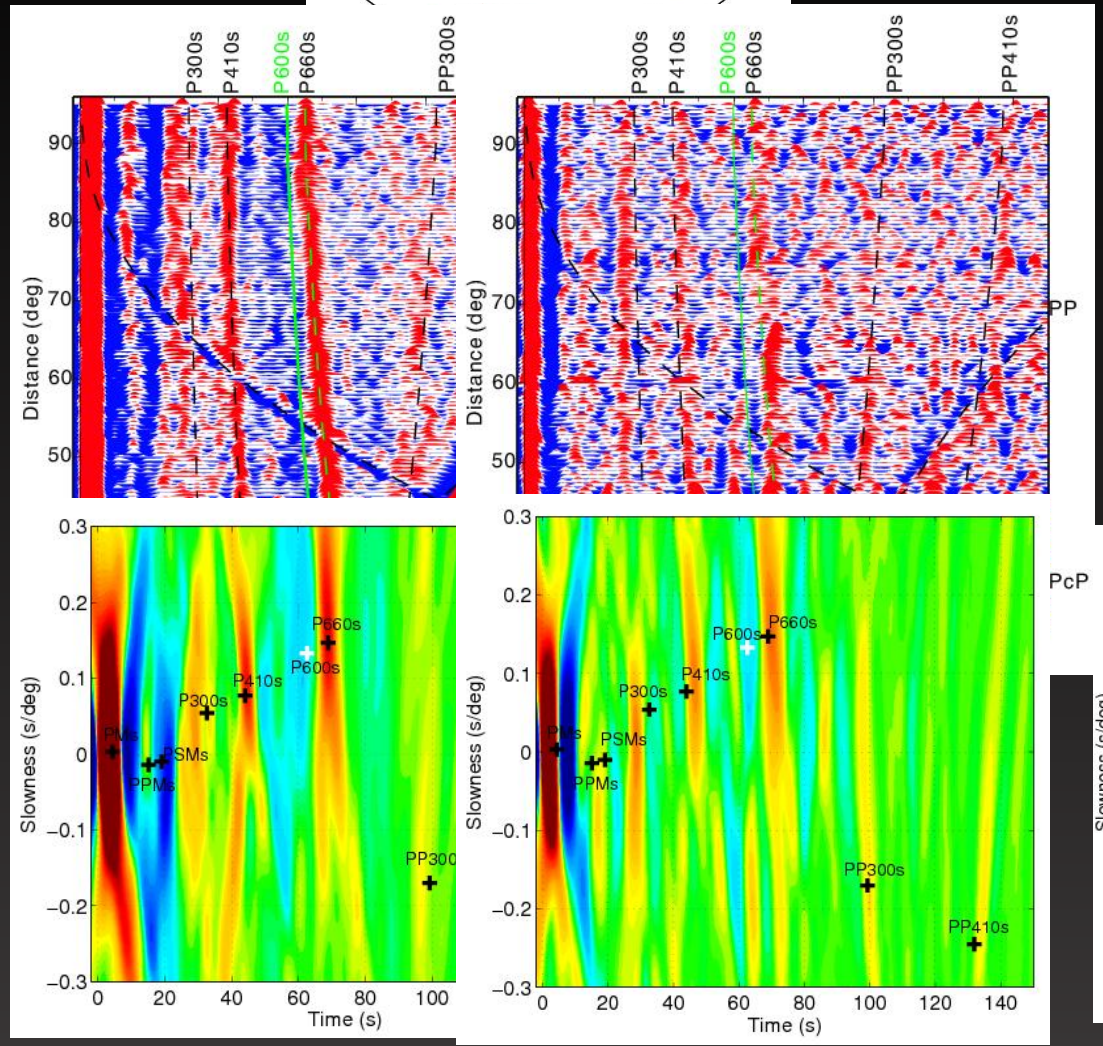


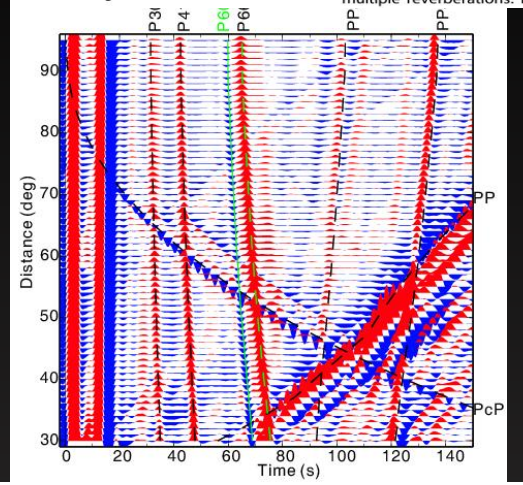
Basalt/hartzburgite density reversal

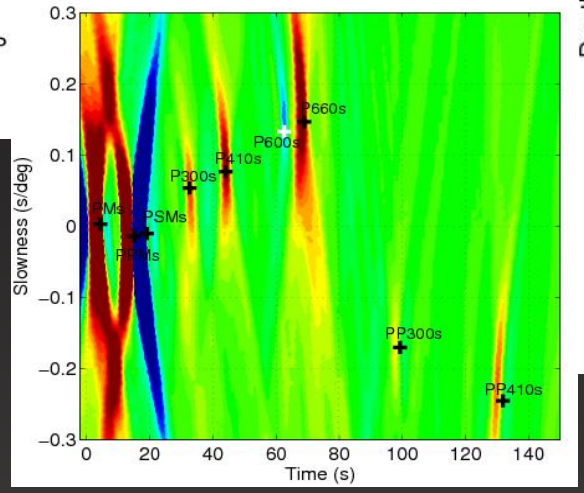
Ringwood, 1991; 1994

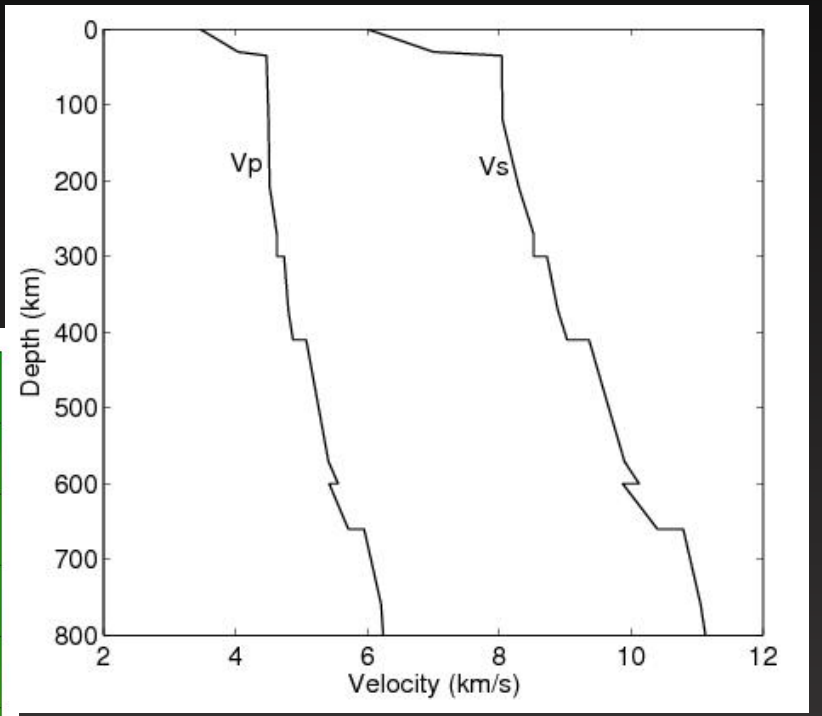
Former crust/lithosphere near the 660











AGU PUBLICATIONS

Geophysical Research Letters

RESEARCH LETTER
10.1002/2013GL058918

Key Points:
- Global receiver function stacks revealed mantle stratification
- A positive 300 km and a negative 600 km discontinuity are observed
- Slant-stack technique identifies the primary conversions from the multiples

Supporting Information:
- Readme
- Figures S1–S3

A ubiquitous low-velocity layer at the base of the mantle transition zone

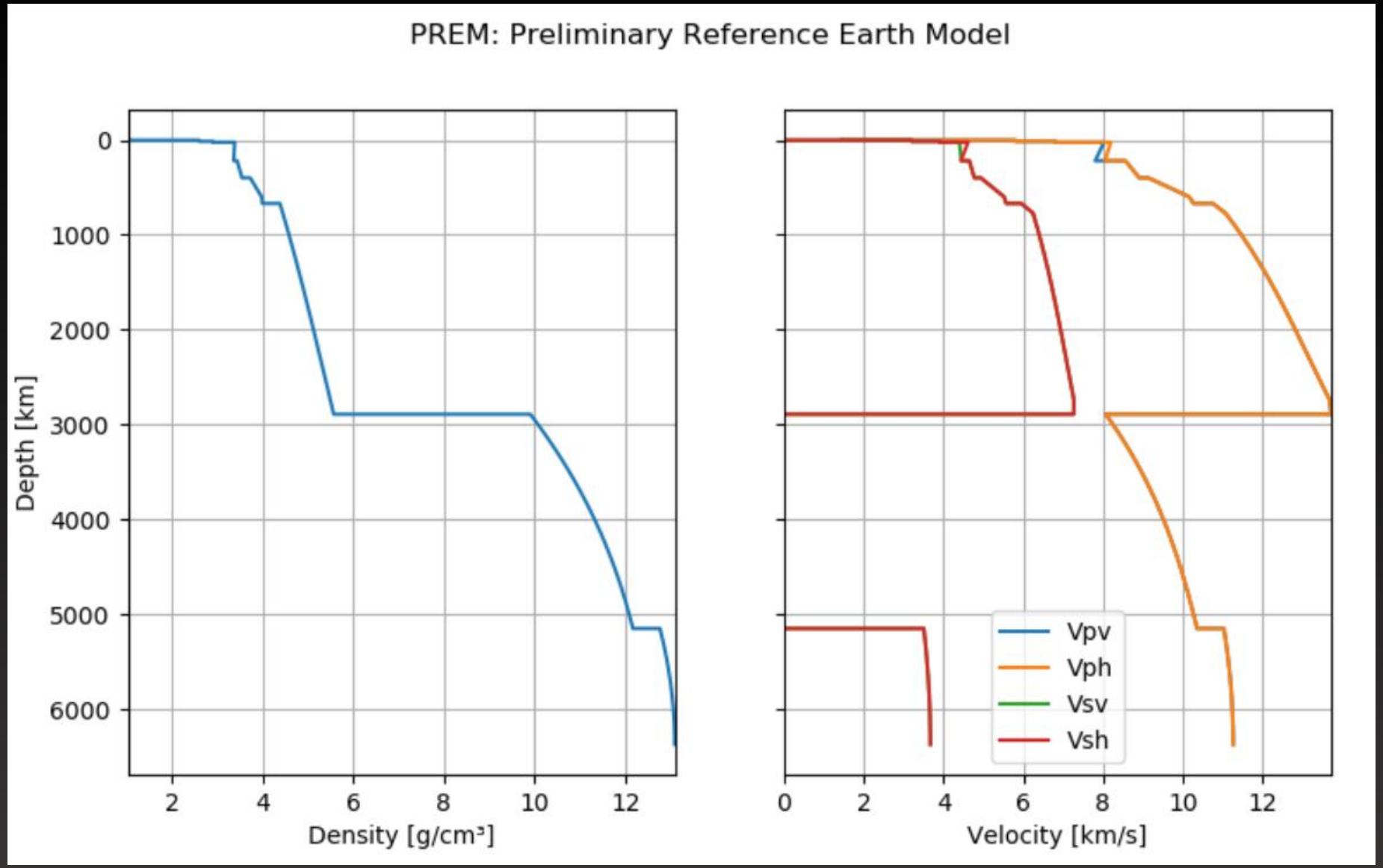
Xuzhang Shen[1], Xiaohui Yuan[2], and Xueqing Li[2]

[1]Lanzhou Institute of Seismology, China Earthquake Administration, Lanzhou, China, [2]Deutsches GeoForschungsZentrum GFZ, Potsdam, Germany

Abstract Global stacks of receiver functions clearly exhibit the upper mantle stratification. Besides the most prominent seismic discontinuities, such as the Moho and the 410 and 660 km discontinuities, a negative discontinuity is detected at a depth of ~600 km, indicating a low-velocity layer at the base of the mantle transition zone. The slant-slack technique helps to identify the primary conversions from the multiple reverberations. Presence of the negative 600 km discontinuity underneath both continent

(Shen et al., 2014)

The most fundamental model in Earth science



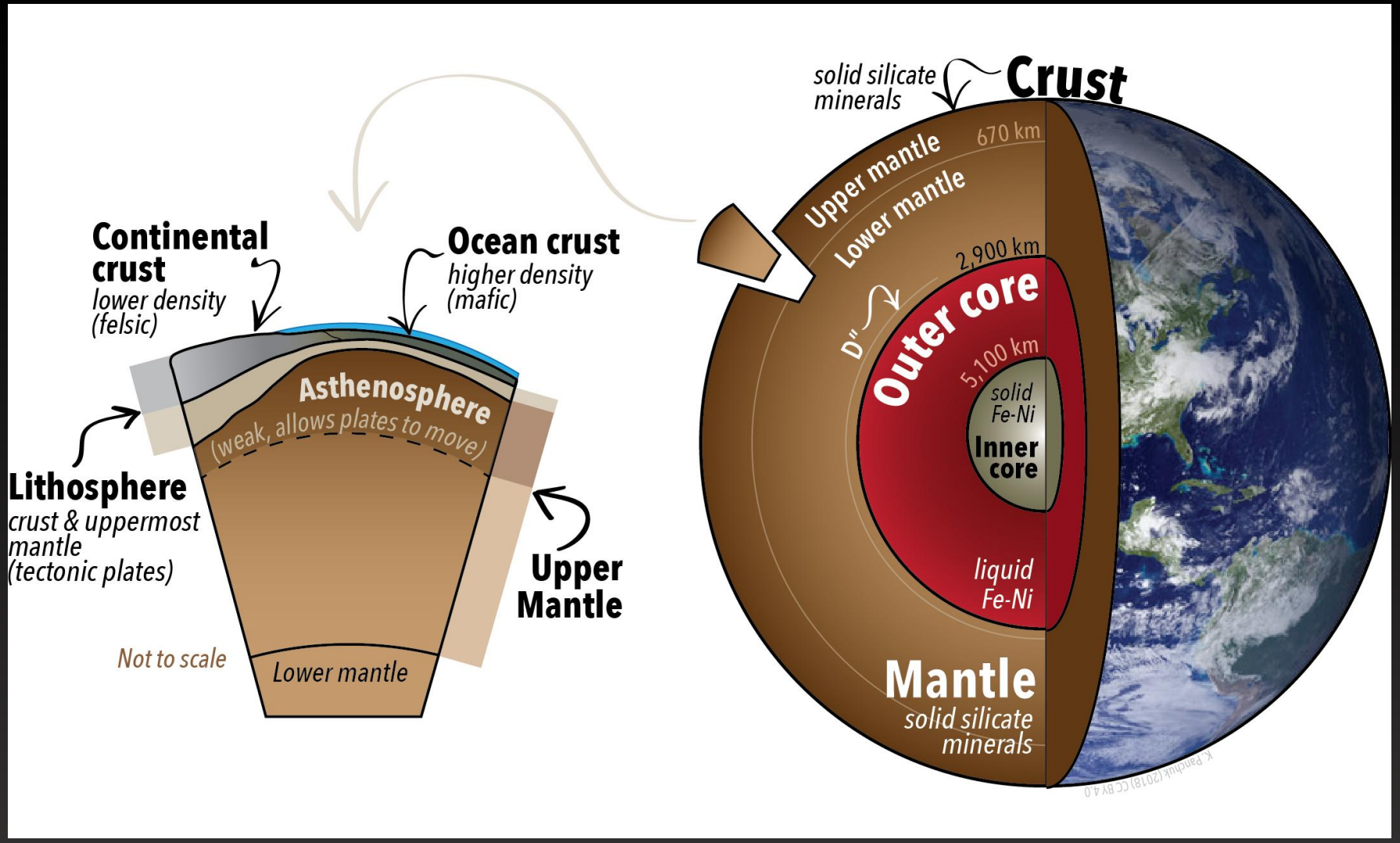
Dziewonsky, 1981

Comparison of different global models

Model	PREM	IASP91	AK135 and AK135-F
Reference	Dziewonski and Anderson, 1981, PEPI[1]	Kennett and Engdahl, 1991, GJI[12]	*Kennett et al., 1995*[12], and *Montagner and Kennett et al., 1996*, GJI[16]
Data used	Body waves, normal modes, surface waves, surface wave dispersion, astronomical observations	Bodywaves ($6*10^6$ measurements)	Bodywaves relocated with IASP91, bodywave differentials, plus normal modes (in AK135-F only)
Period	1 s with attenuation corrections for 200 s	1 s	1 s
Regional bias	Crust thickness is weighted average of continent and ocean, mantle unbiased	Continental crustal thickness used as seismometers are on continents. Upper mantle more biased than lower mantle	AK135: continental thickness used as seismometers on continents, upper mantle more biased than lower mantle. AK135-F: Average crustal structure, upper mantle more biased than lower mantle.
Water layer	Yes: 3km thick	No	Yes: 3km thick
Resolved parameters	Vp, Vs, Q, density	Vp, Vs	Vp, Vs, plus Q and density (in AK135-F only)
Features	Upper mantle discontinuity at 220 km depth	Vp better resolved than Vs	Outer core well resolved by PKP differential travel times, density and Q from Montagner and Kennett (1996)
Anisotropic/Isotropic	Transverse anisotropy of 2-4% from 80-220 km depth	Isotropic	Isotropic
Best uses in seismology	Long period studies	Body-wave studies, earthquake relocation	Body-wave studies specifically core, earthquake relocation

https://seismo.berkeley.edu/wiki_cider/REFERENCE_MODELS

Layered earth

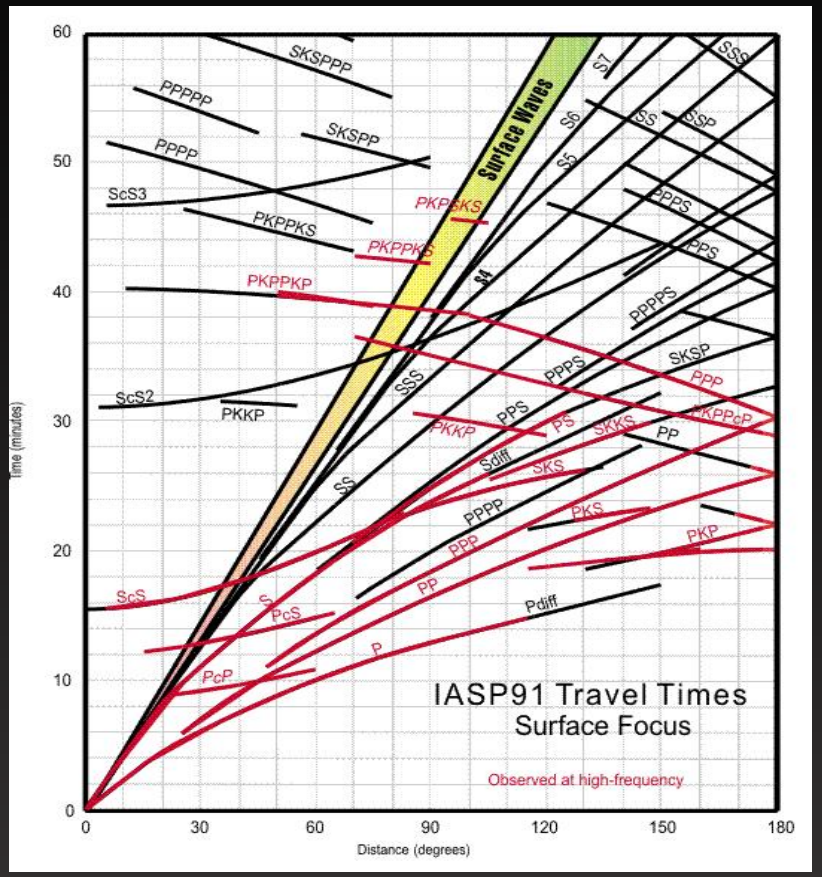


Deeper regions, particularly the inner and outer core, have relatively simpler material compositions.

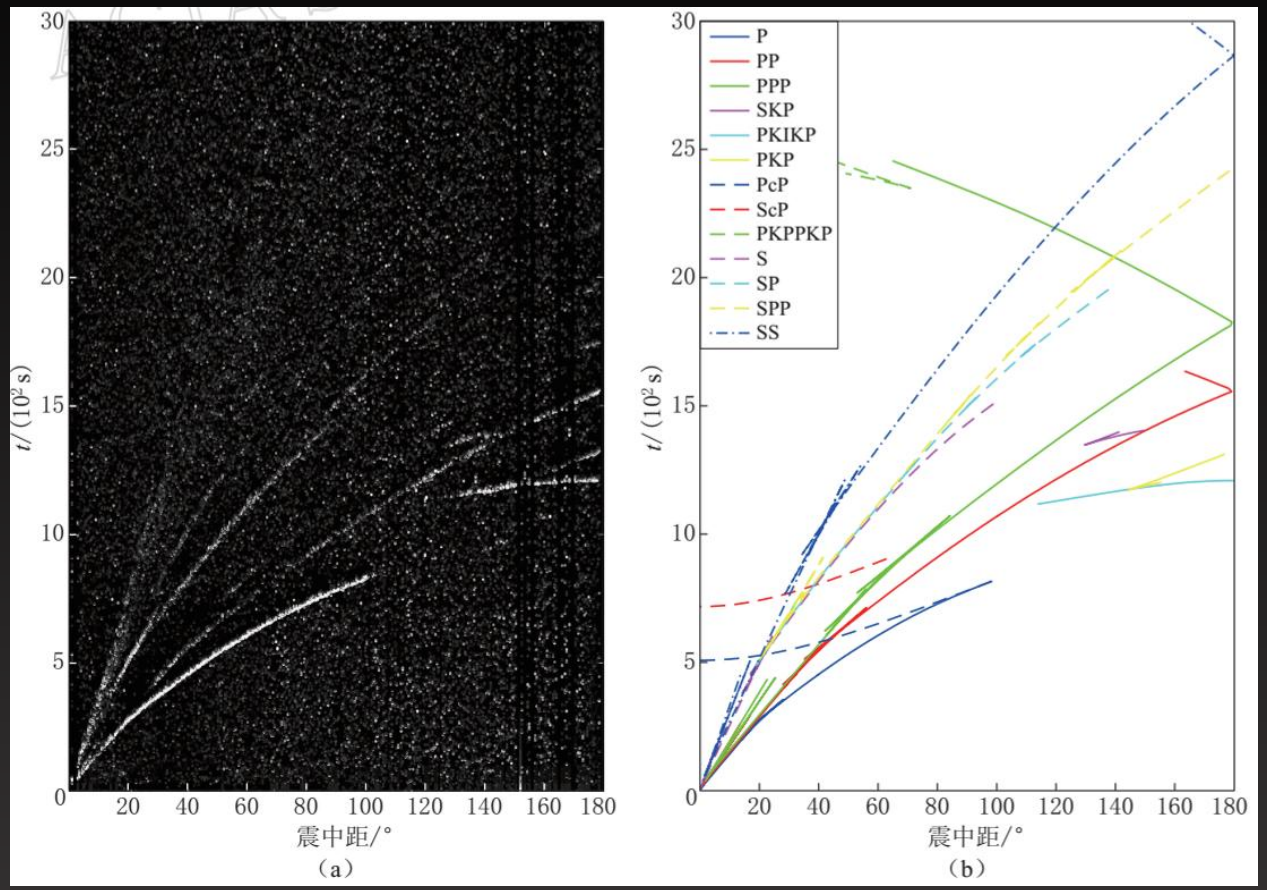
https://openpress.usask.ca/app/uploads/sites/29/2018/03/earth_interior.png

The Fascinating One-Dimensional Layered Earth Model

The one- dimensional layered Earth model looks simple yet is a landmark achievement of centuries- long Earth exploration. Its theoretical arrival times and waveforms can account for roughly 80% of seismic observations.



Travel-time tables of various seismic phases predicted by the IASP91 Earth model



Travel-time curves obtained by stacking multi-year waveforms at the Lanzhou short-period CTBTO station

秦满忠，沈旭章., 2014

1-D Structure: Rapidly Rotating Inner Core（1996）



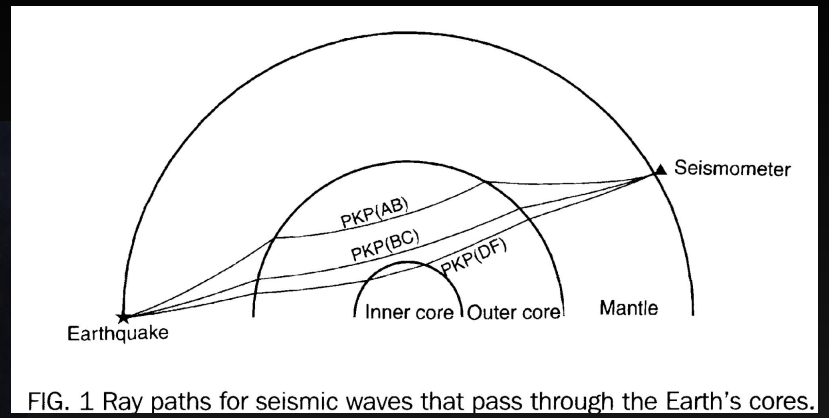
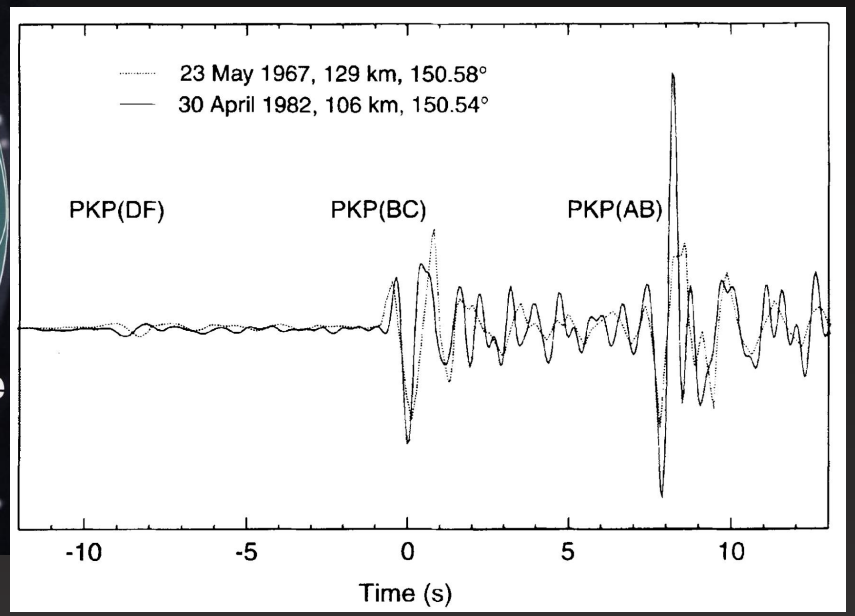
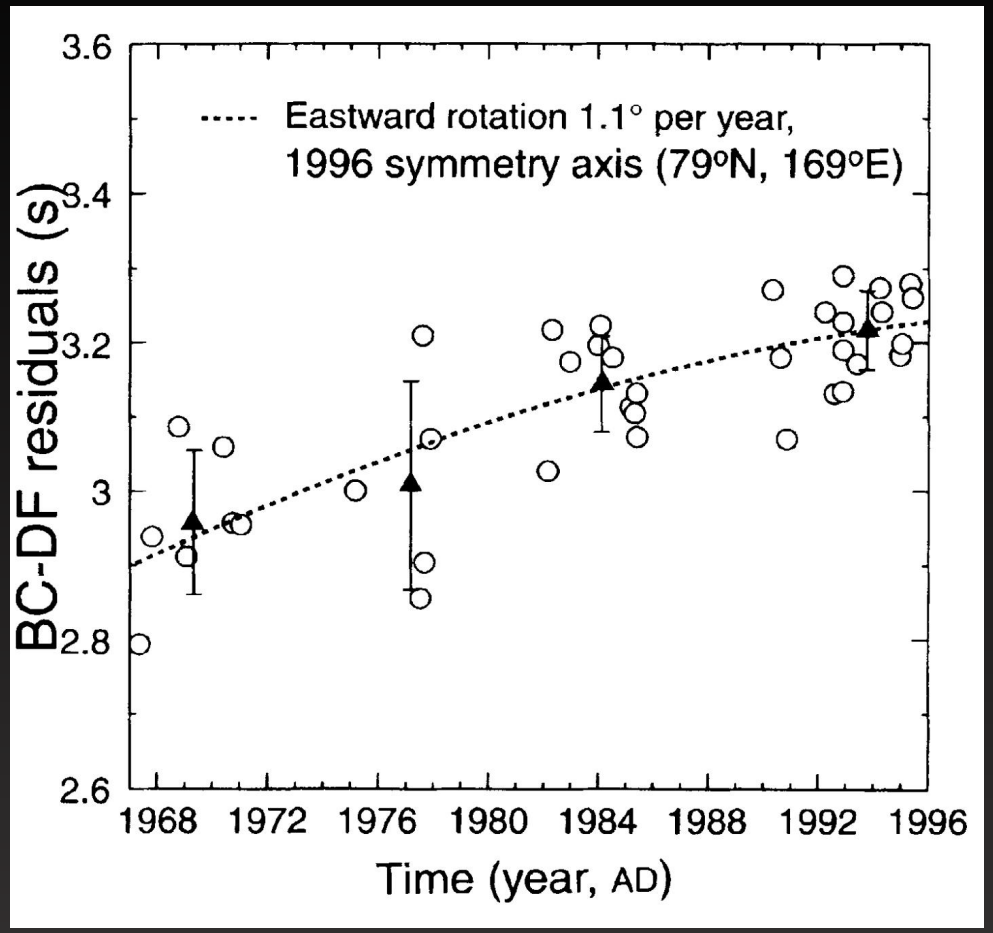


FIG. 1 Ray paths for seismic waves that pass through the Earth's cores.





The inner core rotates an extra 0.3–0.5° per year, completing approximately one extra rotation every 1000 years.

X. Song and P. Richards, 1996

1-D Structure: The inner core rotation rate is not as fast as previously thought (2023).

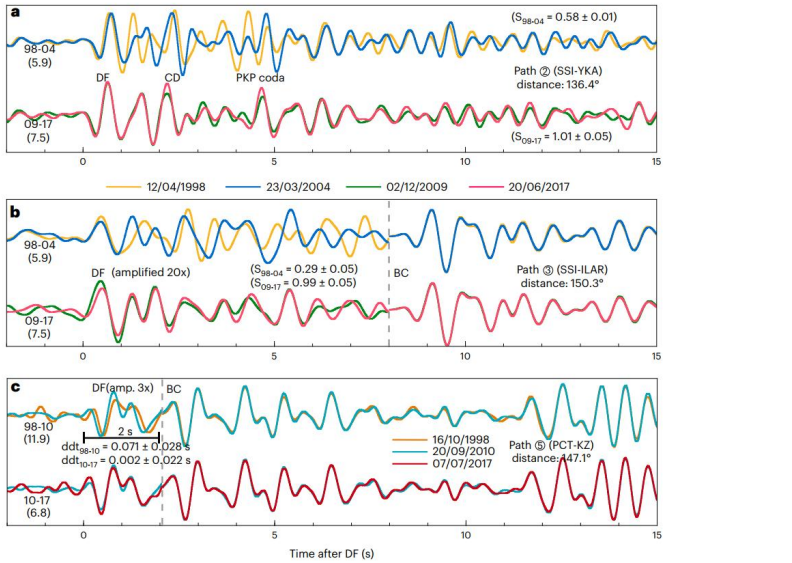


Fig. 2 | Examples highlighting a pattern change in the inner-core temporal changes in the recent decade. a,**b**, Waveforms from an SSI multiplet along Paths 2 and 3 showing the pattern change in *S*. The last two digits of the event years and time lapse (in years) are labelled on the left. For Path 2 at CD distance range (**a**), the normalized waveforms are aligned by cross-correlation of the entire window. For Path 3 at BC distance range (**b**), they are aligned with BC, and the weak inner-core waves and the background noise preceding the dashed line (onset of BC) are amplified. **c**, Waveforms from a PCT multiplet along Path 5 showing the pattern change in DF relative arrival times (ddt). It is plotted in the same way as **b**. The horizontal 2-s segment is the DF time window used to measure the ddt.

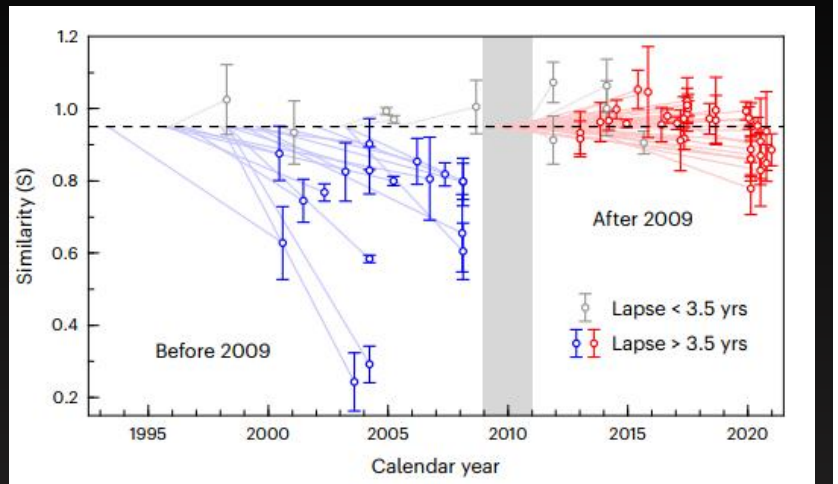


Fig. 3 | *S* of the inner-core waves from two subsets of doublets. In one subset (left), both events of a doublet are before 2009; in the other subset (right), both events are after 2009. Each line segment plots a doublet from the origin time of the earlier event and the reference *S* of 0.95 (the dashed horizontal line) to the origin time of the later event and the corresponding *S* horizontally and vertically, respectively. Each error bar represents an *S* measurement ± its measurement error (σ_s; see Methods). The shaded vertical bar indicates the 95% CI for the time of the turning point for the pattern change from the ddt data (see main text).

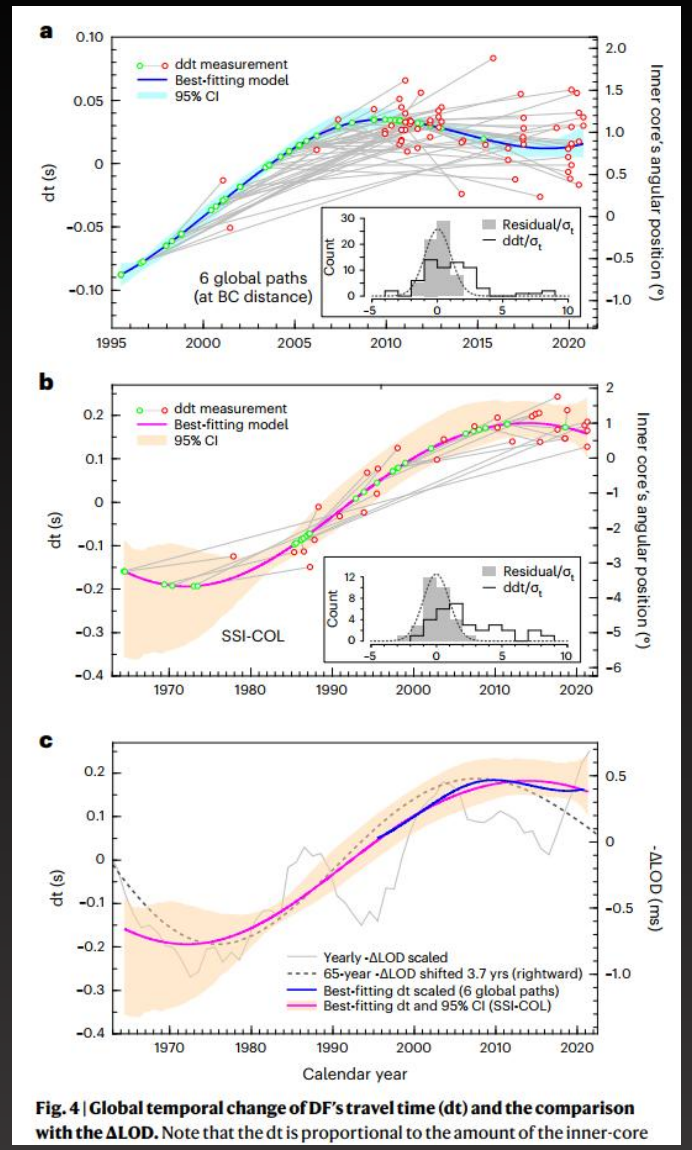
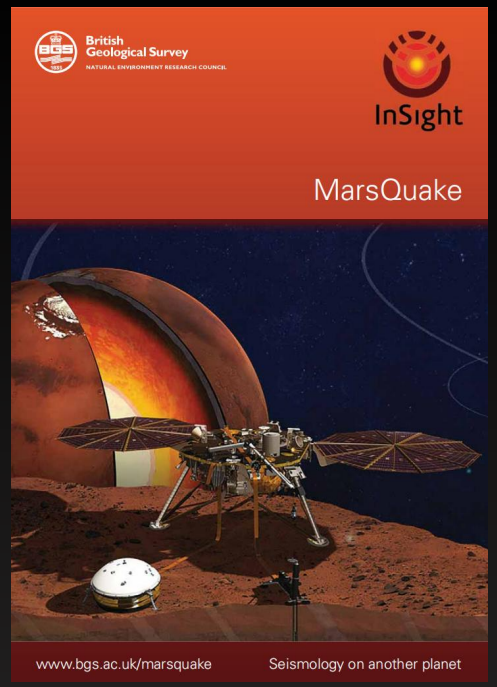


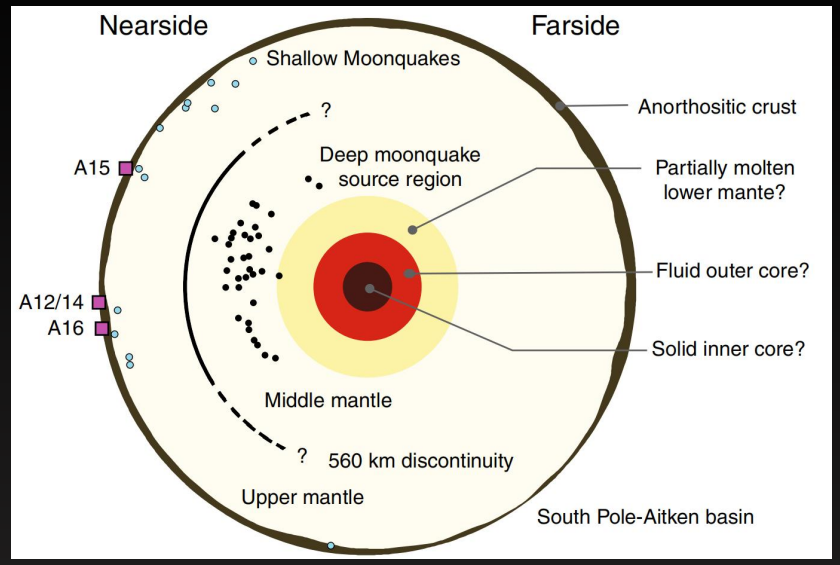
Fig. 4 | Global temporal change of DF's travel time (dt) and the comparison with the ΔLOD. Note that the dt is proportional to the amount of the inner-core

Since the early 1970s, the Earth's inner core rotated faster than the Earth's surface. It became nearly synchronous with the surface around 2009, and thereafter began to rotate more slowly than the surface. It is inferred that the differential rotation of the inner core may oscillate with a period of approximately 70 years. This study provides new constraints on the dynamic processes in the deep Earth and the core − mantle coupling mechanism, and helps us understand how the deep Earth spheres operate.

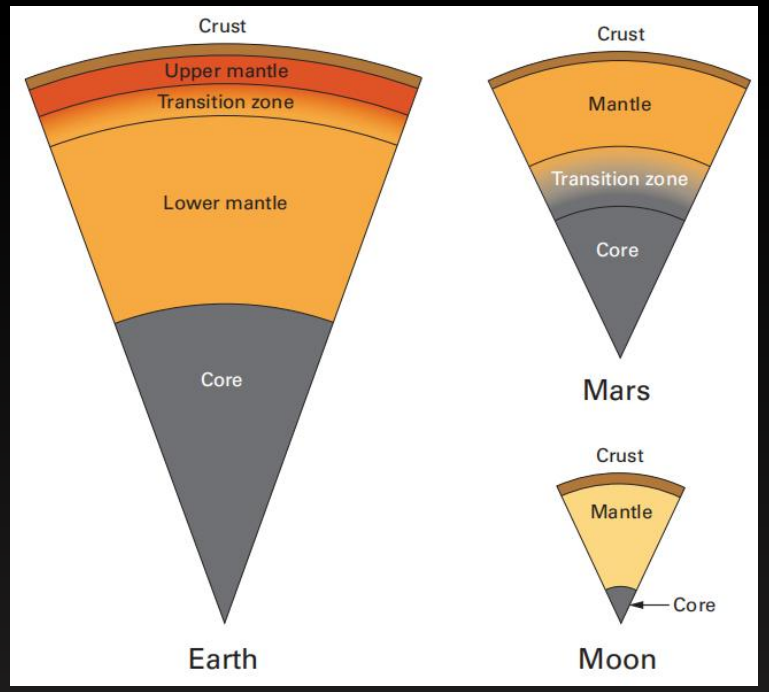
Yang and Song, 2023

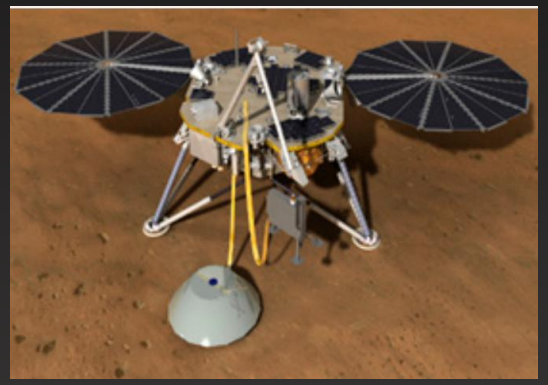
Moonquake and Marsquake

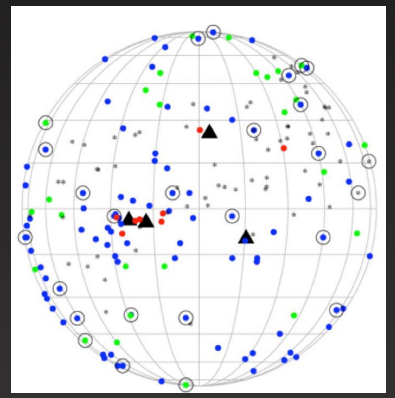


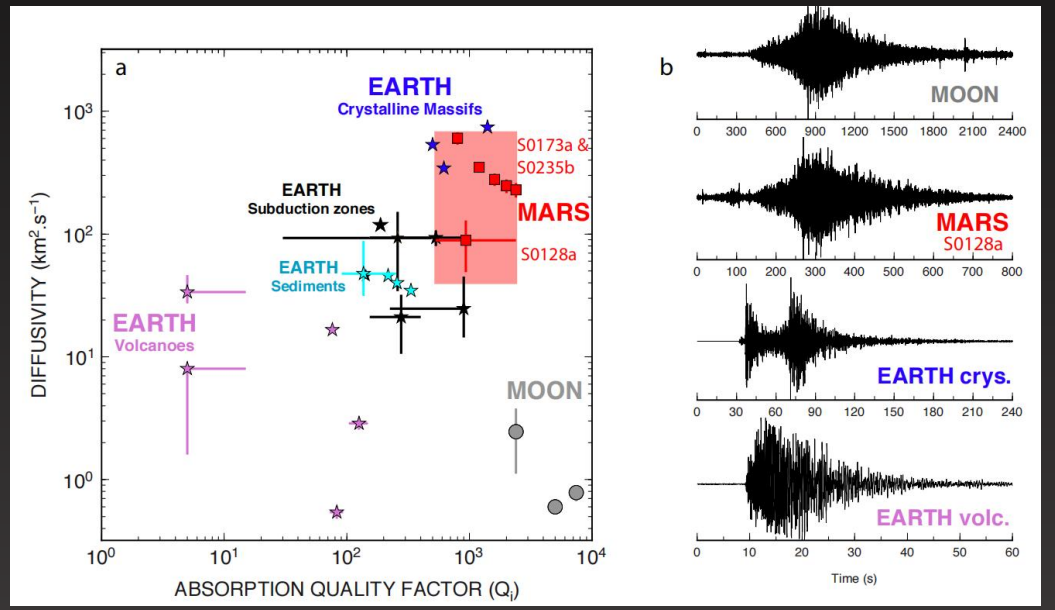


Mimoun et al., 2012









Lognonné et al., 2020

Where do the Earth and other planets come from? Where are they heading?

Martian solid inner core

Article

Seismic detection of a 600-km solid inner core in Mars

https://doi.org/10.1038/s41586-025-09361-9

Received: 15 May 2024

Accepted: 4 July 2025

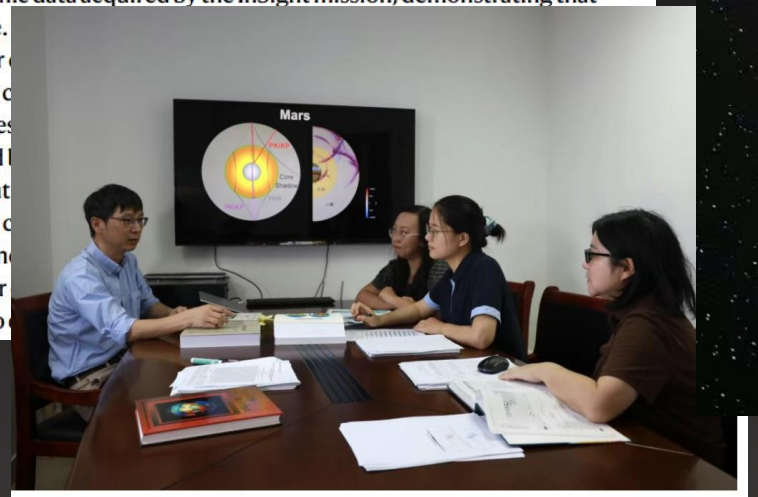
Published online: 3 September 2025

Open access

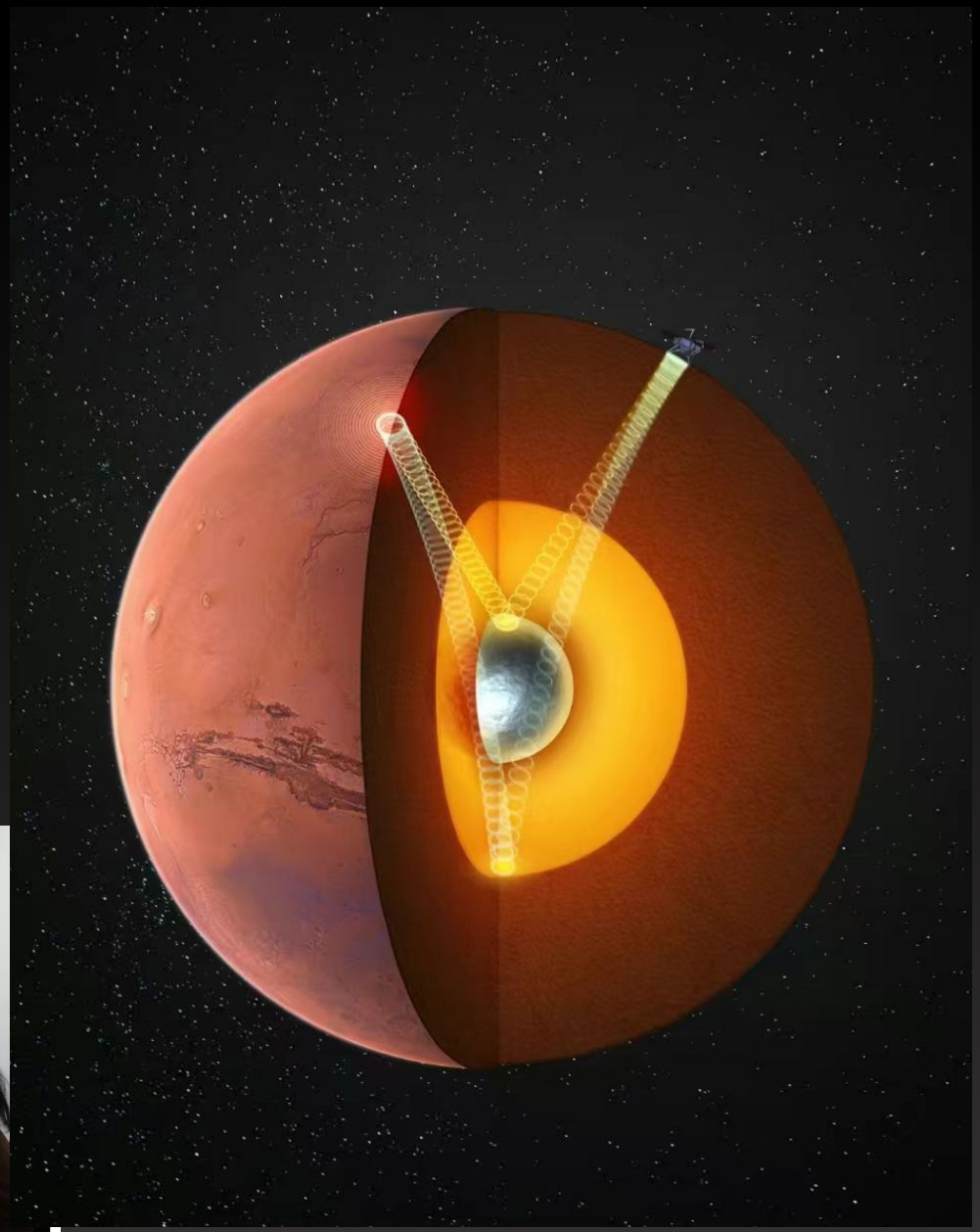
Check for updates

Huixing Bi[1,2], Daoyuan Sun[1,2]✉, Ningyu Sun[2,3], Zhu Mao[1,2], Mingwei Dai[1,2] & Douglas Hemingway[4]

For rocky planets, the presence of a solid inner core has notable implications on the composition and thermal evolution of the core and on the magnetic history of the planet[1–3]. On Mars, geophysical observations have confirmed that the core is at least partially liquid[4–7], but it is unknown whether any part of the core is solid. Here we present an analysis of seismic data acquired by the InSight mission, demonstrating that Mars has a solid inner core.
phase, PKKP, and the inner
inner core. Our inversions c
613 ± 67 km, with a compres
core boundary, supported
properties imply a concent
segregated from the outer c
anchor point for understan
relationship between inner
could provide insights into

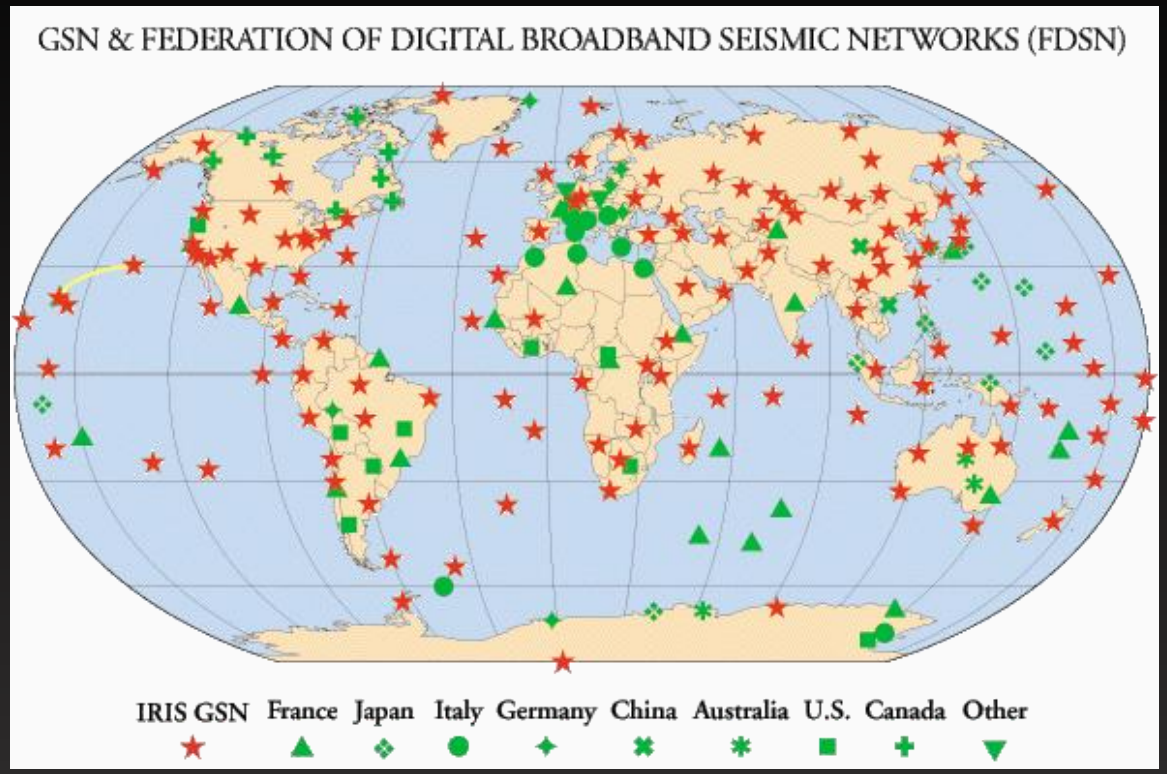


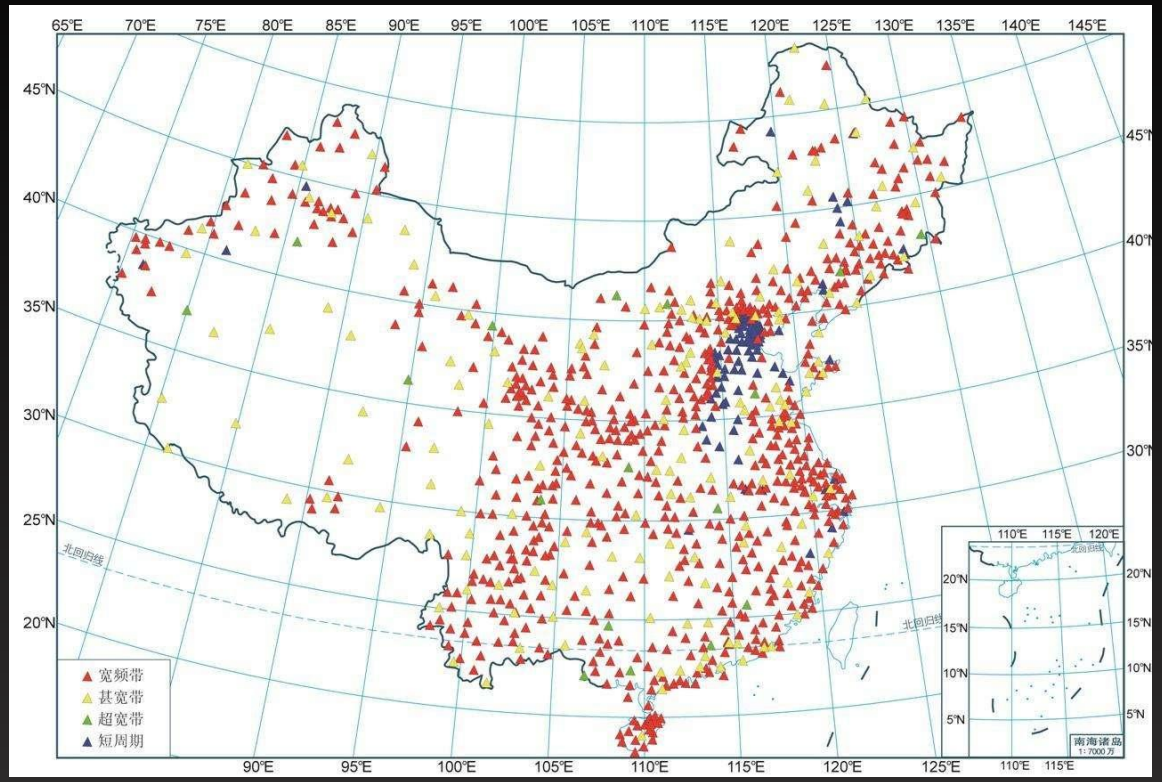
中国科大教授孙道远（左一）与团队成员讨论研究进展



- Research history of the layered Earth
- Secondary discontinuities within the Earth's interior
- 3D Earth

Global and reginal seismic network





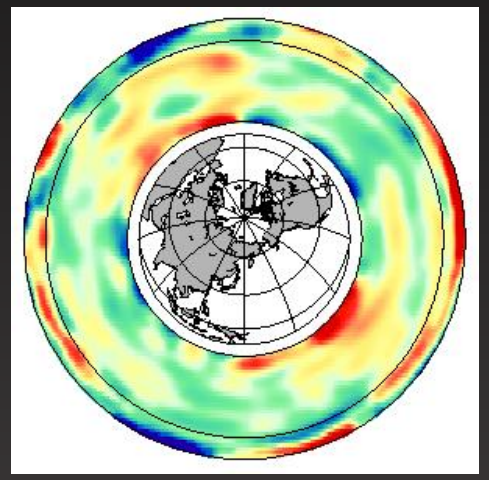
Seismic body wave tomography



Seismic body wave tomography

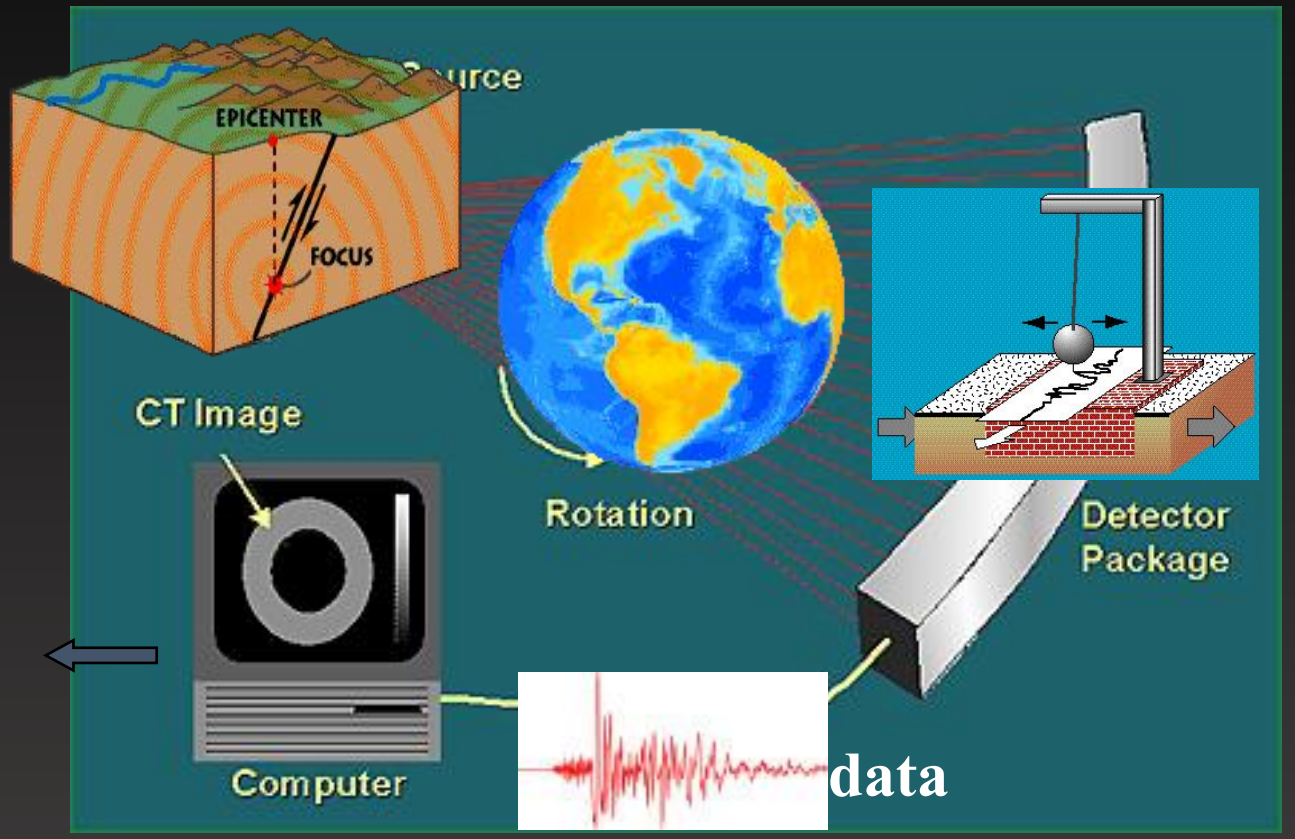


SeismicTomography

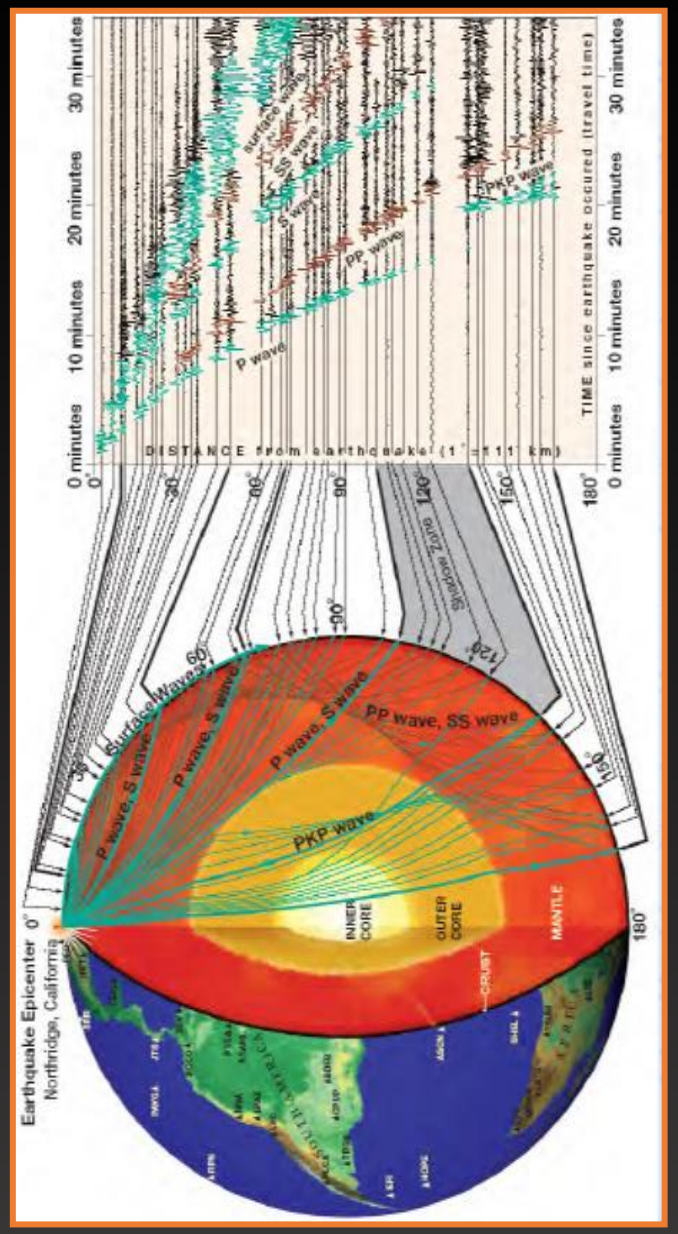


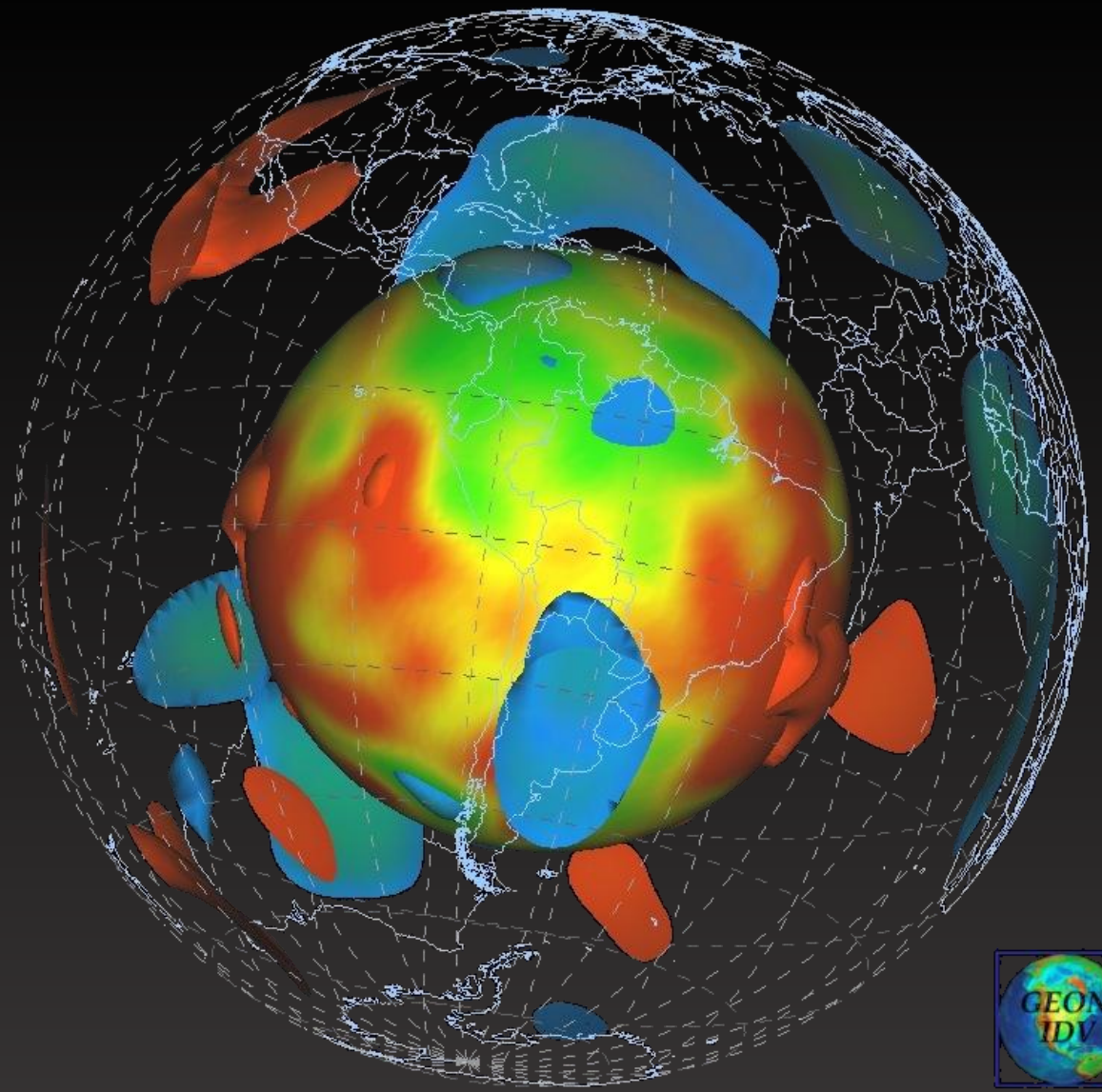
Medical Tomography

CT (Computerized tomography) Scan



Passive-source seismology for revealing deep Earth structure

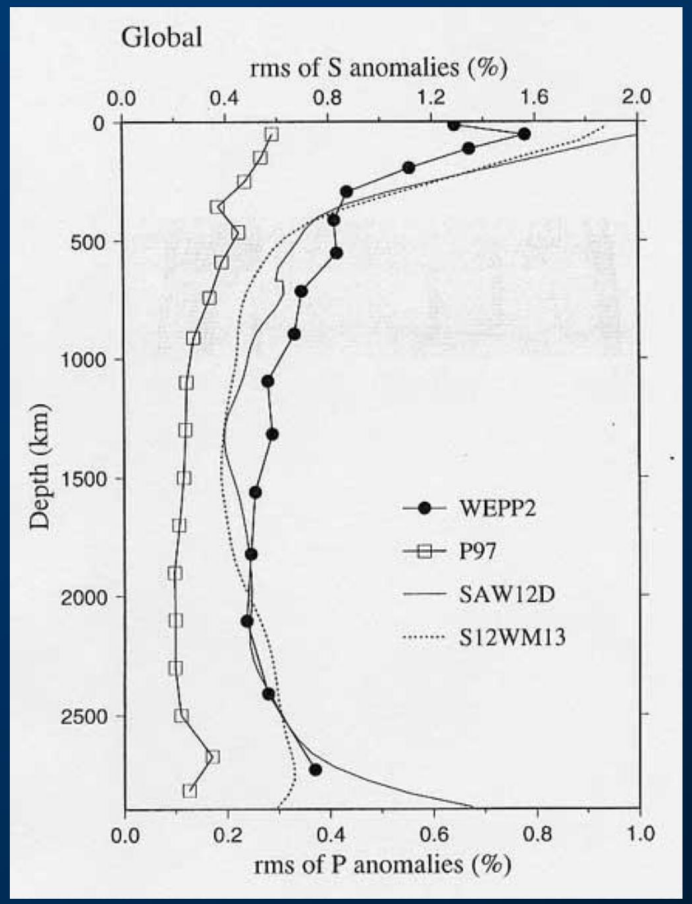


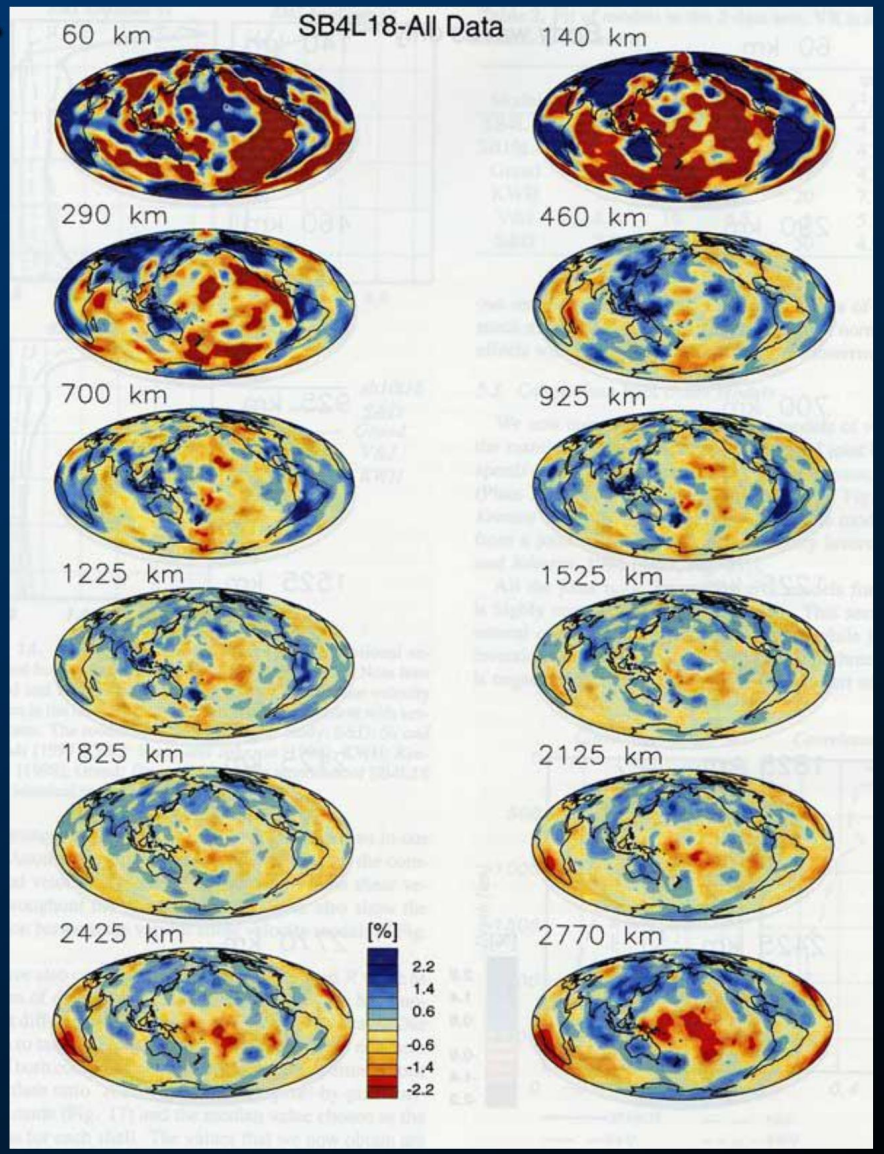


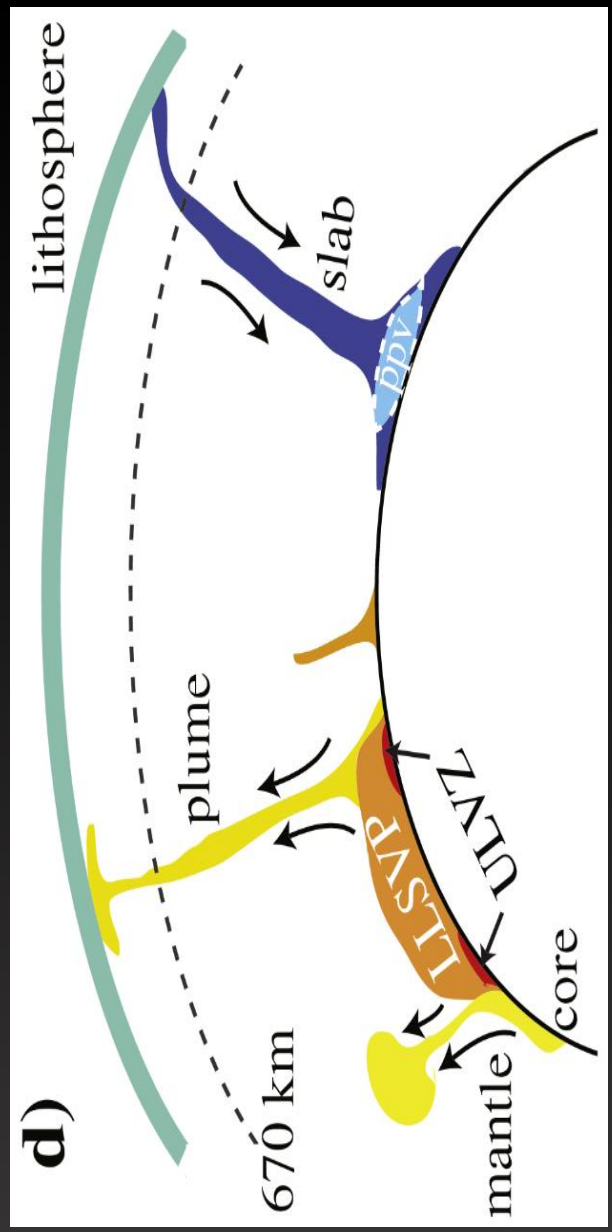
https://ds.iris.edu/media/product/emc-desktoptools/images/UNAVCO_IDV_tomog_REM_HR_4deg_tomography.jpg

Global tomography

Depth Distribution of Heterogeneities

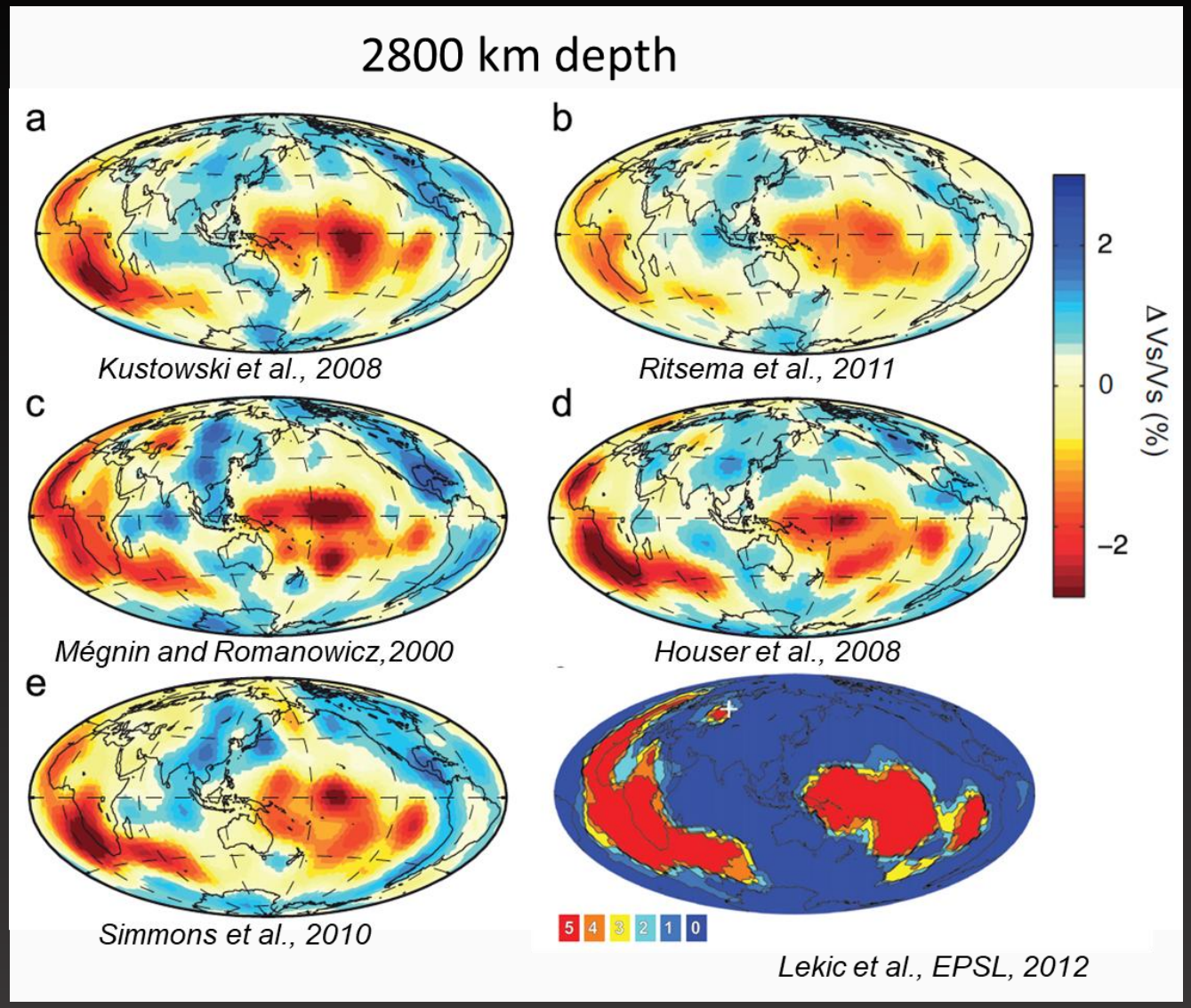






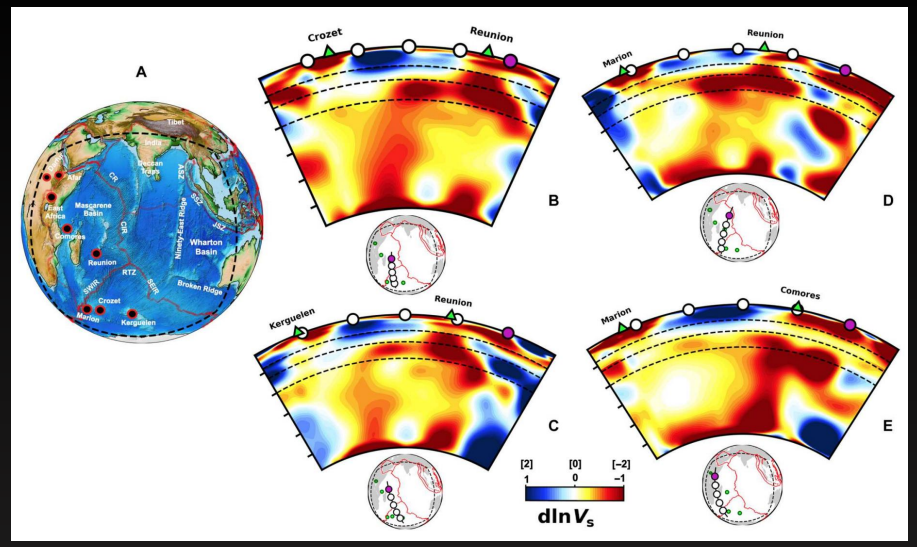
Ishii and Tromp, 2001

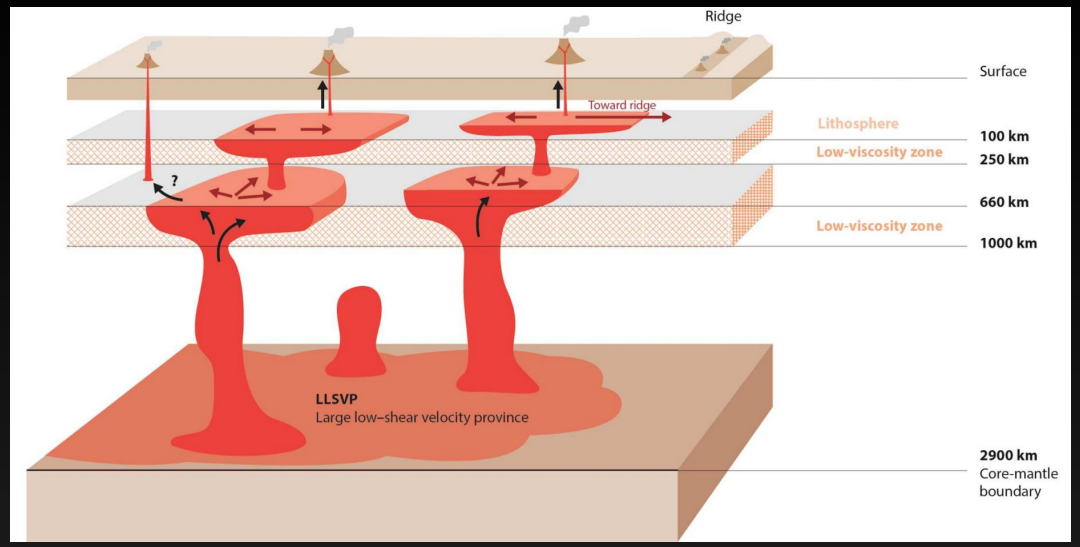
(Large Low Shear Velocity Provinces，LLSVPs)

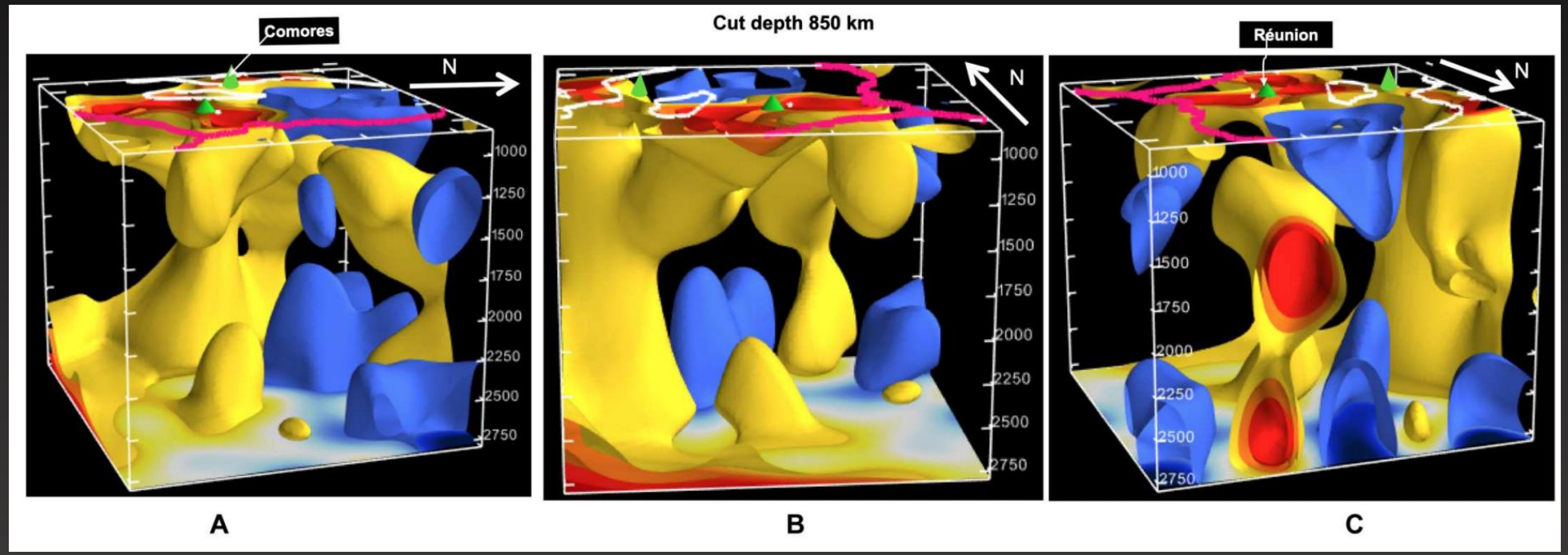


- Two large-scale shear-wave velocity provinces exist at the global core-mantle boundary, beneath the Pacific and Africa.
- Results from different studies show good consistency.
- 2–9% of mantle by mass
- Sharp boundaries
- Spatially correlated with hotspots
- Thermochemical anomalies
- Small-scale ultra-low velocity zones (ULVZ) exist; partial melting? (ULVZ, partial melts?)
- Long-term stability (?)

Big mantle pluse revealed by 3D earth tomography

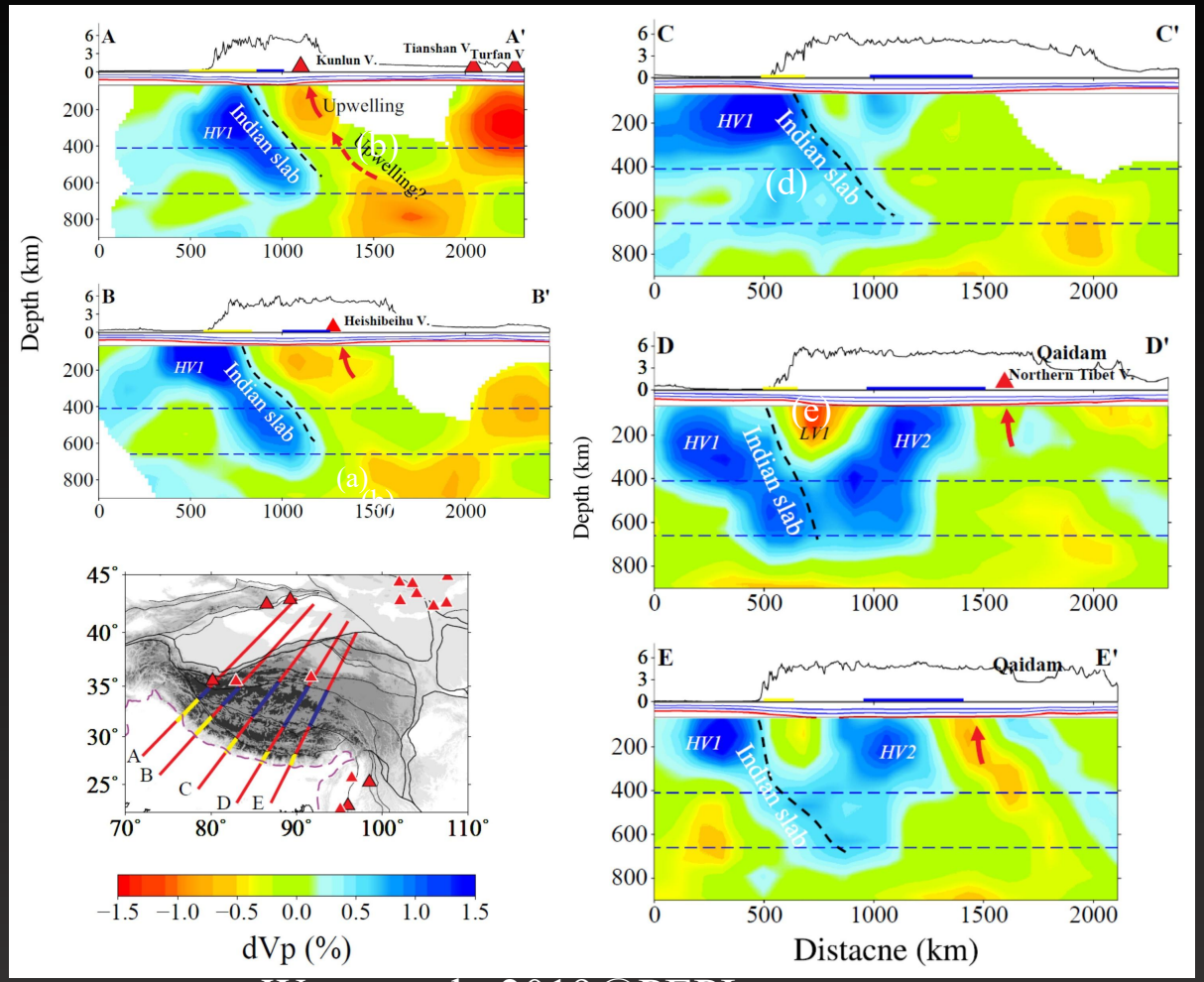






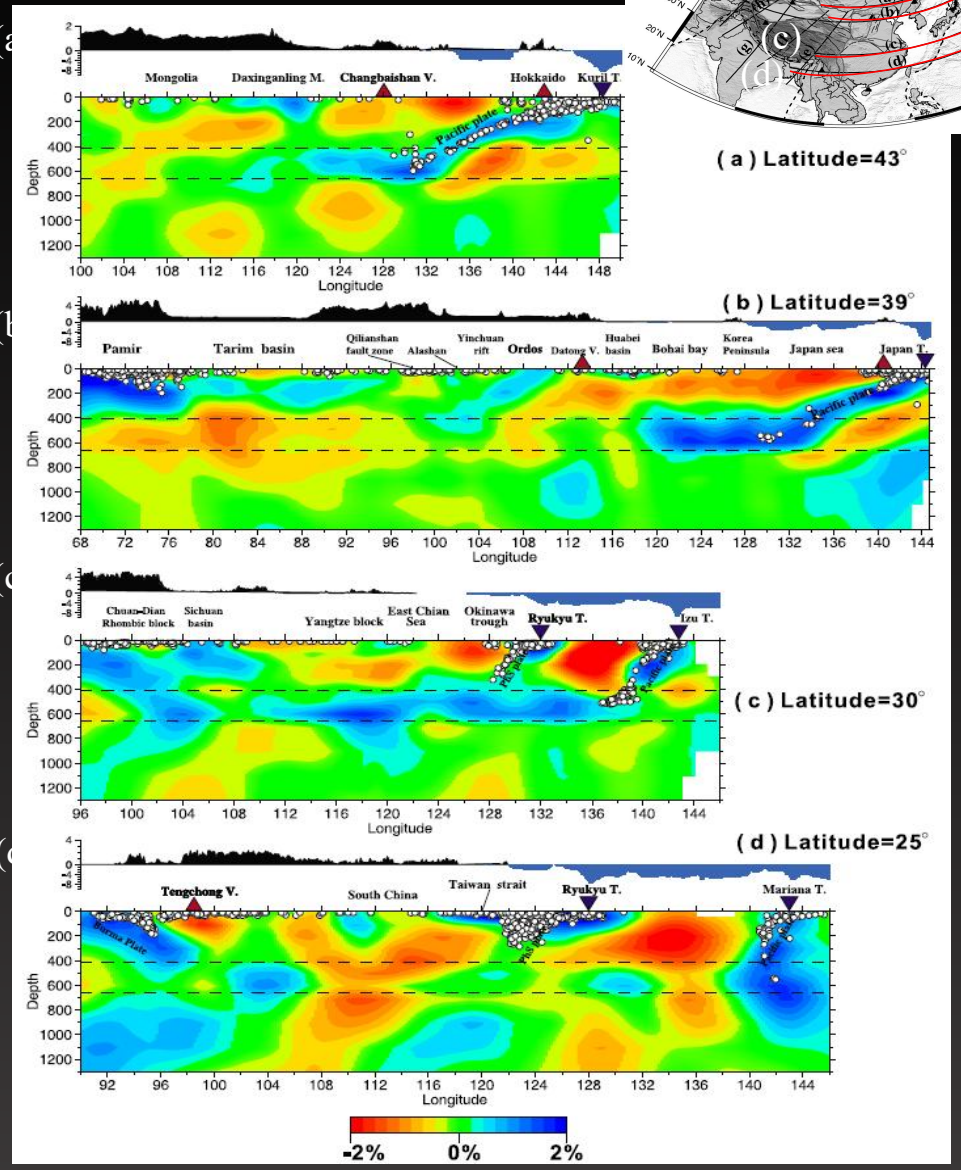
Wamba et al, 2023

Travel time imaging unveils the deep geometry of the Pacific and Indian slab.

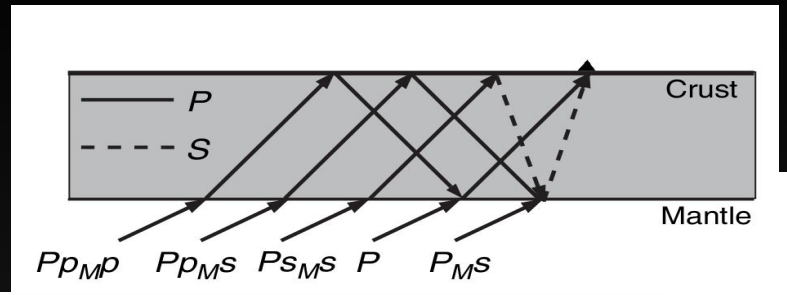


Wang et al., 2019@PEPI

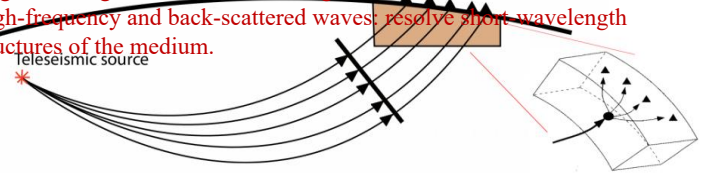
Huang et al., 2006@JGR

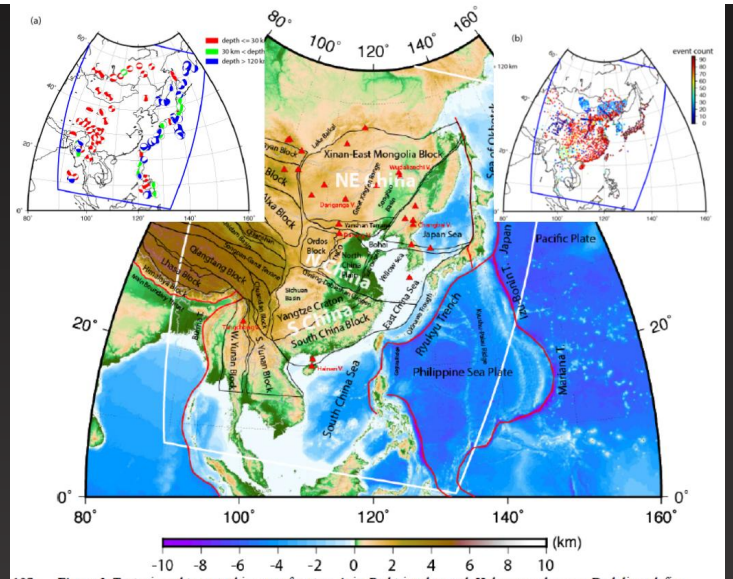


Full waveform Inversion (FWI)



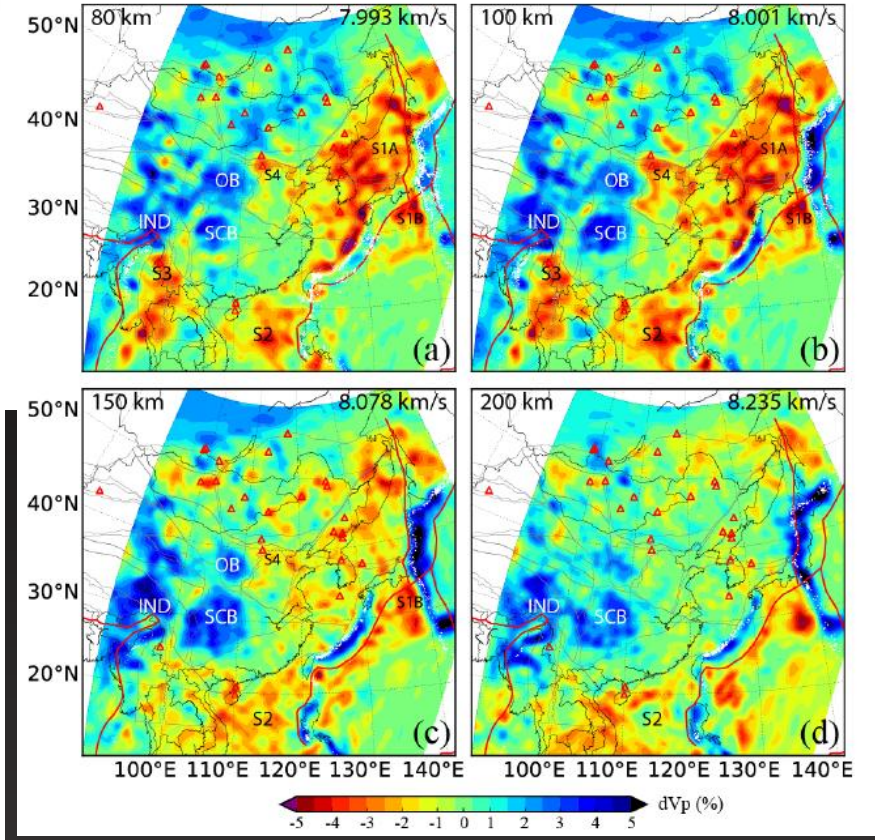
Low-frequency and forward-scattered waves: resolve medium- to long-wavelength structures in the target medium.
High-frequency and back-scattered waves: resolve short-wavelength structures of the medium.





127 **Figure 3.** Tectonic and topographic map of eastern Asia. Red triangles mark Holocene volcanoes. Dark lines define
128 main tectonic units and basins. "V." stands for volcano, and TNCO: Trans-North China Orogenic belt. Tectonic unit
129 boundaries are included in later figures as grey lines for reference. Red lines delineate plate boundaries. The white
130 box denotes the simulation region.

Upper Mantle Structure beneath Eastern Asia: Seismic Full-Waveform Tomography (80–800 km)



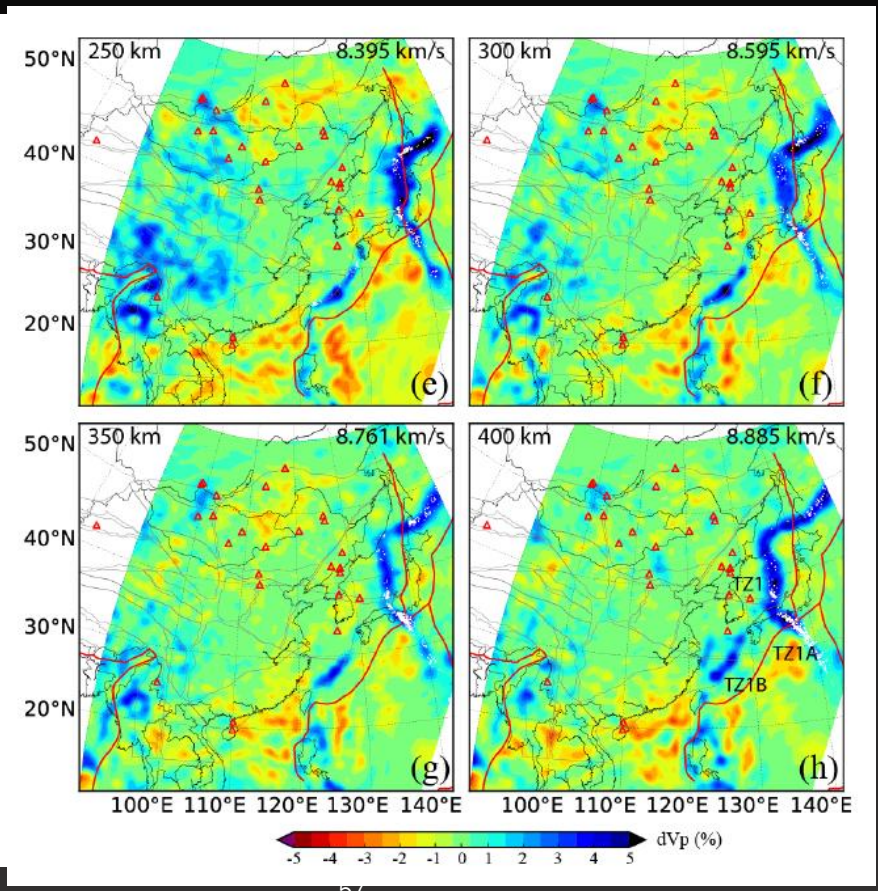
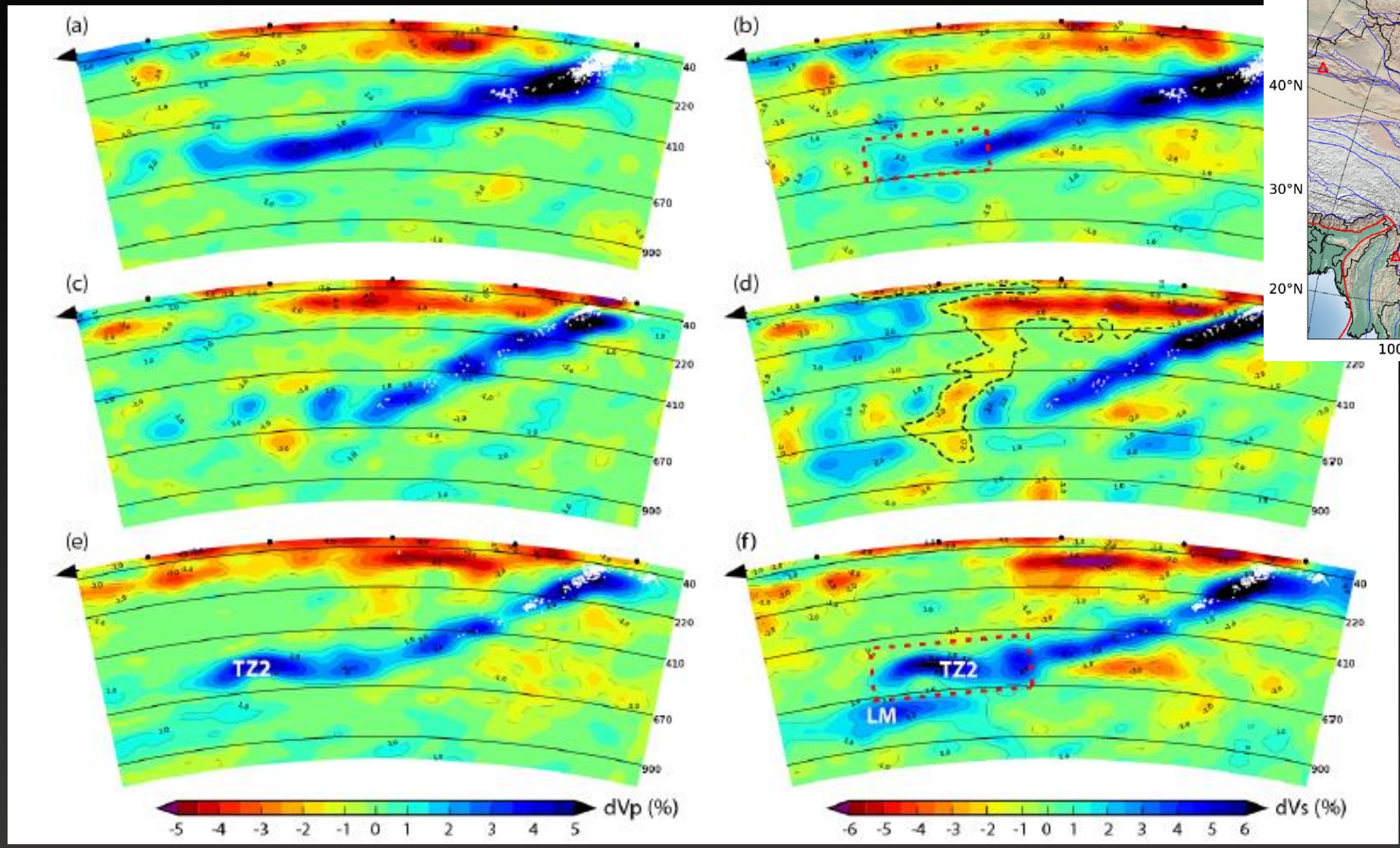
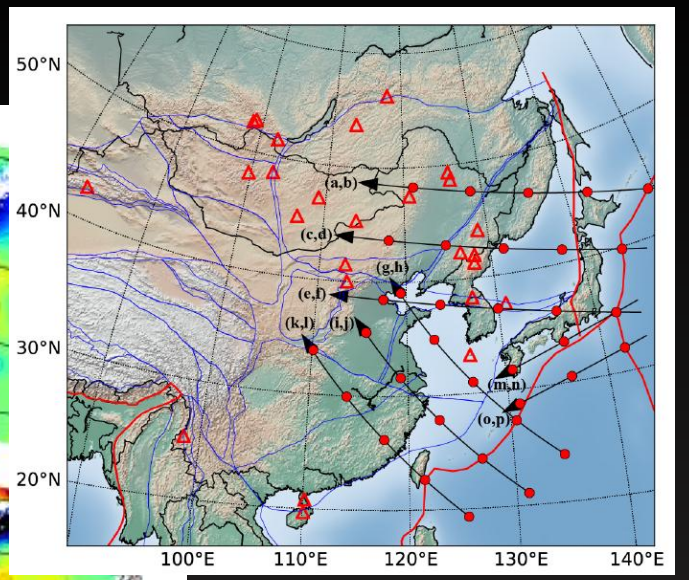


Figure 12. Horizontal cross sections of relative perturbations in isotropic P-velocity at depths ranging from 80 km to 800 km. The number on the left top of each figure shows the depth and the number on the right top shows the average velocity at this depth. OB: Ordos Basin, SCB: Sichuan Basin, IND: Indian plate.

Tao et al., 2018@JGR

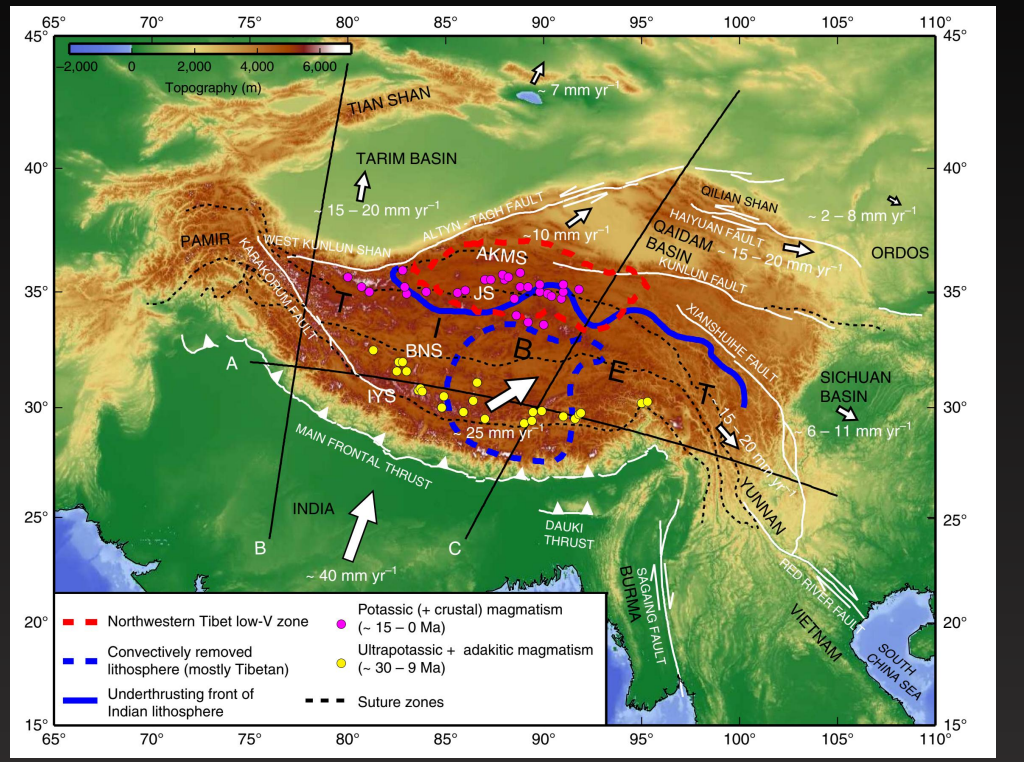
Full-waveform imaging unveils the deep geometry of the Pacific slab subducting beneath Asia.

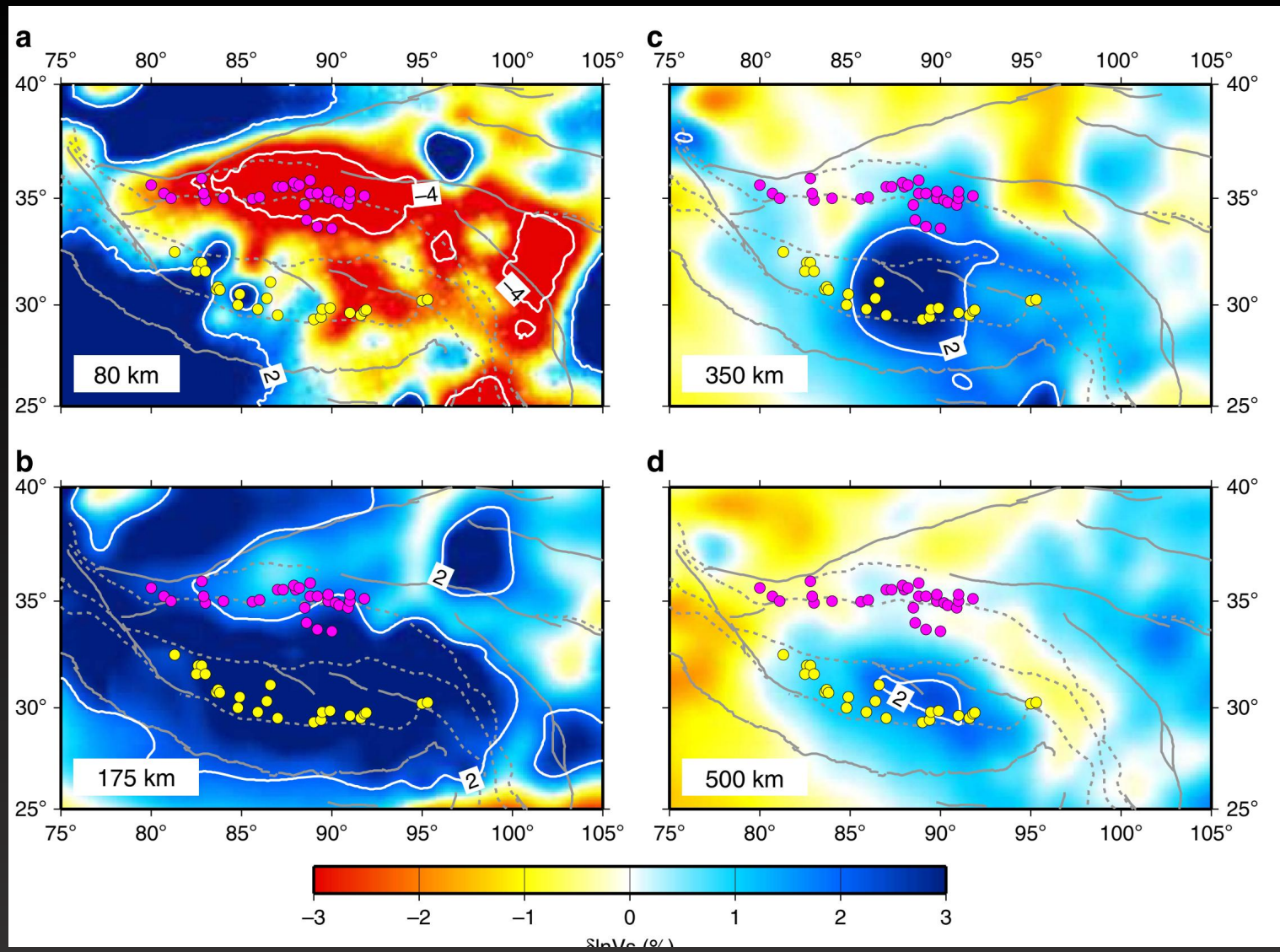




Tao et al., 2018@JGR

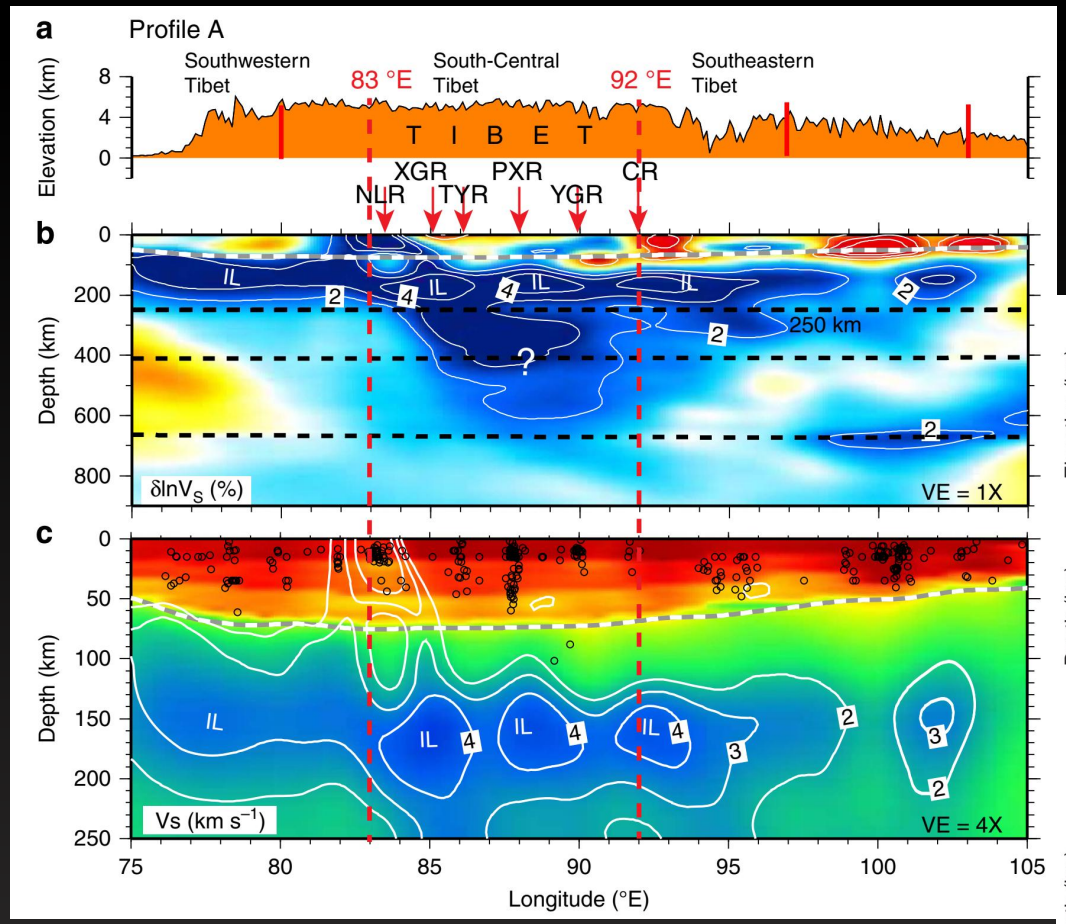
Subduction of the Indian Plate Indicated by Tomographic Results

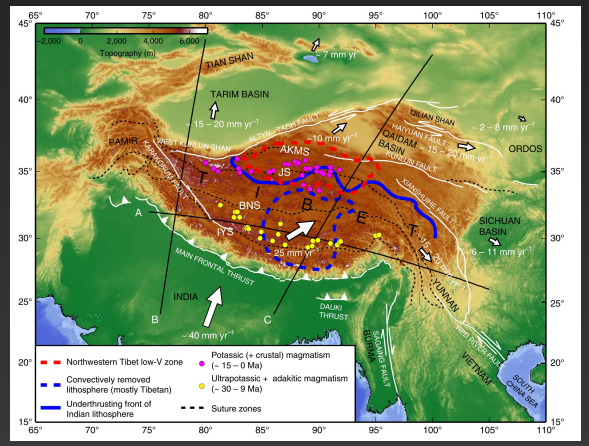


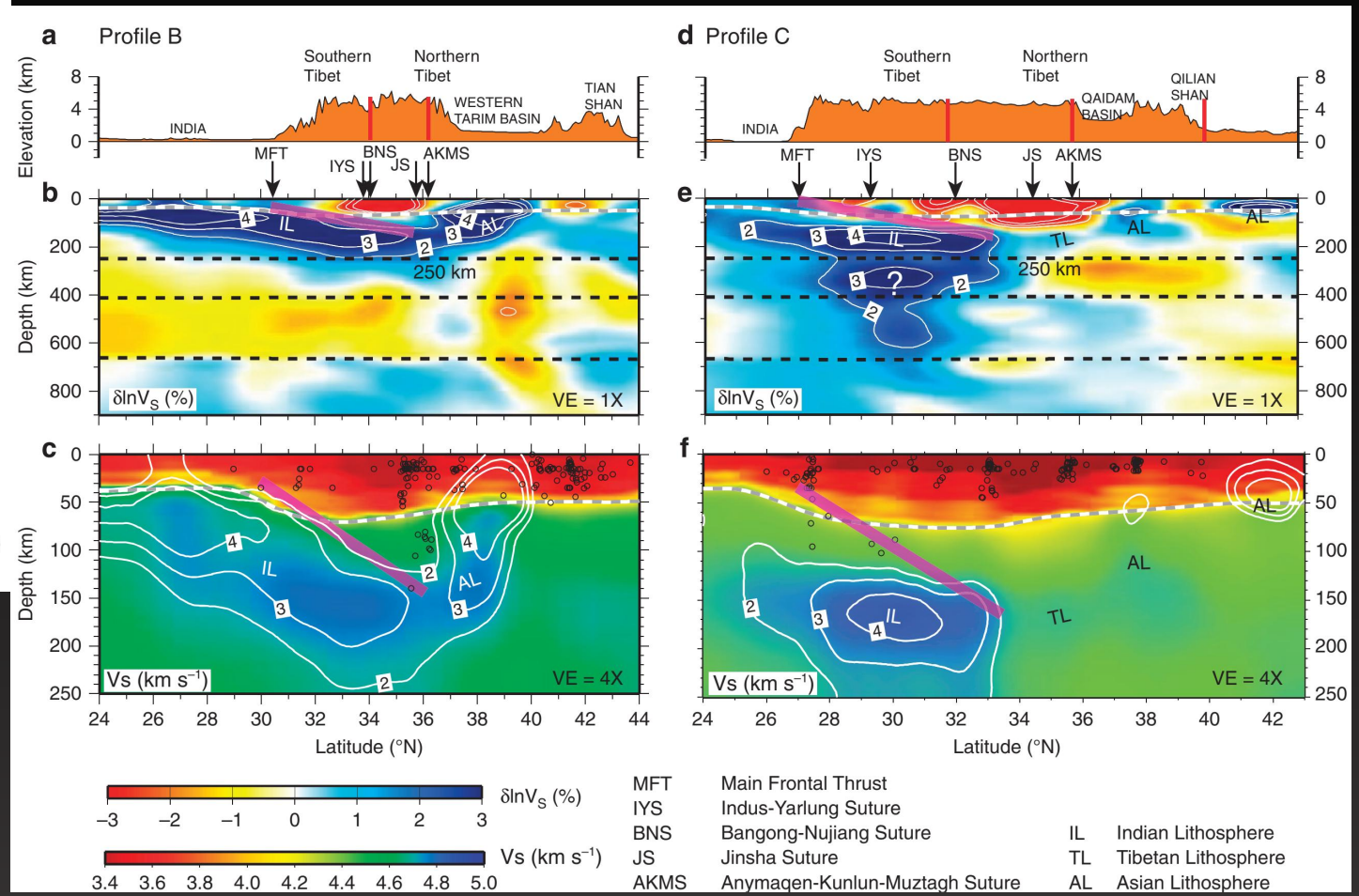


Chen et al., 2017@*Nature Comunication*

Subduction of the Indian Plate Indicated by Tomographic Results

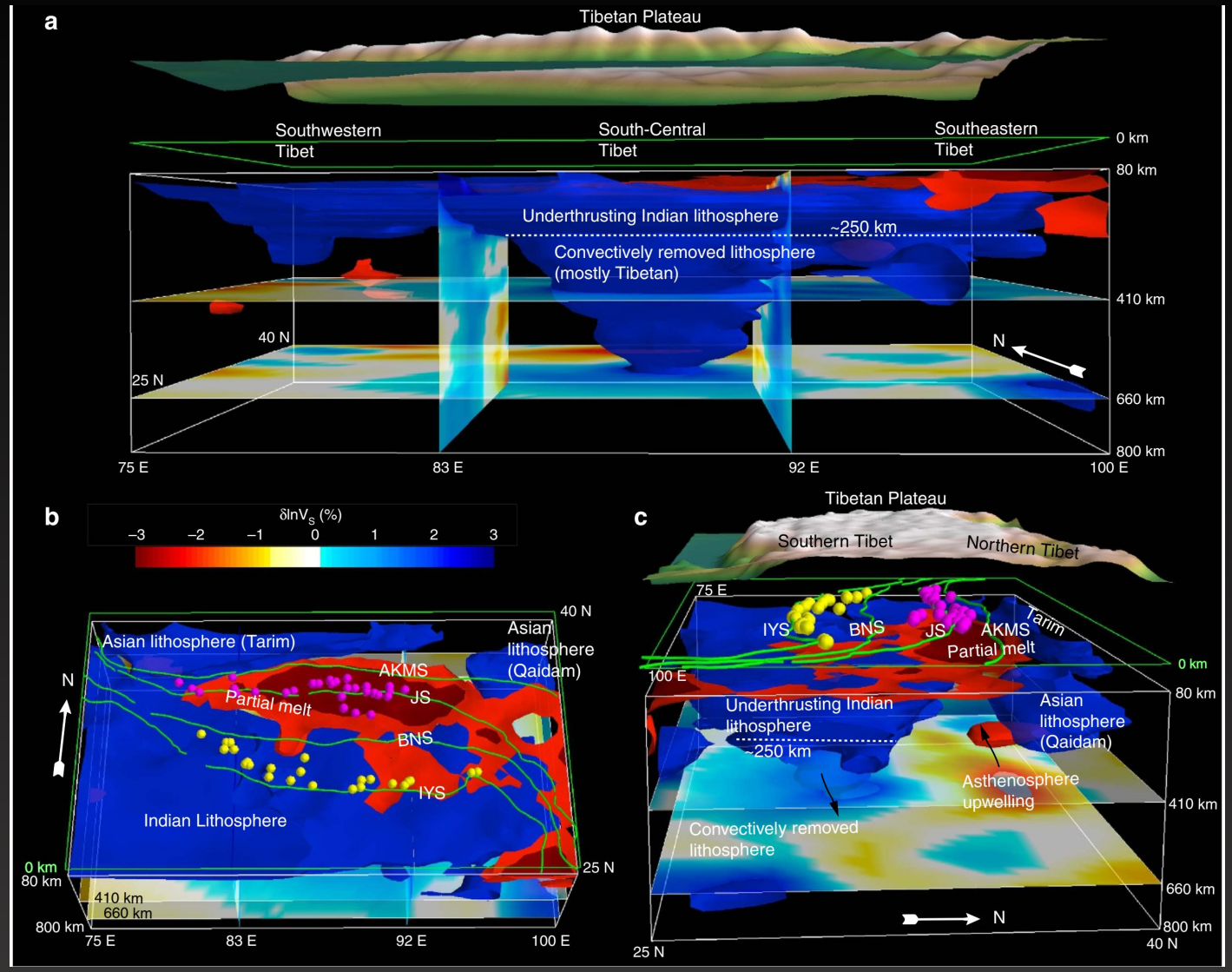






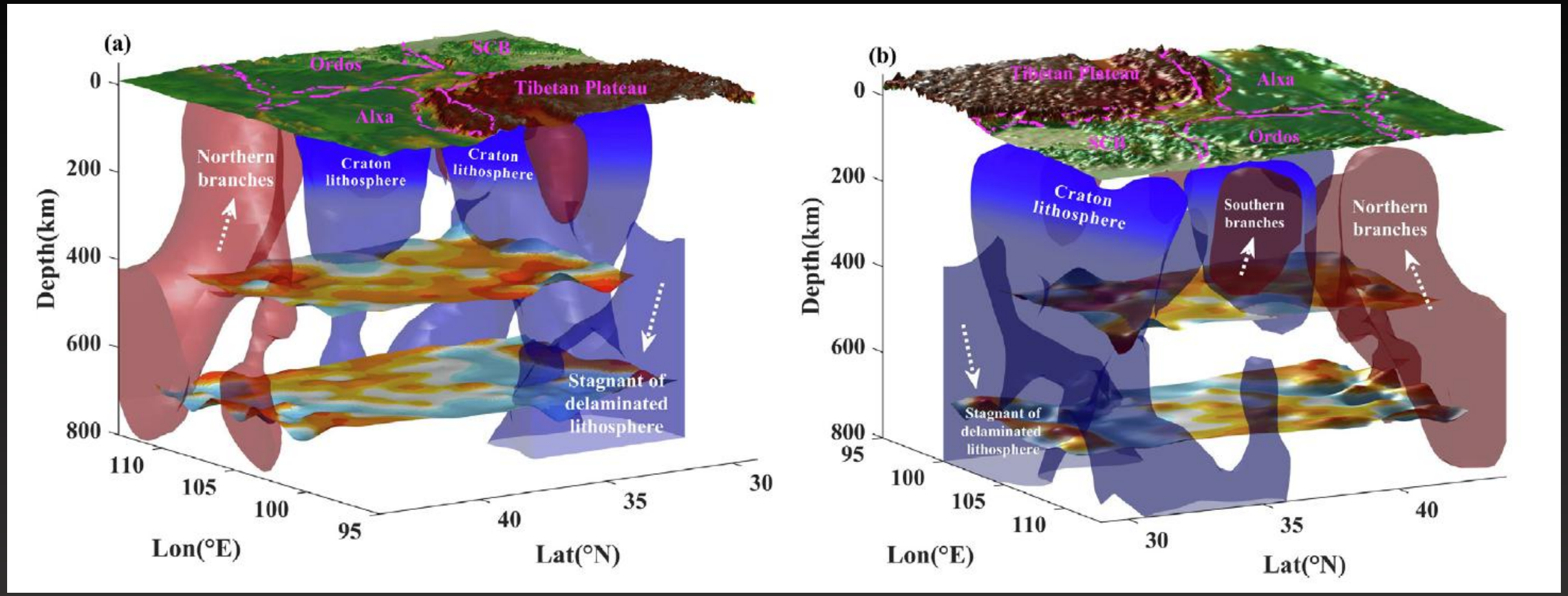
Chen et al., 2017

Subduction of the Indian Plate Indicated by Tomographic Results



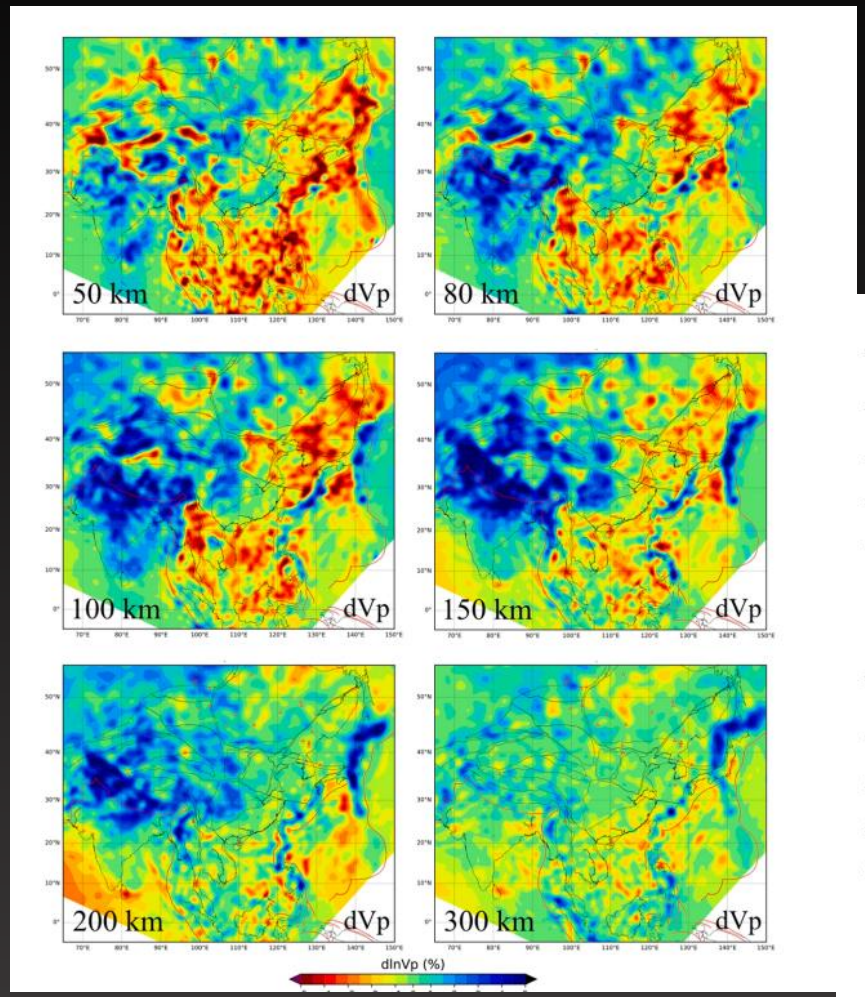
Chen et al., 2017@*Nature Comunication*

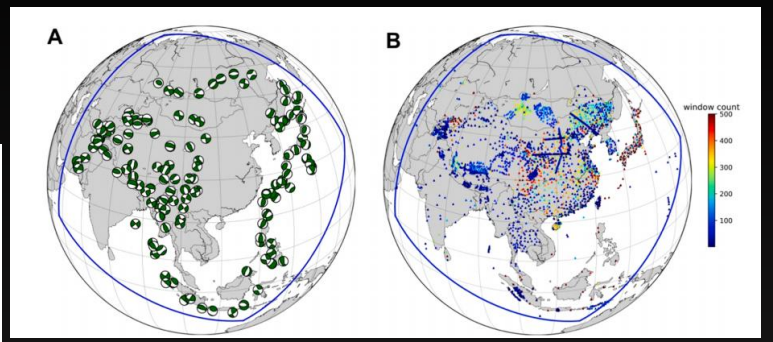
Geodynamic processes revealed by the deep structures beneath the NE margin of the Tibetan Plateau



Huang et al., 2019

Full-waveform imaging unveils the deep geometry of the East Asia.





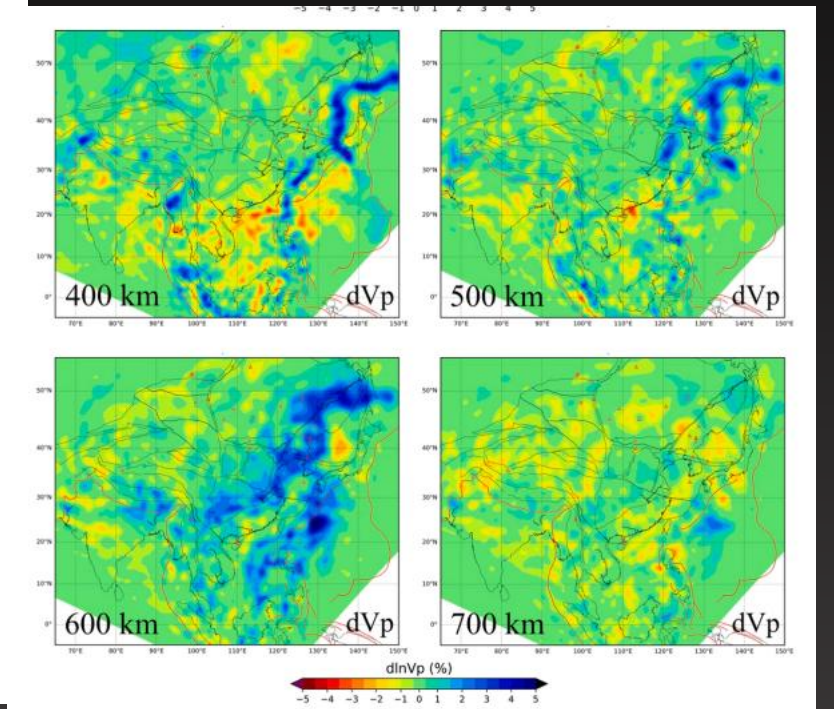
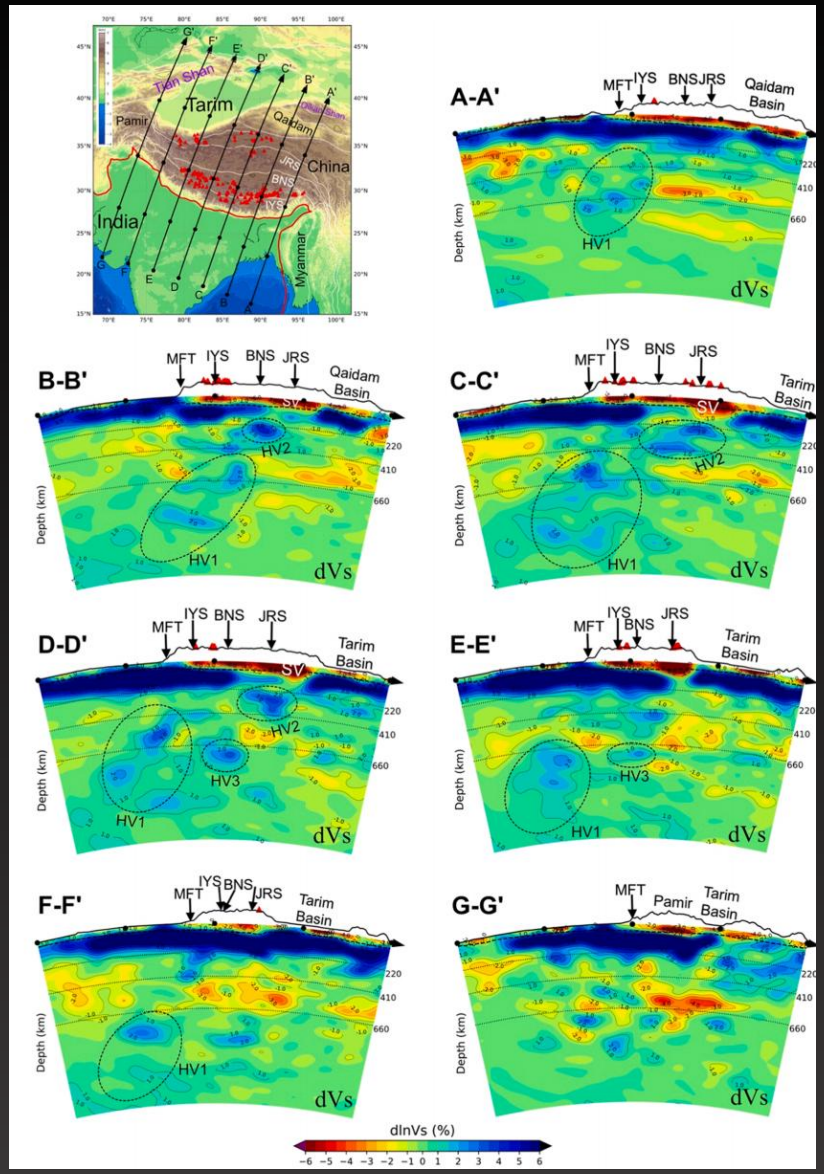
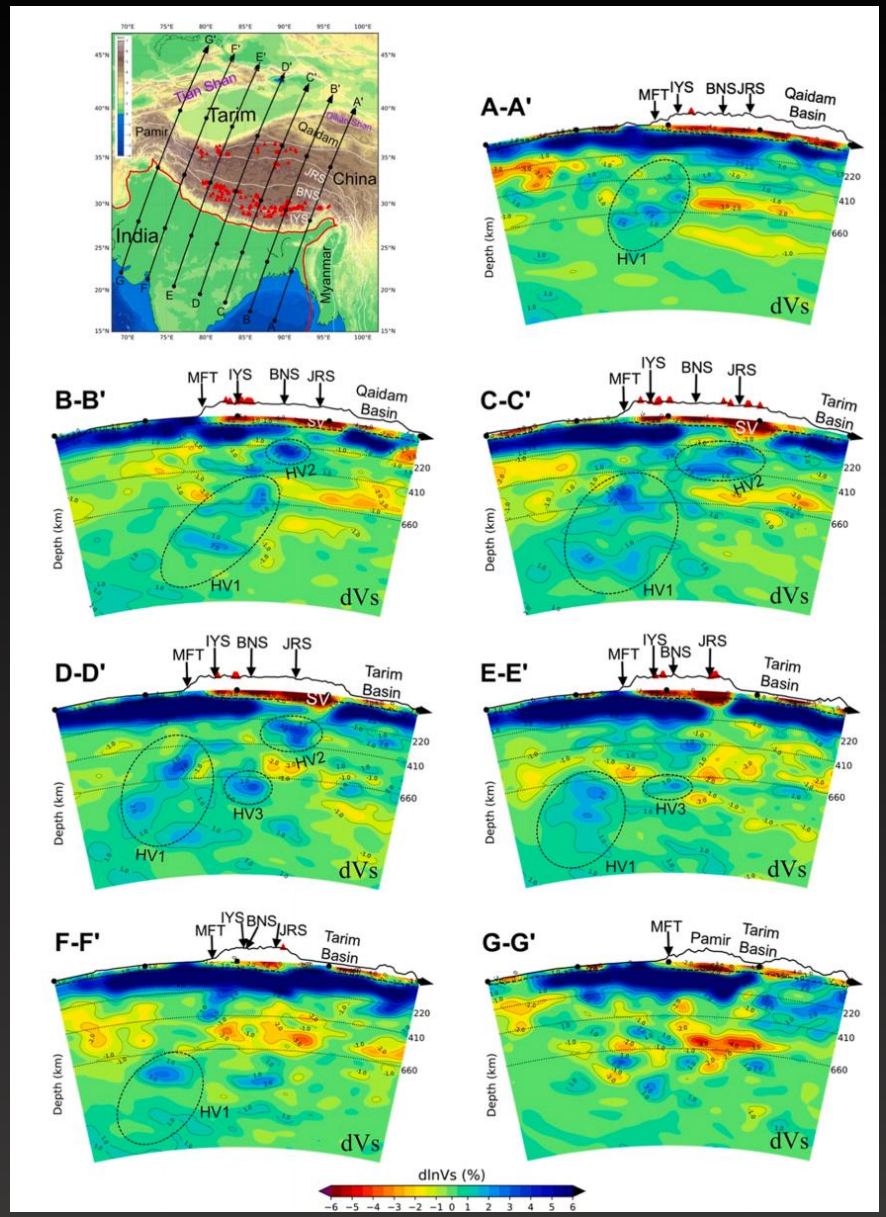


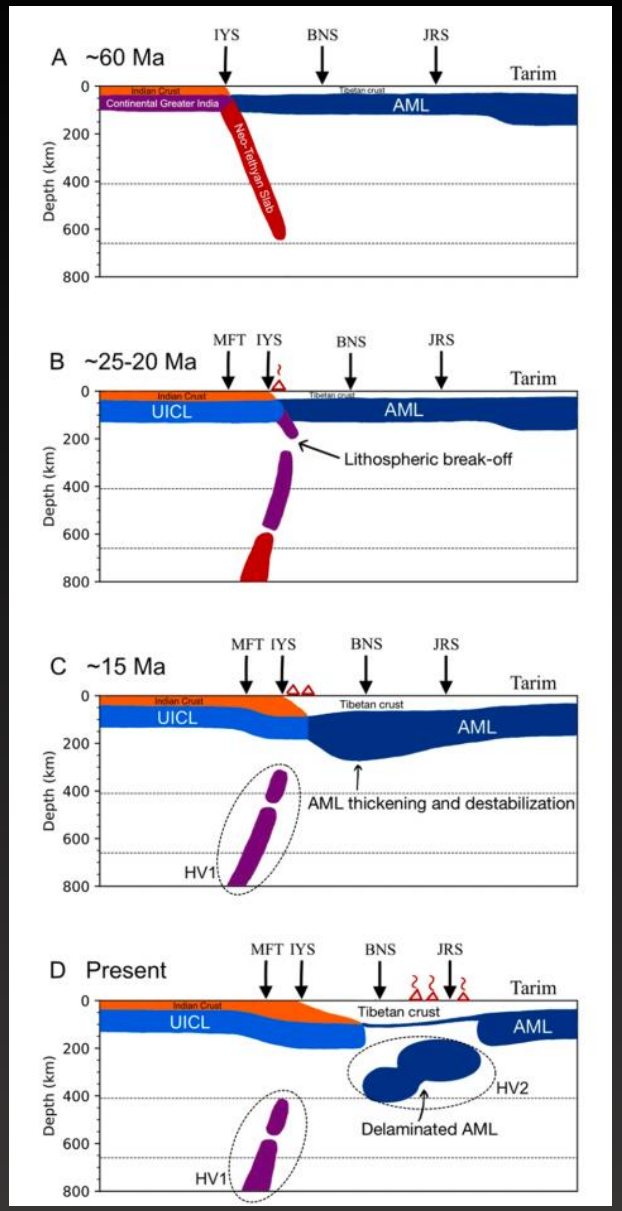
Fig. 5. Same as Fig. 4, but for P-wave velocity perturbations.



Liu et al., 2024@*EPSL*

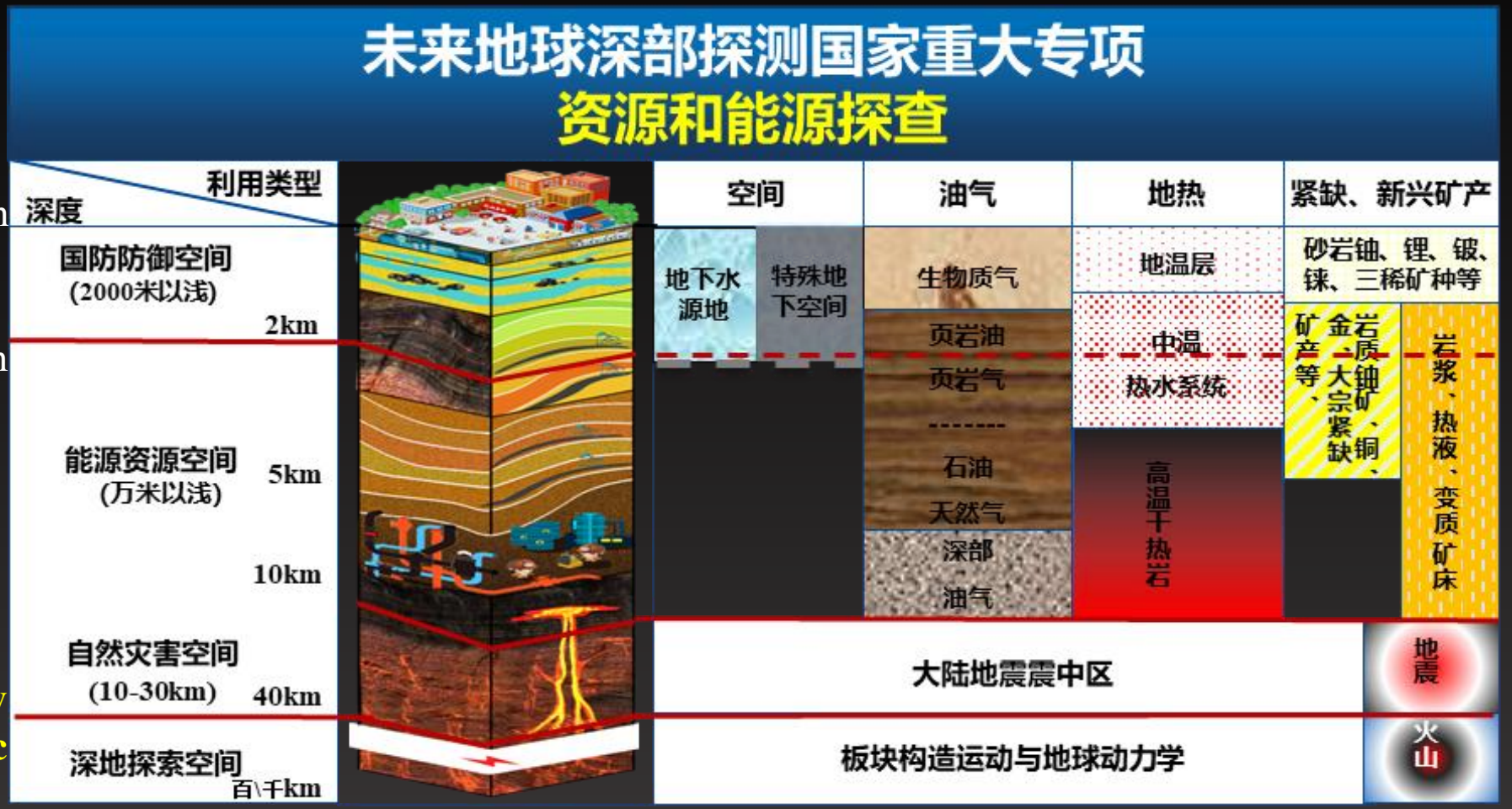
Deep structures record what has happened over the long geological time.





Deep Earth Exploration: A Discipline with Strong Vitality for the Future

- The greatest challenge in probing deep Earth structures does not lie in the innermost regions of the Earth, **but in the shallow part that is most closely linked to human activities.** Shallow exploration is tightly connected with national energy and resource demands, industrial production earthquake hazard mitigation and other fields. High precision and high resolution are fundamental requirements for shallow subsurface exploration. **Deep Earth exploration will remain a key and hot frontier for scientific research in the future.**



Thank you!